國立交通大學

統計學研究所

碩士論文

雙閘極暨絕緣層上矽場效應電晶體有效位勢量子修正模式的線性迴歸

Application of Linear Regression to Effective Potential of Double-Gate and Silicon-on-Insulator Metal-Oxide-Semiconductor Field-Effect Transistors

研 究 生：張景嵐

指導教授：周幼珍　博士

李義明　博士

中華民國九十五年七月

雙閘極暨絕緣層上矽場效應電晶體有效位勢量子修正模式的線性迴歸

Application of Linear Regression to Effective Potential of Double-Gate and Silicon-on-Insulator Metal-Oxide-Semiconductor Field-Effect Transistors

研 究 生：張景嵐　　Student：Ching-Lan Chang

指導教授：周幼珍　博士　　Advisor：Dr. Yow-Jen Jou

李義明　博士　　Advisor：Dr. Yiming Li

國立交通大學

統計學研究所

碩士論文

A Thesis

Submitted to Institute of Statistics

National Chiao Tung University

in partial Fulfillment of the Requirements

for the Degree of

Master

in

Statistics

July 2006

Hsinchu, Taiwan

中華民國九十五年七月

© Copyright by Ching-Lan Chang 2006

All Rights Reserved

雙閘極暨絕緣層上矽場效應電晶體有效位勢量子修正模式的線性迴歸

學生：張景嵐

指導教授：周幼珍 博士
李義明 博士

國立交通大學 統計 學研究所 碩士班

摘　　要

現今在系統晶片積體電路中的半導體元件尺寸已經縮小到奈米刻度的尺寸，隨著尺寸的縮小，因應各種特殊設計，半導體元件中氧化層的厚度也隨之變薄。因為氧化層厚度變薄的因素，在氧化層及通道的界面便產生了能量井，量子效應也就產生。在模擬上我們該如何考慮所謂的量子效應，是一個重要的議題。

傳統上，為了模擬量子效應會加入水丁格(Schrödinger equation)方程式在半導體方程式中。然而，水丁格方程式在數值計算上相當耗時及會有數值收斂上的麻煩，在二維度或三維度空間中邊界條件的設定也不容易。為了避免此方程式在模擬上的困難，許多替代的量子修正模型也陸續被提出，在這許多的模型中，大都還是存在著偏微分方程式。近年來被提出的有效位勢(effective potential)理論，是一個簡單的積分方程式。除此之外，在演算法中也大大的改善了耗時的缺點。不過在有效位勢模型中，存在著一個具有不確定性的變數(波包的標準差，standard deviation of wave packet)。隨著標準差的變化，所模擬得到的結果也會有所差異。為了得到正確的值，吾人利用波松-水丁格方程式的結果為基準，調整波包的標準差以達到兩者的結果最為接近。而另外一個問題隨之出現，隨著元件外加不同的條件(偏壓、氧化層厚度…等等)，標準差的值也會隨之變化。

在此論文中，所探討的元件結構為雙閘極以及絕緣層上矽金屬氧化物半導體場效電晶體為主，探討不同的條件對波包的標準差的影響為何。吾人在各種不同的外加條件下，以波松-水丁格方程式的結果為基準，求出各個不同的波包標準差值。接著利用統計的方法，建立出波包標準差以及各外加條件的模型。首先，我們以散佈圖觀察各外加條件對波包的標準差的關係圖，發現之間並沒有複雜的關係，所以我們建立一個二階的線性模型。經過變數轉換得到不錯的結果。

在此提出的模型在結構，外加條件上有所限制，可以將此模型的適用性擴展到更多結構、或是特性相似的半導體元件上。文章中所提出的統計方法可以廣為應用在其他的半導體元件特性分析上。

Application of Linear Regression to Effective Potential of Double-Gate and Silicon-on-Insulator Metal-Oxide-Semiconductor Field-Effect Transistors

student：Ching-Lan Chang

Advisors：Dr. Yow-Jen Jou
Dr. Yiming Li

Department of Institute of Statistics
National Chiao Tung University

ABSTRACT

Within the next decade or so, it is expected that gate lengths will shrink to 45 nm or less in devices found in integrated circuits. Quantum effects are known to occur in the channel region of MOSFET devices, in which the carriers are confined in a triangular potential well at the semiconductor-oxide interface. How might we expect quantum mechanics to arise in the transport through these small devices?

Typically, these effects are quantified by a simultaneous solution of the Schrödinger and Poisson equations, which can be a very time consuming procedure if it needs to be incorporated in realistic device simulations. Besides, different methods are proposed to include quantization effects in simulation of carrier transport in nanoscale devices. For instance, Hansch, MlDA, Van Dort, Density Gradient model … etc. Among these approaches, Density Gradient method are used generally. However, the quantum potential is defined in terms of the second derivative of the square root of local density. Such and approach is highly sensitive to noise in the determination of the local carrier density. Recently, Ferry propose an efficient method, effective potential, to include quantum effects. This approach avoids complex computation. Later, an more complicated effective potential is develop, but it is not included in our discussion.

Effective potential method is quite convenient to calculate. However, one variable, standard deviation of wave packet, in the model influence the results quite significantly. Unfortunately, value of this parameter is not known exactly. How to determine the value is an interesting problem.

In this thesis, we do some simulations with various conditions to calibrate value of the variable by Schrödinger equation. And try to establish a model of standard deviation of wave packet by using statistical methods. First, we draw the scattering plots and find that correlations between outer conditions and value of standard deviation of wave packet are simple. So we just establish a second order multiple linear model. We get results which are satisfied through power transformation. The model is established corresponding to double-gate and silicon-on-insulator (SOI) MOSFET structures. Though the model is not suitable for any structure, conditions of devices. This method can be expanded to establish other models more generally.

誌　謝

這份論文能夠順利完成，首先感謝我的指導老師 周幼珍老師給予我最大自由度，讓我可以繼續完成感興趣的研究，並在課業以及生活上不吝惜的指導及支持。其次，我要感謝我另一共同指導老師 李義明老師，感謝老師指導我論文方向脈絡，以及研究的能力激發有著深厚的影響。

論文口試期間，承蒙清華大學統計學研究所周若珍教授、以及國家高速網路與計算中心羅仕京博士撥冗細審，並會予寶貴意見與殷切指正使本論文更臻完備。

研究室方面，我要感謝周宏穆學長、建松、煒昕、柏賢、宏榮教導我許多元件物理的觀念，真的讓我獲益匪淺；紹銘學長、陳璞學長、傳盛學長、正凱學長、彥羽學長在程式上以及論文給予相當大的幫助。

統研所方面，感謝豐洋、育仕、玉均、雅靜、穎劭、婉文；不僅在統計的知識上會給予幫助，也在我學習的路上給予許多的建議。

我還要感謝我的好朋友們，哲名、信揚、義富、全豐、智國、穎慈、岱融。雖然現在大家都各分東西，但是總在最恰當的時候，給予最恰當的鼓勵、安慰、歡笑。並且在論文中各方面的問題提供協助。

最後最應該感謝的是我的爸爸，媽媽，和我的姐姐以及金龍，支持我在統計之外，往半導體學習。這期間即便我承受在大的壓力、不開心、不耐煩、及挫折，還是一直在鼓勵我、幫我調適心情。現在終於完成論文畢業了，真的很感謝你們。

感謝這段期間大家對我的包容、關懷與愛護。這篇論文，這個工作，以及我在交大的一切成長，沒有你們，是完全沒有辦法達成的，一切的功勞都歸因於全部的人。謝謝大家一直挺我鼓勵我，使我順順利利的度過這段非凡且精采的日子。在此將這篇論文獻給所有關心我以及我所愛的人，謝謝你們。

本論文感謝行政院國家科學委員會(計畫編號 NSC-93-2115-E-492-008、NSC-94-2115-E-009-084)、卓越沿續計畫(計畫編號 NSC-94-2752-E-009-003-PAE、NSC-95-2752-E-009-003-PAE)、五年五百億計畫、經濟部科專計劃(計畫編號 93-EC-17-A-07-S1-0011)以及台灣積體電路製造股份有限公司之資助。

張景嵐 謹誌

中華民國九十五年七月 于風城交大

Contents

Abstract (in Chinese) v

Abstract (in English) vii

Acknowledgments (in Chinese) ix

List of Tables xv

List of Figures xvi

1 Introduction 1

1.1 Background 1

1.2 Motivation 3

1.3 Outline 4

2 Classical and Quantum Mechanical Transport Models 5

2.1 Double-Gate and Silicon-On-Insulator Metal-Oxide-Semiconductor Field-Effect Transistors 6

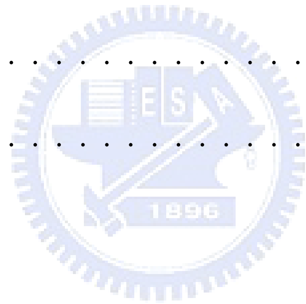

2.2 Classical Drift-Diffusion Model 11

2.3 Quantum Mechanical Model 14

3 Effective Potential 20

3.1 Fundamental of the Effective Potential 21

3.2 Ferry's Effective Potential Approach 24

4 The Linear Regression 32

4.1 Scattering Plot 33

4.2 Multiple Linear Regression 34

4.2.1 Model Expression 34

4.2.2 Estimation of The Model Parameters 35

4.2.3 Hypothesis Testing in Multiple Linear Regression 39

4.2.4 Variable Selection in Regression Analysis 42

4.3 Residual Analysis 45

4.3.1 Normal Probability Plot 45

4.3.2 Plot of Residuals against the Fitted Values 46

4.4 Power Transformation 47

5 Results and Discussion 49

5.1 Calibration of Ferry's Effective Potential 50

5.2 Data Collection by Using Device Simulation Tool 53
5.3 Modelling and Simulation Results 54
5.3.1 Modelling Double-Gate MOSFET 54
5.3.2 Accuracy of Model of Double-Gate MOSFET 74
5.3.3 Modelling Double-Gate and SOI MOSFETs 77
5.3.4 Accuracy of Model of Double-Gate and SOI MOSFET 90
5.4 Discussion 95

6 Conclusions **96**

6.1 Summary 97
6.2 Future Work 98
References 99

Appendix A

Effective Potential Source Code of Matlab 107

Appendix B

ISE Commands for Classical Transport and Schrödinger Equation 109
B.1 MDraw Commands 110
B.2 Dessis Commands 111
B.2.1 key words 114

Appendix C

Energy Band of Double-Gate MOSFET 116

Appendix D

A Brief Instruction to SPSS 123

List of Tables

4.1 ANOVA table for significance of regression in multiple regression 41

5.1 Correlation Table 56

5.2 ANOVA table for significance of regression in multiple regression in double-gate MOSFET 56

5.3 Residual statistics in double-gate MOSFET 57

5.4 Coefficients table in double-gate MOSFET 57

5.5 ANOVA table for significance of regression in multiple regression 77

5.6 Residual statistics 78

5.7 Coefficients table 78

List of Figures

2.1 3D double-gate schematic diagram 7
2.2 2D double-gate schematic diagram 8
2.3 A energy band profile for the double-gate MOSFET used in the simulation . 9
2.4 3D SOI schematic diagram 10
2.5 Flow chart of Poisson and Continuity equations in ISE 13
2.6 Flow chart of SP Equation in ISE 17
2.7 Potential of SP equations 18
2.8 Electron density of SP equations 19
3.1 Flow chart of Ferry's effective potential 27
3.2 Potential from Ferry's effective potential 28
3.3 Electron density of Ferry's effective potential 29
3.4 Calibration of electron density of Ferry's effective potential by SP equations - I 30

3.5 Calibration of electron density of Ferry's effective potential by SP equations - II . . . 31

4.1 Example of scattering plot . . . 33

4.2 The Box-Cox likelihood plot . . . 48

5.1 Classical electron density and electron density corrected by SP equations of double-gate MOSFET . . . 51

5.2 Electron density corrected by Ferry's effective potential with various standard deviation of wave packet of double- gate MOSFET . . . 52

5.3 Scattering Plot : Channel length vs. standard deviation of wave packet . . . 59

5.4 Scattering plot : Gate voltage vs. Standard deviation of wave packet . . . 60

5.5 Scattering plot : Drain voltage vs. Standard deviation of wave packet . . . 61

5.6 Scattering plot : Thickness of bulk vs. Standard deviation of wave packet . 62

5.7 Scattering plot : Thickness of oxide vs. Standard deviation of wave packet . 63

5.8 Scattering plot : Doping concentration vs. Standard deviation of wave packet 64

5.9 Normal plot I . . . 65

5.10 Scattering plot : Fitted value against residual I . . . 66

5.11 Likelihood plot of power transformation . . . 67

5.12 Normal plot II . . . 68

5.13 Scattering plot : Fitted value against residual II . . . 69

5.14 Normal plot III 70
5.15 Scattering plot : Fitted value against residual III 71
5.16 Normal plot IV 72
5.17 Scattering plot : Fitted value against residual IV 73
5.18 Comparison of electron density 75
5.19 Scattering plot : Id-Vg curve 76
5.20 Likelihood plot of power transformation 80
5.21 Scattering plot : Thickness of oxide vs. Standard deviation of wave packet . 81
5.22 Scattering Plot : Channel length vs. standard deviation of wave packet . . . 82
5.23 Scattering plot : Thickness of bulk vs. Standard deviation of wave packet . 83
5.24 Scattering plot : Gate voltage vs. Standard deviation of wave packet 84
5.25 Scattering plot : Drain voltage vs. Standard deviation of wave packet 85
5.26 Scattering plot : Doping concentration vs. Standard deviation of wave packet 86
5.27 Scattering plot : Structure vs. Standard deviation of wave packet 87
5.28 Normal plot 88
5.29 Scattering plot : Fitted value against residual I 89
5.30 Comparison of electron density 91
5.31 Scattering plot : Id-Vg curve of double-gate MOSFET 92
5.32 Comparison of electron density 93

5.33 Scattering plot : Id-Vg curve of SOI 94

C.1 Energy band plot of various thickness of bulk 117

C.2 Energy band plot of various doping concentration 118

C.3 Energy band plot of various gate voltage 119

C.4 Energy band plot of various thickness of oxide 120

C.5 Energy band plot of various drain voltage 121

C.6 Energy band plot of various channel length 122

D.1 SPSS-I 124

D.2 SPSS-II 125

D.3 SPSS-III 126

D.4 SPSS-IV 127

D.5 SPSS-V 128

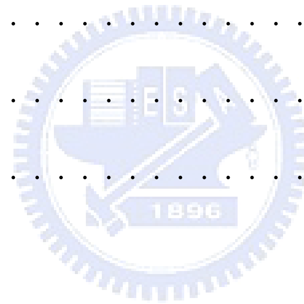

Chapter 1

Introduction

1.1 Background

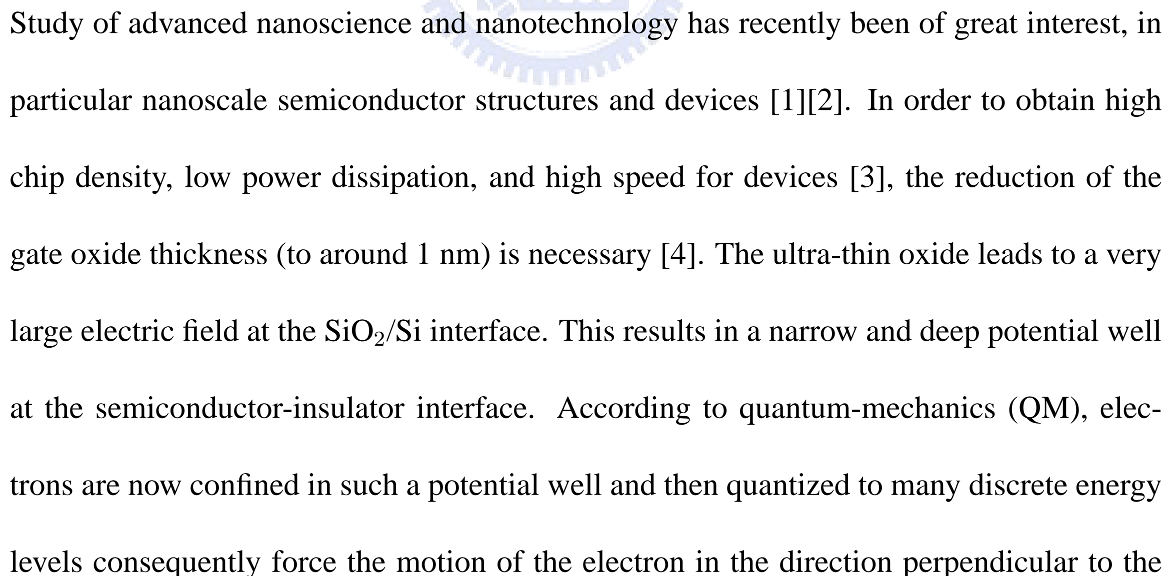

Study of advanced nanoscience and nanotechnology has recently been of great interest, in particular nanoscale semiconductor structures and devices [1][2]. In order to obtain high chip density, low power dissipation, and high speed for devices [3], the reduction of the gate oxide thickness (to around 1 nm) is necessary [4]. The ultra-thin oxide leads to a very large electric field at the SiO_2/Si interface. This results in a narrow and deep potential well at the semiconductor-insulator interface. According to quantum-mechanics (QM), electrons are now confined in such a potential well and then quantized to many discrete energy levels consequently force the motion of the electron in the direction perpendicular to the

silicon-insulator interface [5][6]. Since the quantum effect becomes noticeable in the deep-submicron devices and a mere classical description of the physics is not sufficient for an accurate calculation of the inversion-layer charge, in order to understand the characteristics of a nanoscale device, it is important to take quantum mechanical effects into account.

In principle, the Schrödinger-Poisson (SP) equations are the most accurate way to handle the problem of the inversion-layer charge density, but it is not suitable for engineering applications especially for the two- and three-dimensional cases. This is not only because it is computationally expensive but also because it is difficult to generalize to the multi-dimensional case (e.g. how to deal with the boundary condition in the 3-D case). Thus it is important to find a method which can produce a result similar to the quantum mechanically calculated one but requires only about the same computation cost as that of the classical calculation. Over the last two decades, various quantum mechanical correction methods are proposed. Among these approaches, the effective potential has the easiest numerical computation, but is too sensitive to the fitted parameter. The value usually used is 5 Å. Is the value exact? It is suspect. So determination of this parameter is an important issue.

1.2 Motivation

There are several approaches have been proposed to replace solving Schrödinger equation to include the quantum effects. And accuracy is highly believable. However, computation of algorism is also time-consuming. The effective potential Ferry proposed has been advanced which has the advantages of easy numerical implementation and almost guaranteed convergence. And this approach are widely used and compared with other models [7][8][9][10]. We calibrate effective potential method by the results from SP equations to determine the suitable standard deviation of the wave packet, a parameter in the effective potential formula. Value of the variable people usually use is 0.5 nm. However, result from effective potential approach is quite sensitive to the parameter. Different applied voltage, thickness of oxide, doping and other conditions will cause different values of the parameter. In order to choose better value of this parameter in simulation with various conditions. The objective of this thesis is to model the correlation between the parameter and other conditions of devices. In this thesis, we try to use statistical method to analysis the model of double-gate and SOI (Silicon-on-Insulator) MOSFETs (Metal-Oxide-Semiconductor Field-Effect Transistor). And these statistical approaches may be extended to more general structures or devices with other conditions.

1.3 Outline

There are six chapters in this thesis. In Chapter 2, classical drift-diffusion model and classical quantum mechanical transport model-SP will be introduced. Chapter 3 presents Ferry's effective potential, including its merit, shortcomings, and comparison between SP equations and Ferry's effective potential. Chapter 4 will present some statistical methods used in our analyzing. In the chapter 5, we will show the results and some discussion according to statistical analyzing results. Finally, we draw some conclusions and suggest the future works in Chapter 6.

Chapter 2

Classical and Quantum Mechanical Transport Models

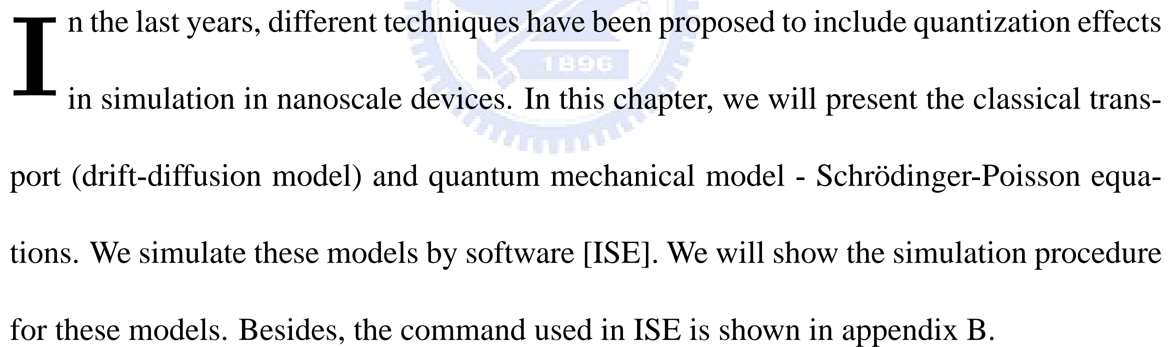

In the last years, different techniques have been proposed to include quantization effects in simulation in nanoscale devices. In this chapter, we will present the classical transport (drift-diffusion model) and quantum mechanical model - Schrödinger-Poisson equations. We simulate these models by software [ISE]. We will show the simulation procedure for these models. Besides, the command used in ISE is shown in appendix B.

2.1 Double-Gate and Silicon-On-Insulator Metal-Oxide-Semiconductor Field-Effect Transistors

Figure 2.1 and 2.2 show 3D and 2D schematic diagrams of double-gate MOSFET. Our simulation focuses on this structure. Figure 2.3 shows the energy band profile for a double-gate MOSFET. From Fig. 2.3, we can find there are potential wells in the direction perpendicular to the SiO_2/Si interface (Region1). Therefore, quantum effects are often considered in the direction which is confined [16]. In our simulation, we solve 2D Poisson equation and 2D electron current continuity equation [17]. All quantum mechanisms are considered in one-dimension (1D) along x direction. So, 1D Schrödinger equation is considered (in the direction x) [42][18]. Also, effective potential method presented in Chapter 3 is corrected in one-dimension.

For double-gate MOSFETs, if one of gate is increased thick enough and gates voltage equal to 0, then we can treat it as SOI (Fig. 2.4). Because of the thick oxide, there will be only one potential well.

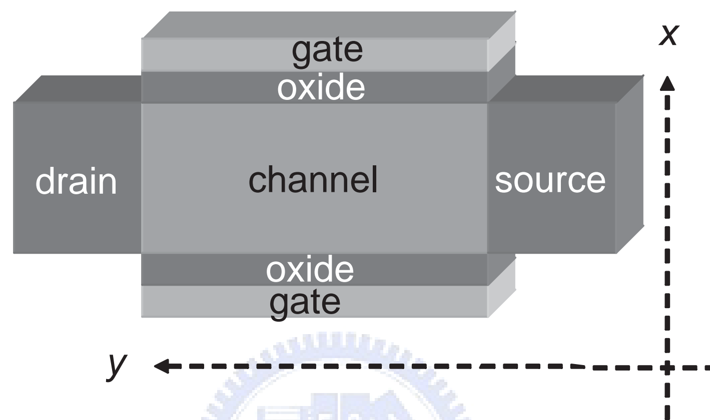

Figure 2.1: 3D double-gate schematic diagram. Scales in our simulation are following: thickness of oxide: 1 nm $\sim$ 2 nm; channel length: 20 nm $\sim$ 50 nm; thickness of film: about 0.5*channel length; doping of source and drain: 1e20 / cm^3; doping of film: 1e16 $\sim$ 5e17 / cm^3.

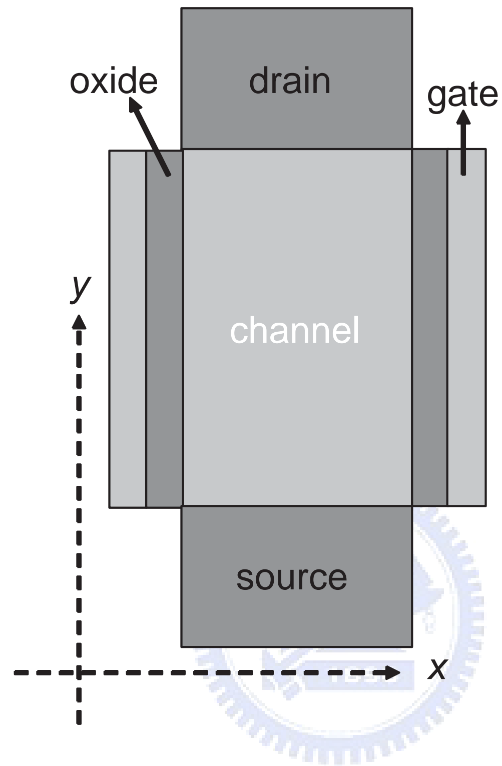

Figure 2.2: 2D double-gate schematic diagram. In our research, we consider 2D model except quantum correction. And quantum correction will be consider in x direction for each y.

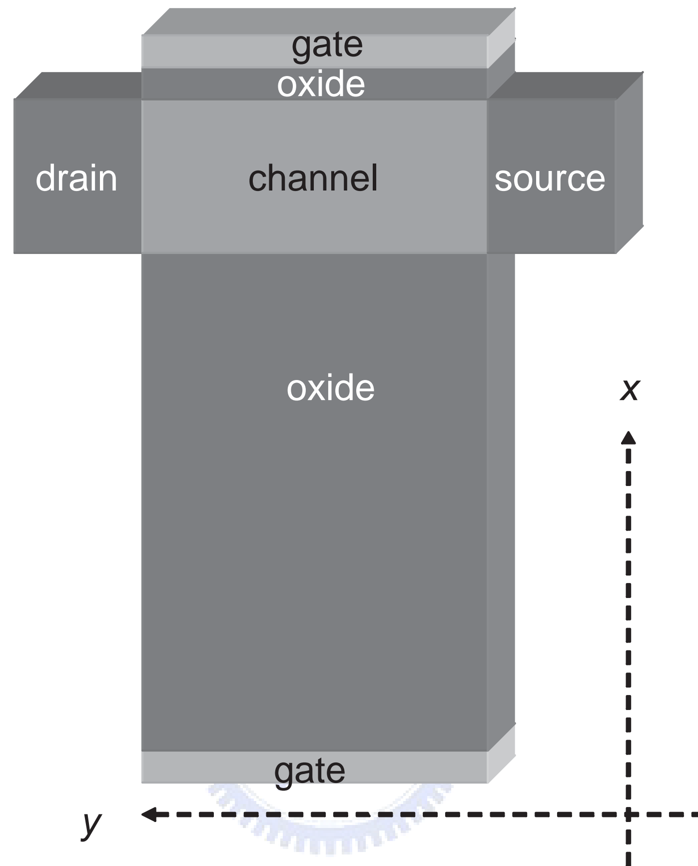

Figure 2.3: A energy band profile for the double-gate MOSFET in x direction. When voltage is applied on gate, there will be potential well (Region 1) if the oxide is thin enough. And then there will be quantum mechanism. E_{lim} is the energy level corresponding to the classical regime.

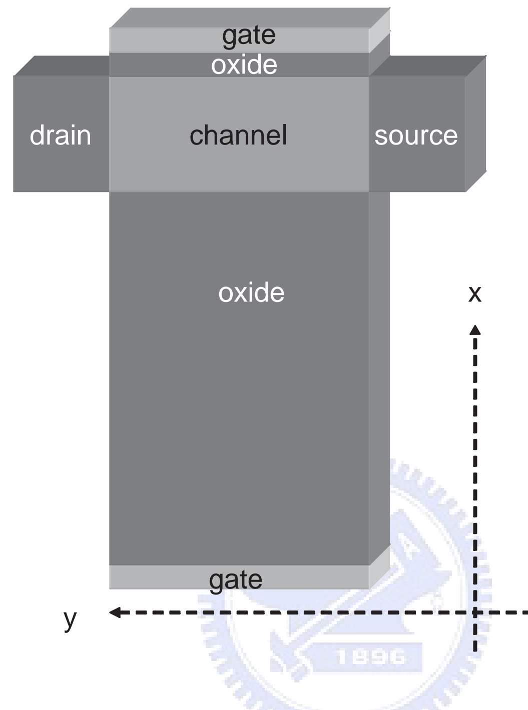

Figure 2.4: 3D SOI schematic diagram. If we let one oxide in double-gate MOSFET is thick enough, then it will become SOI structure. In this thesis, we set one of thickness of oxide is equal to 200 nm. And whose gate voltage is equal to 0 V. Other conditions are the same as Fig. 2.1.

2.2 Classical Drift-Diffusion Model

Essentially, the continuity equations and the Poisson equation have to be satisfied when we consider a device with nonequilibrium applied voltage

$$\triangle V = \frac{-\rho}{\varepsilon_s} = \frac{q}{\varepsilon_s}(n - p + D), \tag{2.1}$$

$$\frac{\partial n}{\partial t} = -\frac{1}{q}\nabla \cdot J_n + (G_n - R_n), \tag{2.2}$$

$$\frac{\partial p}{\partial t} = -\frac{1}{q}\nabla \cdot J_p + (G_p - R_p).$$

Eq. 2.1 is the Poisson equation, where V is potential, ρ is space charge density, ε_s is permittivity of silicon, n is electron density, p is hole density, and D is doping. Eq. 2.2 are continuity equations for electron and hole. Where J is current density, G and R are the generation term and recombination term, respectively [13].

In Poisson equation, Consider the Boltzmann relation. At thermal equilibrium the relation is given by

$$n = n_i \cdot exp(\frac{E_F - E_i}{kT}) \equiv n_i \cdot exp[\frac{q(V - \phi)}{kT}], \tag{2.3}$$

$$p = n_i \cdot exp(\frac{E_i - E_F}{kT}) \equiv n_i \cdot exp[\frac{q(\phi - V)}{kT}],$$

where ϕ is the potential corresponding to the Fermi level. When the voltage is applied, the relation becomes

$$n \equiv n_i \cdot exp[\frac{q(V - \phi_n)}{kT}], \tag{2.4}$$

$$p \equiv n_i \cdot exp[\frac{q(\phi_p - V)}{kT}],$$

where ϕ_n and ϕ_p are the quasi-Fermi levels for electrons and holes, respectively[12]. Therefore, Poisson equation becomes a function of potential and quasi Fermi-levels.

In continuity equations, assume $(G_n - R_n) = (G_p - R_p) = 0$ to simplify the equations. At the stable state, Eq. 2.2 becomes,

$$\nabla \cdot J_n = 0, \tag{2.5}$$

$$\nabla \cdot J_p = 0,$$

where

$$J_n = -q\mu_n n \nabla V + qD_n \nabla n, \tag{2.6}$$

$$J_p = -q\mu_p p \nabla V - qD_p \nabla p.$$

μ is mobility, D_n and D_p are diffusion coefficient for electron and hole.

Thus, we can get the potential, ϕ_n, and ϕ_p self-consistent by solving Eq. 2.1 and Eq. 2.5 repeatedly [12] [13] until the results are convergent [14][15]. The flow is shown as Fig. 2.5. Potential solved from these equations is classical, without considering any other mechanism.

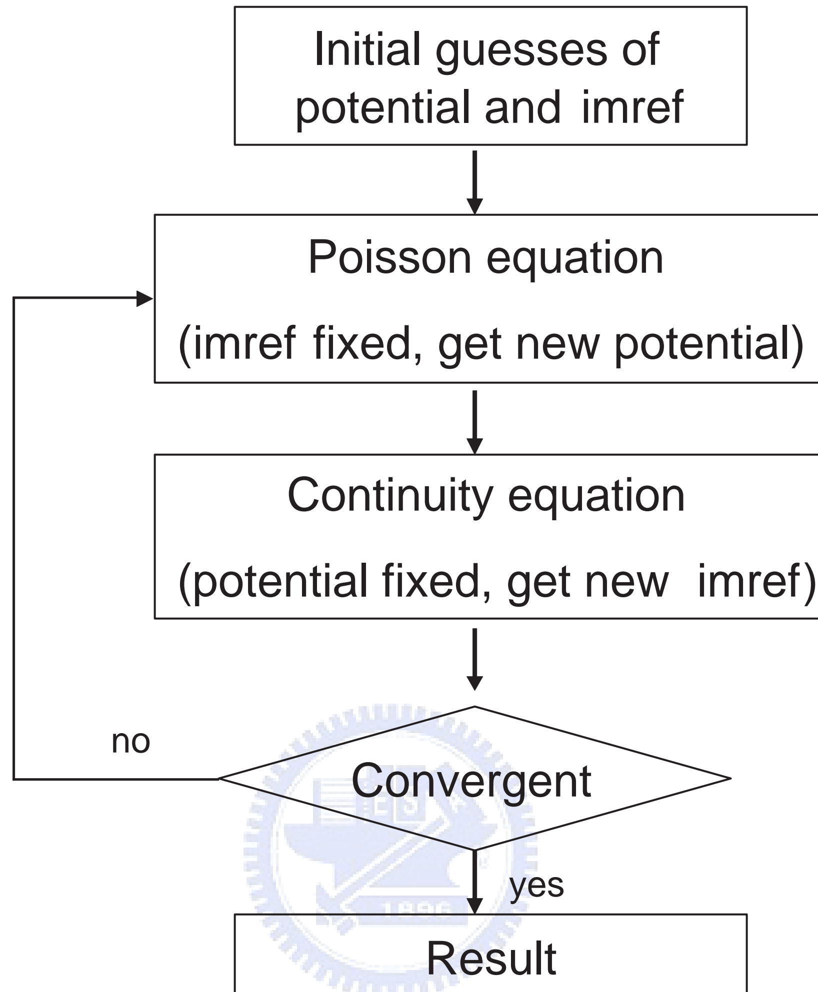

Figure 2.5: Flow chart of Poisson and Continuity equations in ISE (imref : quasi Fermi-levels). Here, potential and imref are unknown. First, we have initial guesses of both. Then we solve Poisson equation by given imref, and solve continuity equation by given potential. The algorithm will be terminated until potential and imref are convergent.

2.3 Quantum Mechanical Model

As the size of devices decreasing, quantum effects are included in simulation. In principle, the Schrödinger Equation have to be considered to describe the quantum effects. However, it is not efficient to solve Schrödinger Equation.

Conventionally, we consider the Schrödinger Equation to include the quantum effects. Following is 1-D Schrödinger Equation,

$$\Delta\psi(x) + \frac{2m^*}{\hbar^2}(E - V(x))\psi(x) = 0, \tag{2.7}$$

where ψ is the wave function, m^* is the effective mass, $\hbar$ is the Planck's constant, E is total energy, and V is potential. We can rewrite Eq. 2.7 as

$$[-\frac{\hbar^2}{2m^*} \cdot \frac{\partial^2}{\partial x^2} + V(x)]\psi(x) = E\psi(x). \tag{2.8}$$

From Eq. 2.8, we can know that the Schrödinger equation is an eigenvalue problem [29]. For given potential, we can get the subbands and wave function. Therefore, we can get charge density from subbands and wave function. Charge density calculated from Schrödinger equation includes quantum effects.

Based on the model described above, the charge density in the silicon layer is given by

$$\rho = -q(n - p + D).$$

For the p-type substrate, the hole density p is calculated by the Boltzmann approximation as before,

$$p = n_i \cdot exp[\frac{q(\phi_p - V)}{kT}],$$

whereas the electron density n_q contained in the subbands which are lower then E_{lim} and is given by [19][20][21][22][23][24]:

$$n_q = \frac{qV_T}{\pi\hbar^2}\sum_{k=1}^{2} g_k m_{jk} \sum_j ln[\frac{1 + exp(\frac{E_F - E_{jk}}{k_B T})}{1 + exp(\frac{E_F - E_{lim}}{k_B T})}]|\psi_{jk}|^2, \tag{2.9}$$

where E_F is the electron quasi-Fermi level, g_k is the degeneracy factor of the kth valley, ψ_{jk} is the wave function of the jth level in the kth valley and m_{jk} is the parallel effective mass in the kth valley. For (100) silicon, there is a two-fold degenerate pair of valleys with a larger effective mass (along the transverse direction), $m^* = 0.916m_0$,which comprises the lowest subband. The four-fold degenerate valleys have a lighter effective mass $m^* = 0.190m_0$, and lie higher in the subband ladder. E_{lim} is the energy level corresponding to the classical regime. Treating the density of states classically above the energy level E_{lim} limits the j and k values in the summation such $E_{jk} \leqq E_{lim}$ in the polycryatalline layer, classical treatment is usually assumed.

Under quantum effects, We get new charge density from Schrödinger equation. However, potential will change simultaneously. In order to get potential under quantum effects, we have to solve Poisson equation by using new charge density. Because potential and charge

density influence each other. So, we have to solve Poisson and Schrödinger equations repeatedly until convergent. Flow chart is shown as Fig. 2.6. Fig. 2.7, and Fig. 2.8 show the comparison of potential and carrier density between classical results and Schrödinger equation.

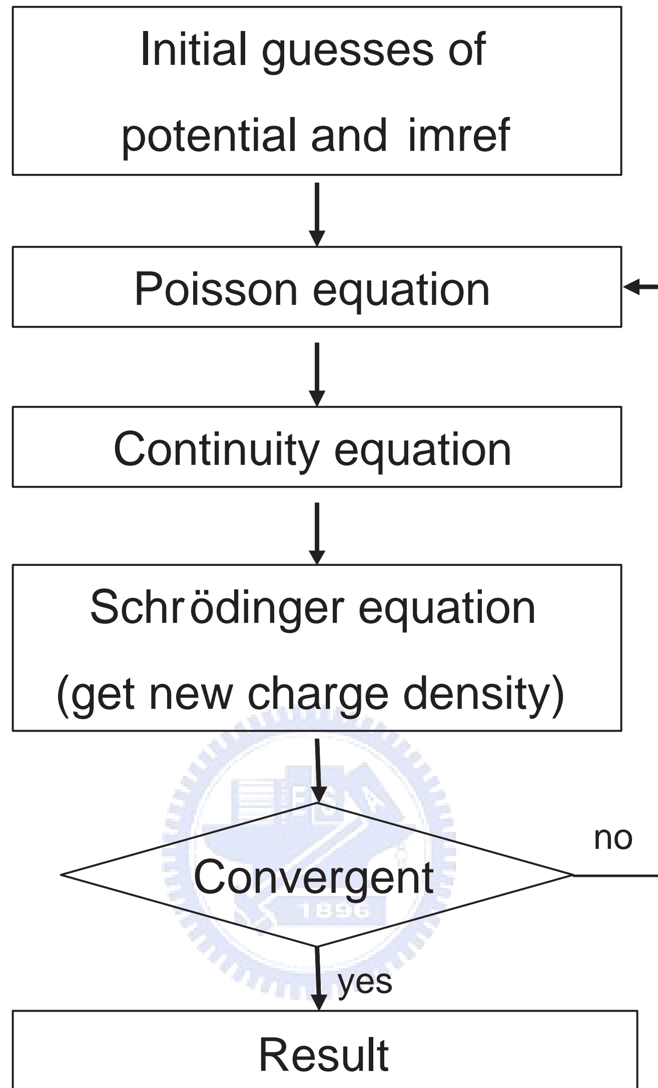

Figure 2.6: Flow chart of SP Equation in ISE. Steps of Poisson equation and continuity are the same as statement in Fig. 2.5. Here, we solve Schrödinger equation to correct carrier density to include quantum effect.

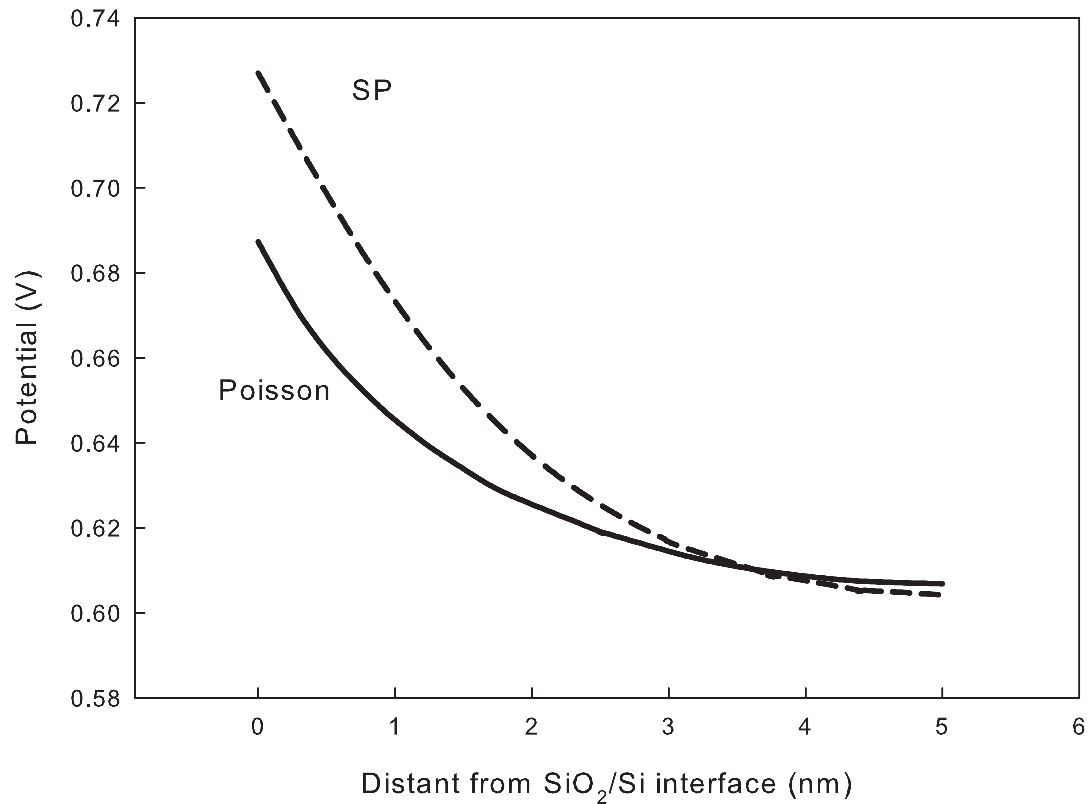

Figure 2.7: Solid line is potential solved from classical transport, dash line is potential solved by SP equations. Potential after quantum corrected is mush higher than classical. We only show half curves because of symmetry of double-gate MOSFET. tox = 1 nm, Vd = Vg = 0.6 V, tsi = 10 nm, Lg = 20 nm, N = 1e22 / m^3.

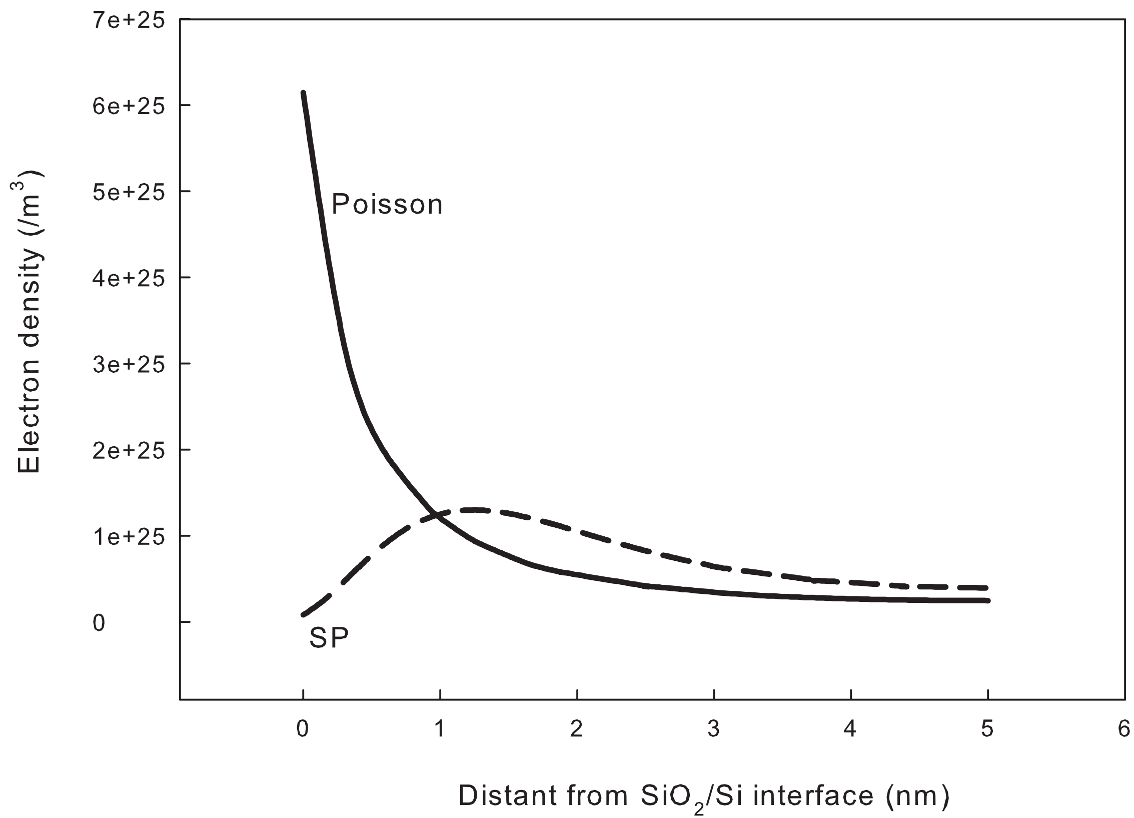

Figure 2.8: Solid line is electron density derived from classical transport; dash line is electron density derived from SP equations. The serious change nearby the SiO_2/Si interface arises from quantum effect. We only show half curves because of symmetry of double-gate MOSFET. tox = 1 nm, Vd = Vg = 0.6 V, tsi = 10 nm, Lg = 20 nm, N = 1e22 / m^3.

Chapter 3

Effective Potential

In an effective potential approach, one replaces the quantum distribution function by a classical distribution function with a modified potential. Thus, all the quantum effects in the system are modelled solely through the forces acting on the electron. Effective potentials are derived from a quantum mechanical description, either directly from the Schrödinger Equation or from a quantum kinetic transport equation for the Wigner function.

3.1 Fundamental of the Effective Potential

The idea of quantum potential is quite old and originates from the hydrodynamic formulation of quantum mechanics, first introduced by de Broglie and Madelung, and later developed by Bohm. one begins with the one particle Schrödinger Equation, of the form

$$i\hbar\frac{\partial\psi}{\partial t} = -(\frac{\hbar^2}{2m})\nabla^2\psi + V(x)\psi, \tag{3.1}$$

The wave function is written in complex form in terms of its amplitude $R(r,t)$ and phase $S(r,t)$ as

$$\psi(r,t) = R(r,t)exp[iS(r,t)/\hbar]. \tag{3.2}$$

When substituted back into the Schrödinger Equation, one arrives at the following coupled equations of motion for the density and phase

$$\frac{\partial R(r,t)}{\partial t} = -\frac{1}{2m}[R(r,t)\nabla^2 S(r,t) + 2\nabla R(r,t)\cdot\nabla S(r,t)], \tag{3.3}$$

$$\frac{\partial S(r,t)}{\partial t} = -[\frac{[\nabla(r,t)]^2}{2m} + V(r,t) - \frac{\hbar^2}{2m}\frac{\nabla^2 R(r,t)}{R(r,t)}]. \tag{3.4}$$

It is convenient to write $\rho(r,t) = R(r,t)^2$, where $\rho(r,t)$ is the probability density. One then obtains

$$\frac{\partial\rho(r,t)}{\partial t} + \nabla\cdot(\rho(r,t)\frac{1}{m}\nabla S(r,t)) = 0, \tag{3.5}$$

$$-\frac{\partial S(r,t)}{\partial t} = \frac{1}{2m}[\nabla S(r,t)]^2 + V(r,t) + Q(\rho,r,t). \tag{3.6}$$

In the classical limit the above equations are subject to a very simple interpretation. The function $S(r,t)$ is a solution of the Hamiltonian-Jacobi equation. If we consider an ensemble of particle trajectories which are solutions of the equations of motion, then from a well-known theorem of mechanics which states that if all of these trajectories are normal to any given surface of constant S, then they are normal to all surfaces of constant S, and $\nabla S(r,t)/m$ equals the velocity vector, v. Therefore, Eq. 3.5 can be rewritten as

$$\frac{\partial \rho(r,t)}{\partial t} + \nabla \cdot [\rho(r,t)v] = 0. \tag{3.7}$$

Since $\rho(r,t)$ is the probability density, ρv is the mean current of particles in the ensemble, and Eq. 3.7 simply expresses conservation of probability or of particles in the ensemble (continuity equation). Also note that Eq. 3.5, 3.6 arising from this so -called Madelung transformation to the Schrödinger Equation, have the form of classical hydrodynamic equations with the addition of an extra potential, often referred to as the quantum or Bohm potential, written as

$$Q = -\frac{\hbar^2}{2mR}\nabla^2 R \approx -\frac{\hbar^2}{2m\sqrt{n}}\frac{\partial^2 \sqrt{n}}{\partial x^2}, \tag{3.8}$$

where the density n is related to the probability density as $n(r,t) = N\rho(r,t) = NR(r,t)^2$, N being the total number number of particles in the ensemble. The Bohm potential essentially represents a field through which the particle interacts with itself. Once we know the field functions, one can calculate the force, os that, if one knows the initial position and momentum of the particle, one can calculate its entire trajectory. This effective potential

approach has been used, for example, in the study of wave packet tunnelling through [35], where the effect of the quantum potential is shown to lower or smoothen barriers and hence allows for the particles to leak through.

An alternative form of the quantum potential was proposed by Iafrate, Grubin and Ferry [30], who derived a form of the quantum potential based on moments of the Wigner-Boltamann equation.the kinetic equation describing the time evolution of the Wigner distribution function [31]. Their form for the quantum potential, based on moments of the Wigner distribution function in a pure state, and involving an expansion of order $O(\hbar^2)$, is given by

$$V_Q = -\frac{\hbar^2}{8m}\Delta(\ln n), \tag{3.9}$$

and is referred to as the Wigner potential, or as the density gradient correction. This form of the Wigner potential is better thought of as a quantum pressure term, which works to modify the actual potential to allow charge penetration into the classically forbidden regions.

Ferry and Zhou derived a form for a smooth quantum potential [36], based on the effective classical partition function of Feynman and Kleinert [28], by linearizing an equation for the equilibrium density matrix. The Feynman-Kleinert effective partition function involves a smoothed potential of the form

$$V_{a^2}(x) = \int \frac{dy}{\sqrt{2\pi a^2}} exp\{-\frac{(x-y)^2}{2a^2}\}V(y), \tag{3.10}$$

where V is the classical potential energy, $a^2 \propto \beta\hbar^2/m$, $\beta = 1/T$ is the inverse temperature, and m is the particle mass. The Ferry-Zhou effective stress represents the difference between the smoothed and the local quantum potential $\hbar^2\nabla^2 n/8mn + V$, where n is the particle density. Their smoothing function is of the form $exp(-(x-y)^2/2a^2)/|x-y|$. Note that the off-diagonal entries in the stress tensor are neglected in [36].

3.2 Ferry's Effective Potential Approach

In analogy to the smoothed potential representations discussed above for the quantum hydrodynamic models, it is desirable to define a smooth quantum potential for use in quantum particle-based simulations. Ferry [33] has suggested an effective potential that emerges from the wave packet description of particle motion, where the extent of the wave packet spread is obtained from the range of wavevectors in the thermal-distribution function. This form for the effective potential allows one to build in certain quantum effects that primarily arise from the non-zero size of the electron wave packet. One arrives at the final result by noting that the potential, in an inhomogeneous system enters the Hamiltonian as [33]

$$H_\nu = \int V(\mathbf{r})n(\mathbf{r})d\mathbf{r} \tag{3.11}$$

Using the non-local form(wave packet description) for the charge leads to

$$
\begin{aligned}
V &= \int drV(r)\sum_i n_i(r) \\
&= \int drV(r)\sum_i \int dr' \exp(-\frac{|r-r'|^2}{\alpha^2})\delta(r'-r_i) \\
&= \sum_i \int dr\delta(r-r_i)\int dr'V(r')\exp(-\frac{|r-r'|^2}{\alpha^2})
\end{aligned}
\tag{3.12}
$$

where the summation over i is a summation over the carriers themselves. The term in the primed integration is now the effective potential, V_{eff}, and the finite size of the electron has been replaced by smoothing of the real potential. In essence, the effective potential, V_{eff}, is related to the potential obtained from the Poisson equation, through an integral smoothing relation

$$
V_{eff}(x) = \int V(x+y)G(y,a_0)dy \tag{3.13}
$$

where G is a Gaussian with the standard deviation a_0. In two dimensions, the formula becomes,

$$
V_{eff}(x,y) = \frac{1}{2\pi a_x a_y}\int\int V(x',y')exp[-\frac{(x-x')^2}{2a_x^2}-\frac{(y-y')^2}{2a_y^2}]dx'dy' \tag{3.14}
$$

where V is the actual potential, and $a_{x,y}$ are the standard deviations of the Gaussian wave packet [34][35][36]. The flow of computing the effective potential is shown as below. However, V_{eff} is quite sensitive to the standard deviation of the wave packet. Fig. 3.2 shows potential derived from Ferry's effective potential with various standard deviation

of wave packet. Fig. 3.3 shows carrier density derived from Ferry's effective potential. From these two figures, we can find that the influence of a is quite significant. So, the determination of its value is an important issue. We calibrate Ferry's effective potential by Schrödinger equation to determine the value of a. Fig. 3.4 shows the comparison between SP equations and Ferry's effective potential with five various values of a. Results from these two methods are closest when $a = 5$ under following condition: thickness of oxide = 20 nm, channel length = 40 nm, thickness of bulk = 24 nm, gate voltage = 0.9 V, and doping concentration = 5e+23 / m^3. Unfortunately, the results are not close anymore when we change the gate voltage from 0.9 V to 1.0 V and keep $a = 5$. See Fig. 3.5.

In terms of computation, Ferry's effective potential is a good approach, but not in terms of sensitivity.

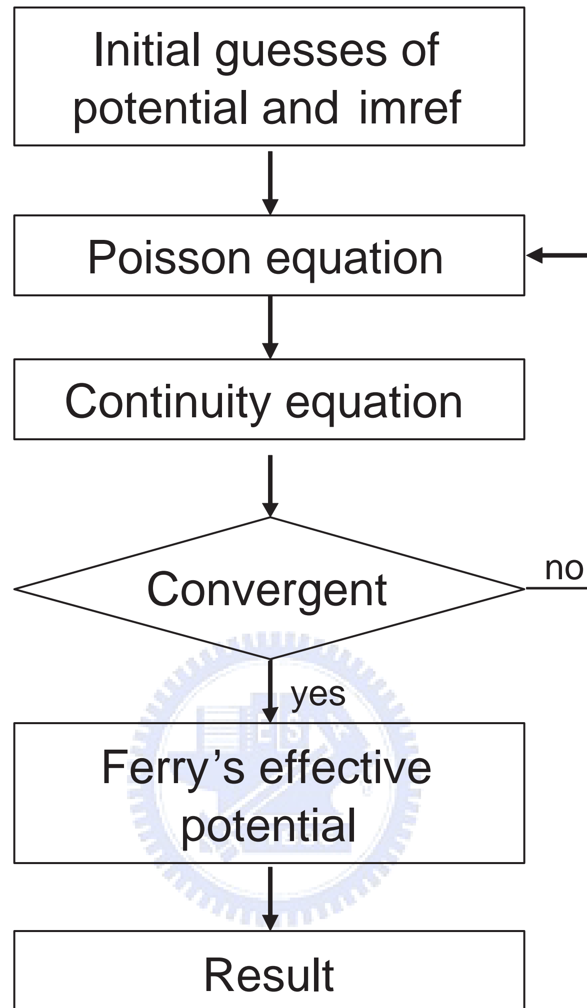

Figure 3.1: Flow chart of Ferry's effective potential. Ferry's effective potential formula don't need to solved in the loop. It just correct the potential which is convergent at last. Algorithm in the loop we simulate by ISE, and calculate Ferry's effective by using our own code.

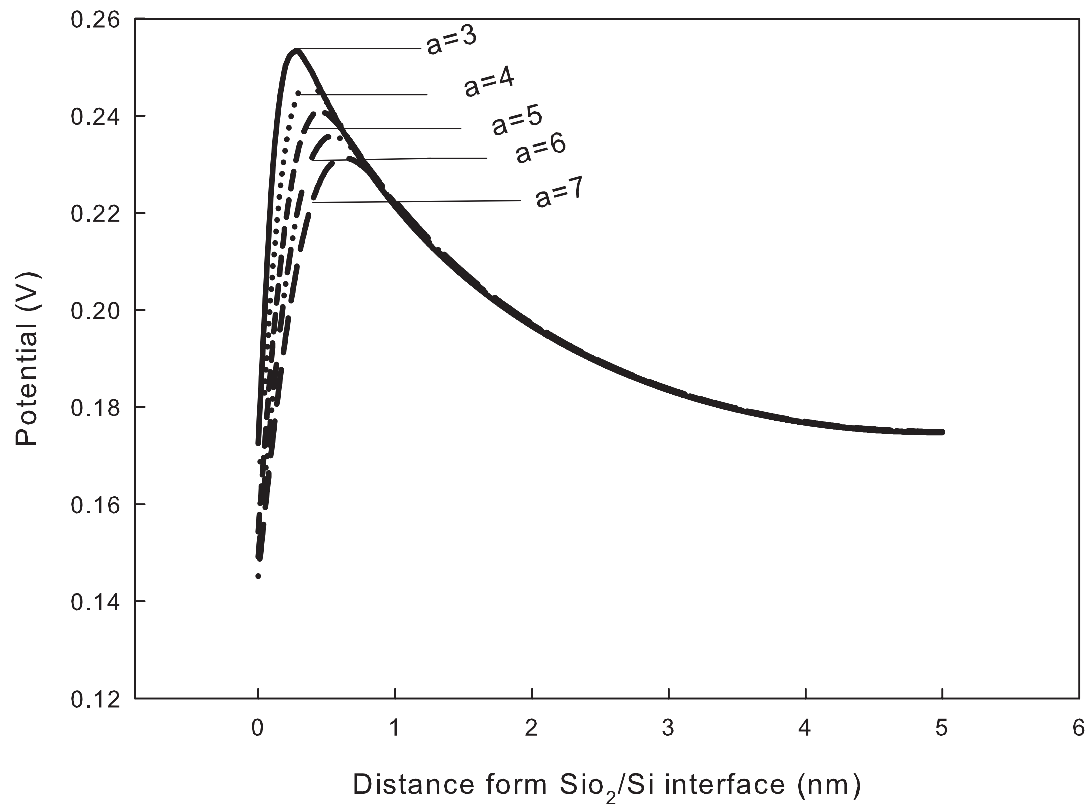

Figure 3.2: Ferry's effective potential of double-gate MOSFET in the direction normal to the semiconductor/oxide interface with various standard deviation of wave packet, a(Å). We only show half curves because of symmetry. Potential shift down as a is increasing. tox = 1 nm, Vd = Vg = 0.6 V, tsi = 10 nm, Lg = 20 nm, N = 1e22 / m^3.

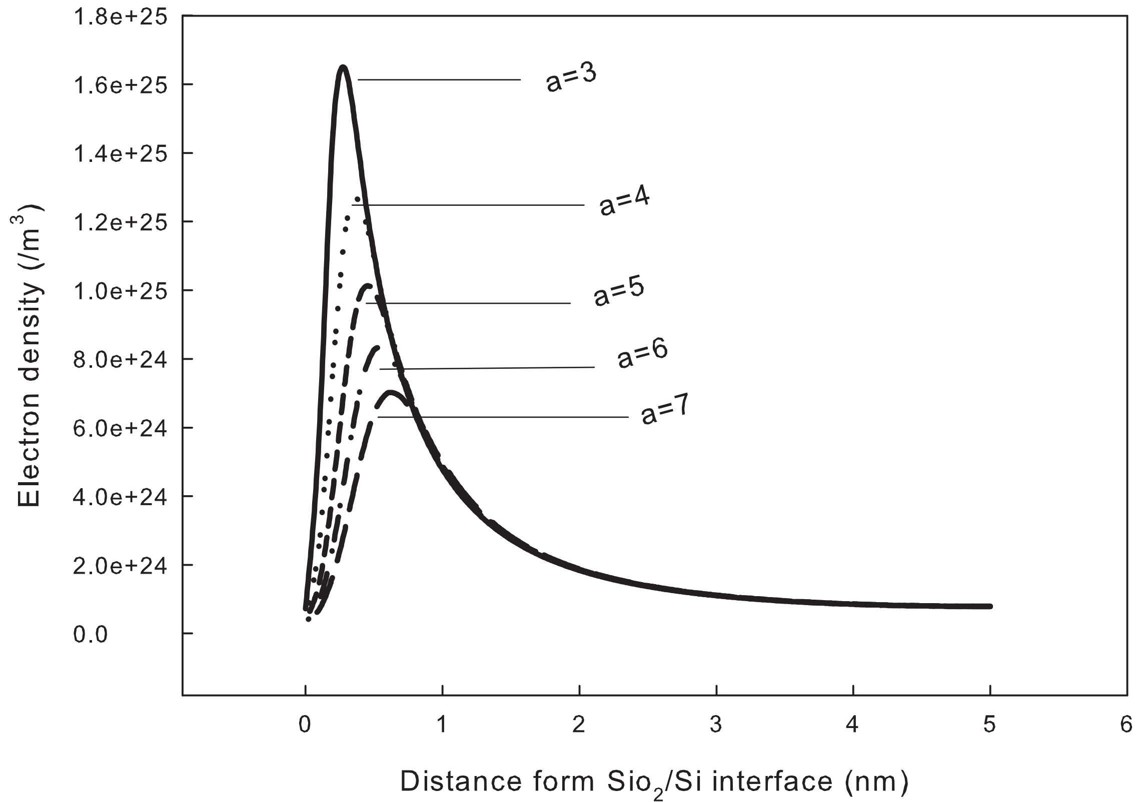

Figure 3.3: Electron density from Ferry's effective potential of double-gate MOSFET in the direction normal to the semiconductor/oxide interface with various standard deviation of wave packet, a(Å). We only show half curves because of symmetry. Carrier density shift down as a is increasing. tox = 1 nm, Vd = Vg = 0.6 V, tsi = 10 nm, Lg = 20 nm, N = 1e22 / m^3.

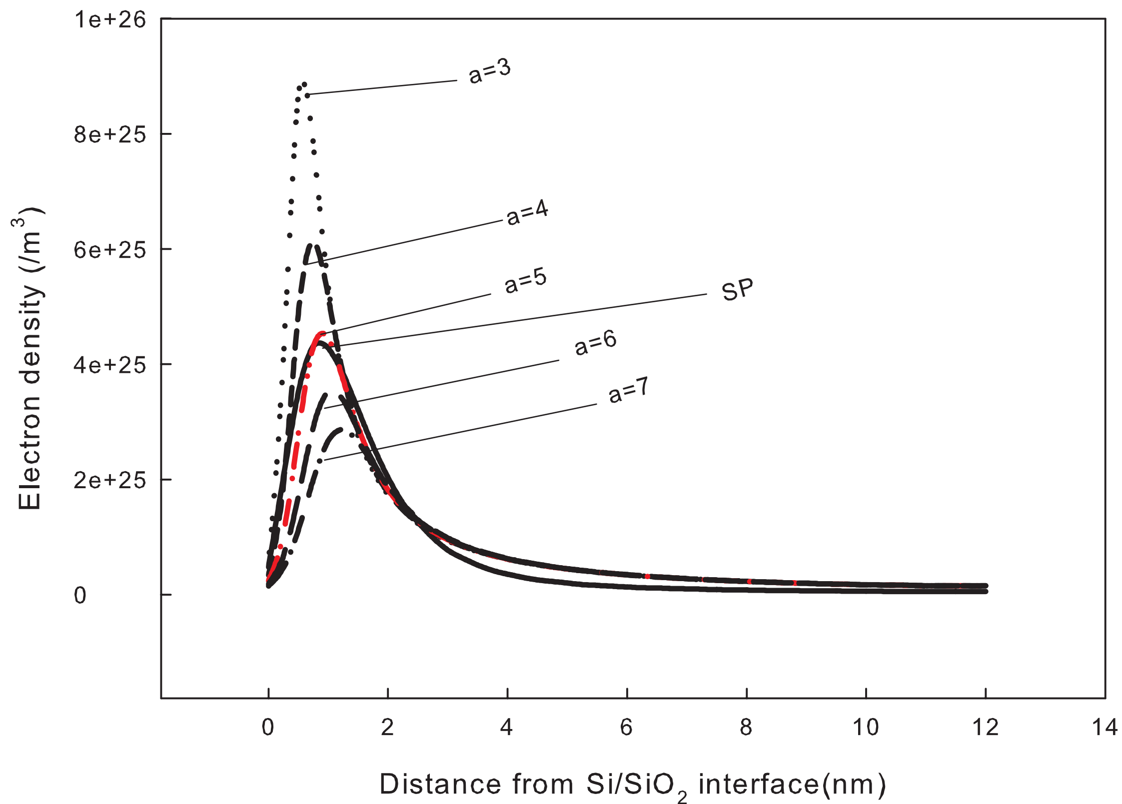

Figure 3.4: Calibration of electron density of Ferry's effective potential by SP equations - I. We only show half curves because of symmetry. (with $tox = 1$ nm, $Lg = 40$ nm, $tsi = 24$ nm, $Vg = 0.9$ V, N = 5e+23 / m^3). We set a = 3, 4, 5, 6, 7 Åto solve carrier density by effective potential. Result is the most close to the result form SP equations when a = 5 Å.

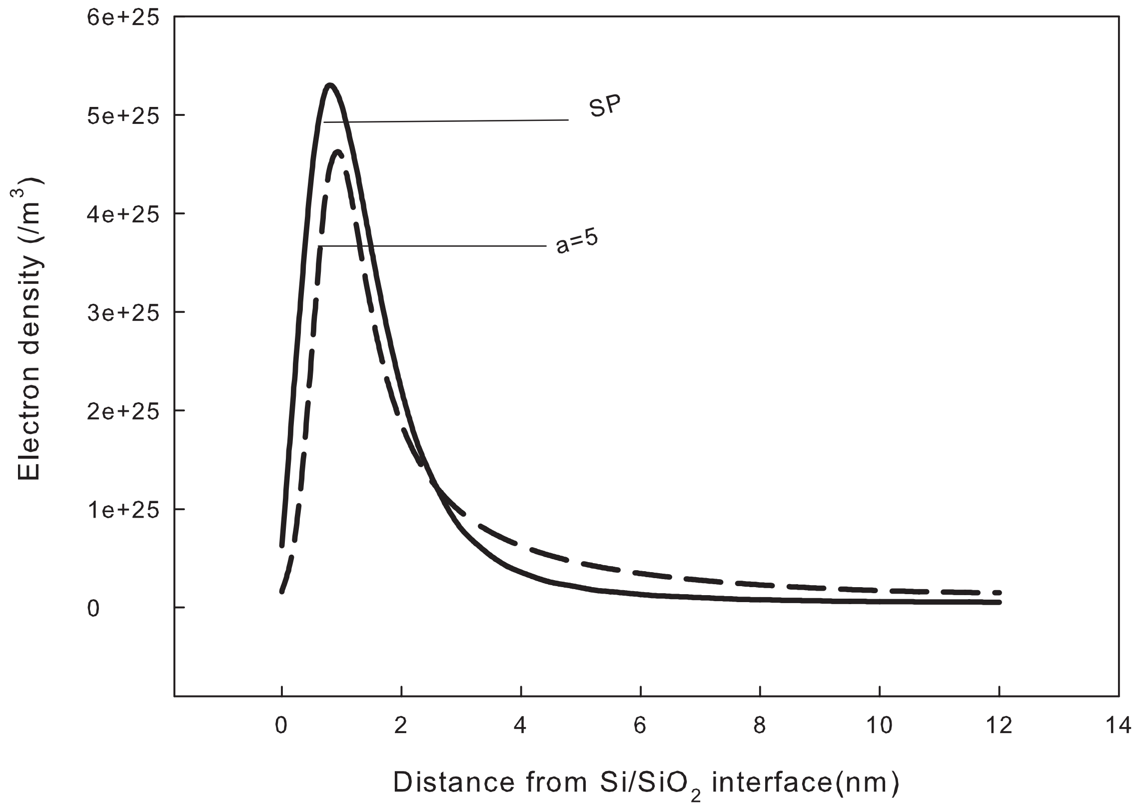

Figure 3.5: Calibration of electron density of Ferry's effective potential by SP equations - II. We only show half curves because of symmetry. (with $tox = 1$ nm, $Lg = 40$ nm, $tsi = 24$ nm, $Vg = 0.9$ V, $N = 5e + 23 \,/\, m^3$). Result from effective is not close to result from SP equations if we set $Vg = 1$ V and keep a = 5 Å.

Chapter 4

The Linear Regression

Most studies and experiments, scientific or industrial, large scale or small, produce data whose analysis is the ultimate object of the endeavor. Statistics is a powerful tool. Regression analysis is a statistical technique for investigating and modelling the relationship between variables. Applications of regression are numerous and occur in almost every field. It is the most important step in our analyzing. Besides regression analysis, there are several statistical methods to assist us in model establishing and checking. In this chapter, we will present statistical approaches will be used in our discussion. Following, we will present scattering plot, multiple linear regression, residual analysis and power transformation.

4.1 Scattering Plot

Scattering Plot is an important tool in statistical analysis. We can approximately know how the correlation between variables before doing further statistical analysis. For example, Fig. 4.1 shows population of U.S.A. from 1790 to 1990. The graph suggest the possibility of fitting a quadratic or exponential trend [37]. Of course, scattering plot is a important basis in statistical analysis.

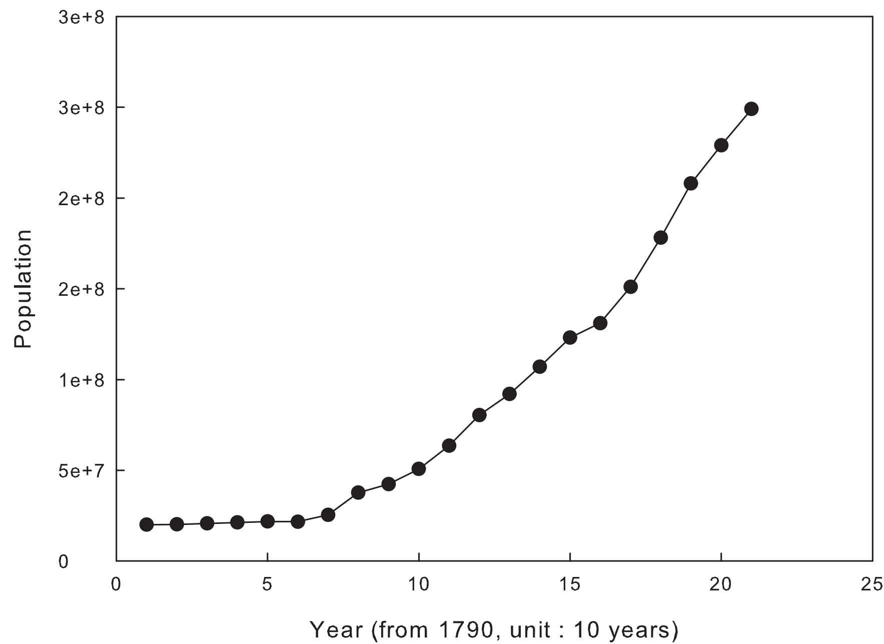

Figure 4.1: Population of the U.S.A at ten-year intervals, 1790-1990. From figure, we find that population increasing as years increasing. And it appears quadratic or exponential trend.

4.2 Multiple Linear Regression

4.2.1 Model Expression

A regression model that involves more than on regressor variables is called a multiple regression model. Simple linear regression model is a special case of multiple linear regression with only one regressor variables.

In general, the response y may be related to k regressor or predictor variables. The model

$$y = \beta_0 + \beta_1 x_1 + \beta_2 x_2 + \cdots + \beta_k x_k + \varepsilon, \tag{4.1}$$

is so-called a multiple linear regression model with k regressors. The parameters $\beta_j, j = 0, 1, \ldots, k$ are called the regression coefficients. This model describes a hyperplane in the k dimensional space of the regressor variables x_j. The parameter β_j represents the expected change in the response y per unit change in x_j when all of the remaining regressor variables $x_i (i \neq j)$ are held constant. For the reason the parameters $\beta_j, j = 0, 1, \ldots, k$, are often called partial regression coefficients.

Multiple linear regression models are often used as empirical models or approximating functions. That is, the true functional relationship between y and $x_1, x_2, \ldots, x_k$ is unknown, but over certain ranges of the regressor variables the linear regression model is an adequate approximation to the true unknown function [38].

4.2.2 Estimation of The Model Parameters

The method of least squares can be used to estimate the regression coefficients in Eq. 4.1. Suppose that $n > k$ observations are available, and let y_i denote the ith observed response and x_{ij} denote the ith observation or level of regressor x_j. We assume that the error term ε in the model has $E(\varepsilon) = 0, Var(\varepsilon) = \sigma^2$, and that the errors are uncorrelated. Furthermore, we assume that the regressor variables $x_1, x_2, \dots, x_k$ are fixed variables, measured without error.

We may write the sample regression model corresponding to Eq. 4.1 as

$$\begin{aligned} y_i &= \beta_0 + \beta_1 x_{i1} + \beta_2 x_{i2} + \cdots + \beta_k x_{ik} + \varepsilon_i \\ &= \beta_0 + \sum_{j=1}^{k} \beta_j x_{ij} + \varepsilon_i \quad , \\ i &= 1, 2, \dots, k. \end{aligned} \tag{4.2}$$

The least-squares function is

$$\begin{aligned} S(\beta_0, \beta_1, \dots, \beta_k) &= \sum_{i}^{n} \varepsilon_i^2 \\ &= \sum_{i}^{n} (y_i - \beta_0 - \sum_{j=1}^{k} \beta_j x_{ij})^2. \end{aligned} \tag{4.3}$$

The function S must be minimized with respect to $\beta_0, \beta_1, \dots \beta_k$. The least-squares estimators of $\beta_0, \beta_1, \dots \beta_k$ must satisfy

$$\frac{\partial S}{\partial \beta_0}|_{\hat{\beta}_0, \hat{\beta}_1, \dots, \hat{\beta}_k} = -2 \sum_{i=1}^{n} (y_i - \hat{\beta}_0 - \sum_{j=1}^{k} \hat{\beta}_j x_{ij}) = 0 \quad , \tag{4.4}$$

and

$$\frac{\partial S}{\partial \beta_j}|_{\hat{\beta}_0,\hat{\beta}_1,\ldots,\hat{\beta}_k} = -2\sum_{i=1}^{n}(y_i - \hat{\beta}_0 - \sum_{j=1}^{k}\hat{\beta}_j x_{ij})x_{ij} = 0 \quad , \tag{4.5}$$

$$j = 1, 2, \ldots, k.$$

Simplifying Eq. 4.4 and Eq. 4.5, we obtain the least-squares normal equations

$$\begin{aligned} n\hat{\beta}_0 + \hat{\beta}_1\sum_{i=1}^{n}x_{i1} + \hat{\beta}_2\sum_{i=1}^{n}x_{i2} + \cdots + \hat{\beta}_k\sum_{i=1}^{n}x_{ik} &= \sum_{i=1}^{n}y_i, \\ \hat{\beta}_0\sum_{i=1}^{n}x_{i1} + \hat{\beta}_1\sum_{i=1}^{n}x_{i1}^2 + \hat{\beta}_2\sum_{i=1}^{n}x_{i1}x_{i2} + \cdots + \hat{\beta}_k\sum_{i=1}^{n}x_{i1}x_{ik} &= \sum_{i=1}^{n}x_{i1}y_i, \\ &\vdots \\ \hat{\beta}_0\sum_{i=1}^{n}x_{ik} + \hat{\beta}_1\sum_{i=1}^{n}x_{ik}x_{i1} + \hat{\beta}_2\sum_{i=1}^{n}x_{ik}x_{i2} + \cdots + \hat{\beta}_k\sum_{i=1}^{n}x_{ik}^2 &= \sum_{i=1}^{n}x_{ik}y_i. \end{aligned} \tag{4.6}$$

Note that there are $p = k + 1$ normal equations, one for each of the unknown regression coefficients. The solution to the normal equations will be the least-squares estimators $\hat{\beta}_0, \hat{\beta}_1, \ldots \hat{\beta}_k$.

It is more convenient to deal with multiple regression models if they are expressed in matrix notation. This allows a very compact display of the model, data. and results. In matrix notation, the model given by Eq. 4.2 is

$$y = X\beta + \varepsilon, \tag{4.7}$$

where

$$y = \begin{pmatrix} y_1 \\ y_2 \\ \vdots \\ y_n \end{pmatrix}, \qquad X = \begin{pmatrix} 1 & x_{11} & x_{12} & \cdots & x_{1k} \\ 1 & x_{21} & x_{22} & \cdots & x_{2k} \\ \vdots & \vdots & \vdots & \vdots & \vdots \\ 1 & x_{n1} & x_{n2} & \cdots & x_{nk} \end{pmatrix}$$

and

$$\beta = \begin{pmatrix} \beta_0 \\ \beta_1 \\ \vdots \\ \beta_k, \end{pmatrix}, \qquad \varepsilon = \begin{pmatrix} \epsilon_1 \\ \epsilon_2 \\ \vdots \\ \epsilon_n \end{pmatrix}. \tag{4.8}$$

In general, y is an $n \times 1$ vector of the observations, X is an $n \times p$ matrix of the levels of the regressor variables, β is a $p \times 1$ vector of the regression coefficients, and ε is an $n \times 1$ vector of random errors. We wish to find the vector of least-squares estimators, $\hat{\beta}$, that minimizes

$$S(\beta) = \sum_{i}^{n} \varepsilon_i^2 = \varepsilon'\varepsilon = (y - X\beta)'(y - X\beta). \tag{4.9}$$

Note that $S(\beta)$ may be expressed as

$$\begin{aligned} S(\beta) &= y'y - \beta'X'y - y'X\beta + \beta'X'X\beta \qquad (4.10) \\ &= y'y - 2\beta'X'y + \beta'X'X\beta. \end{aligned}$$

since $\beta' X' y$ is a 1×1 matrix, or a scalar, and its transpose $(\beta' X' y)' = y' X \beta$ is the same scalar. The least-squares estimators must satisfy

$$\frac{\partial S}{\partial \beta}|_{\hat{\beta}} = -2X'y + 2X'X\hat{\beta} = 0, \tag{4.11}$$

which simplifies to

$$X'X\hat{\beta} = X'y. \tag{4.12}$$

Eq. 4.12 are the least-squares normal equations. They are the matrix analogue of the scalar presentation in Eq. 4.6.

To solve the normal equations, multiply both sides of Eq. 4.12 by the inverse of X'X. Thus, the least-squares estimator of β is

$$\hat{\beta} = (X'X)^{-1} X'y, \tag{4.13}$$

provided that the inverse matrix $(X'X)^{-1}$ exists. The $(X'X)^{-1}$ matrix will always exist if the regressors are linearly independent, that is, if no column of the X matrix is a linear combination of the other columns.

The fitted regression model corresponding to the levels of the regressor variables $x' = [1, x_1, x_1, \ldots, x_k]$ is

$$\hat{y} = x'\hat{\beta} = \hat{\beta}_0 + \sum_{j=1}^{k} \hat{\beta}_j x_j. \tag{4.14}$$

The difference between the observed value y_i and the corresponding fitted value $\hat{y}_i$ is the residual

$$e_i = y_i - \hat{y}_i. \tag{4.15}$$

We may develop and estimator of σ^2 from the residual sum of squares

$$SS_{Ees} \sum_{i=1}^{n} (y_i - \hat{y}_i)^2 = \sum_{i=1}^{n} e_i^2 = y'y - \hat{\beta}' X' y. \tag{4.16}$$

The residual sum of squares has $n - p$ degrees of freedom associated with it since p parameters are estimated in the regression model. The residual mean square is

$$MS_{Res} = \frac{SS_{Res}}{n - p}, \tag{4.17}$$

the expected value of MS_{Res} is σ^2, so an unbiased estimator of σ^2 is given by

$$\sigma^2 = MS_{Res}. \tag{4.18}$$

4.2.3 Hypothesis Testing in Multiple Linear Regression

The test for significance of regression is a test to determine if there is a linear relationship between the response y and any of the regressor variables $x_1, x_2, \ldots, x_k$. This procedure is often thought of as an overall or global test of model adequacy. The appropriate hypotheses are

$$H_0 : \beta_0 = \beta_1 = \cdots = \beta_k = 0,$$

$$H_1 : \beta_j \neq 0, \text{ for at least one } j.$$

Rejection of this mull hypothesis implies that at least one of the regressors $x_1, x_2, \ldots, x_k$ contributes significantly to the model.

The procedure is a generalization of the analysis of variance (ANOVA). The total sum of squares SS_T is partitioned into a sum of squares due to regression, SS_R, and a residual sum of squares, SS_{Res}. Thus

$$SS_T = SS_R + SS_{Res}.$$

If the null hypothesis is true, then SS_R/σ^2 follows a χ^2_k distribution, which has the same number of degrees of freedom as number of regressor variables in the model. Besides, $SS_{Res}/\sigma^2 \sim \chi^2_{n-k-1}$ and that SS_{Res} and SS_R are independent. By the definition of an F statistic,

$$F_0 = \frac{SS_R/k}{SS_{Res}/(n-k-1)} = \frac{MS_R}{MS_{Res}}, \tag{4.19}$$

follows the $F_{k,n-k-1}$ distribution. Therefore, to test the hypothesis $H_0 : \beta_0 = \beta_1 = \cdots = \beta_k = 0$, compute the test statistic F_0 and reject H_0 if

$$F_0 > F_{\alpha,k,n-k-1}, \tag{4.20}$$

where α is significant level. The test procedure is usually summarized in an ANOVA table as follow:

Once we have determined that at least one of the regressors is important, a logical question

Source of Variation	Sum of Squares	Degrees of Freedom	Mean Square	F_0
Regression	SS_R	k	MS_R	$\frac{MS_R}{MS_{Res}}$
Residual	SS_{Res}	$n-k-1$	MS_{Res}	
Total	SS_T	$n-1$		

Table 4.1: ANOVA table for significance of regression in multiple regression. SS_R, SS_{RES}, and SS_T are square error. From Degrees of Freedom, we can know there are n cases and k parameters have to be estimated. Value of F_0 is the criterion to judge whether the model significant is.

becomes which one(s). Adding a variable to a regression model always causes the sum of squares for regression to increase and the residual sum of squares to decrease. We must decide whether the increase in the regression sum of squares is sufficient to warrant using the additional regressor in the model. The addition of a regressor also increases the variance of the fitted value $\hat{y}$, so we must be careful to include only regressors that are of real value in explaining the response. Furthermore, adding an unimportant regressor may increase the residual mean square, which may decrease the usefulness of the model.

The hypotheses for testing the significance of any individual regression coefficient, such as β_j, are

$$H_0 : \beta_j = 0,$$

$$H_1 : \beta_j \neq 0.$$

If $H_0 : \beta_j = 0$ is not rejected, then this indicates that the regressor x_j can be deleted from the model. The test statistic for this hypothesis is

$$t_0 = \frac{\hat{\beta}_j}{\sqrt{\hat{\sigma_2} C_{jj}}} = \frac{\hat{\beta}_j}{se(\hat{\beta}_j)}, \tag{4.21}$$

where C_{jj} is the diagonal element of $(X'X)^{-1}$ corresponding to β_j. The null hypothesis $H_0 : \beta_j = 0$ is rejected if $|t_0| > t_{\alpha/2,n-k-1}$. Note that this is really a partial or marginal test because the regression coefficient β_j depends on all of the other regressor variables $x_i (i \neq j)$ that are in the model. Thus, this is a test of the contribution of x_j given the other regressors in the model.

4.2.4 Variable Selection in Regression Analysis

Because evaluating all possible regressions can be burdensome computationally, various methods have been developed for evaluating only a small number of subset regression models by either add or deleting regressors one at a time. These methods are generally referred to as stepwise-type procedures. They can be classified into three broad categories: (1) forward selection, (2) backward elimination, and (3) stepwise regression, which is a popular combination of procedures 1 and 2.

(a) Forward Selection

This procedure begins with the assumption that there are no regressors in the model other than the intercept. An effort is made to find an optimal subset by inserting regressors into the model one at a time. The first regressor selected for entry into the equation is the one that has the largest simple correlation with the response variable y. Suppose that this regressor is x_1. This is also the regressor that will produce the largest value of the F statistic for testing significance of regression. This regressor is entered if the F statistic exceeds a preselected F value, say F_{IN}. The second regressor chosen for entry is the one that now has the largest correlation with y after adjusting for the effect of the first regressor entered (x_1) on y. We refer to these correlations as partial correlations. They are the simple correlations between the residuals from the regression $\hat{y} = \hat{\beta}_0 + \hat{\beta}_1 x_1$ and the residuals from the regressions of the other candidate regressors on x_1, say $\hat{x_j} = \hat{\alpha_{0j}} + \hat{\alpha_{aj}} x_1, j = 2, 3, \ldots, k$. Suppose that at step 2 the regressor with the highest partial correlation with y is x_2. This implies that the largest partial F-statistic is

$$F = \frac{SS_R(x_2|x_1)}{MS_{Res}(x_1, x_2)}. \tag{4.22}$$

If this F value exceeds F_{IN}, then x_2 is added to the model. In general, at each step the regressor having the highest partial correlation with y is added to the model if its partial F-statistic exceeds the preselected entry level F_{IN}. The procedure terminates either when the partial F-statistic at a particular step does not exceed F_{IN} or when the last candidate

regressor is added to the model.

(b) Backward Elimination

Backward elimination begins with a model that includes all k a candidate regressors. Then the partial F-statistic is computed for each regressor as if it were the last variable to enter the model. The smallest of these partial F-statistics is compared with a preselected value, F_{OUT}. If the smallest partial F value is less than F_{OUT}, that regressor is removed from the model. Now a regression model with $k-1$ regressors is fit, the partial F-statistics for this new model calculated, and the procedure repeated. The backward elimination algorithm terminates when the smallest partial F value is not less than the preselected cutoff value F_{OUT}.

(c) Stepwise Regression

The two procedure described above suggest a number of possible combinations. One of the most popular is the stepwise regression algorithm. Stepwise regression is a modification of forward selection in which at each step all regressors entered into the model previously are reassessed via their partial F-statistics. A regressor added at and earlier step nay now be redundant because of the relationships between it and regressors now in the equation. If the partial F-statistic for a variable is less than F_{OUT}, that variable is dropped from the model. Stepwise regression require two cut off values, F_{IN} and F_{OUT}. Some analysis prefer to

choose $F_{IN} = F_{OUT}$, although this is not necessary. Frequently we choose $F_{IN} > F_{OUT}$, making it relatively more difficult to add a regressor than to delete one.

Among the three selection procedures, stepwise selection is known to be the most effective and is therefore recommended for general use [38][39].

4.3 Residual Analysis

Graphical analysis of residuals is a very effective way to investigate the adequacy of the fit of a regression model and to check the underlying assumptions. In this section, we introduce and illustrate the basic residual plots [41].

4.3.1 Normal Probability Plot

A very simple method of checking the normality assumption is to construct a normal probability plot of the residuals. This is a graph designed so that the cumulative normal distribution will plot as a straight line. Let $e_{[1]} < e_{[2]} < \cdots < e_{[n]}$ be the residuals ranked in increasing order. If we plot $e_{[i]}$ against the cumulative probability $P_i = (i - \frac{1}{2})/n, i = 1, 2, \ldots, n$, on the normal probability plot, the resulting points should lie approximately on a straight line. Substantial departures from a straight line indicate that the distribution is not normal. Usually normal probability plots are constructed by plotting the ranked residual $e_{[i]}$ against the expected normal value $\Phi^{-1}[(i-\frac{1}{2})/n]$, where Φ denotes the standard normal cumulative

distribution. This follows from the fact that $E(e_{[i]}) \simeq \Phi^{-1}[(i - \frac{1}{2})/n]$.

4.3.2 Plot of Residuals against the Fitted Values

A plot of the residuals e_i versus the corresponding fitted values $\hat{y}_i$ is useful for detecting several common types of model inadequacies. If the scattering plot indicates that the residuals can be contained in a horizontal band, then there are no obvious model defects. Else if the plot has strange pattern , then we may try to transform the response variable to improve the model. The outward-opening funnel pattern implies that the variance is and increasing function of response value. A curved plot which is nonlinearity may mean that other regressor variables are need in the model. Transformations on the regressor or the response variable may also be helpful.

4.4 Power Transformation

Generally, transformation are used for three purposes: (1) stabilizing the response variance, (2) making the distribution of the response variable closer to the normal distribution, (3) improving the fit of the model to the data.

We often find that the power family (Eq. 4.23) of transformation is very useful. Box and Cox(1964) have shown how the transformation parameter λ may be estimated simultaneously with the other model parameters. The theory underlying their method uses the method of maximum likelihood.

$$f(y) = \begin{cases} \frac{y^\lambda - 1}{\lambda}, & \lambda \neq 0; \\ \ln y, & \lambda = 0. \end{cases} \tag{4.23}$$

Notice that we cannot select a value of λ by directly comparing the error sums of squares from analysis of y after transformation, because for each value of λ the error sum of squares is measured on a different scale.

In applying the Box-Cox method, we recommend using simple choices for λ, because the practical difference between $\lambda = 0.5$ and $\lambda = 0.58$ is likely to be small, but the square root transformation is much easier to interpret. Fig. 4.2 shows that Likelihood achieves maximum when $\lambda = -0.148$ and 95% confidence interval. By the reason above, we prefer choosing $\lambda = 0$ [40].

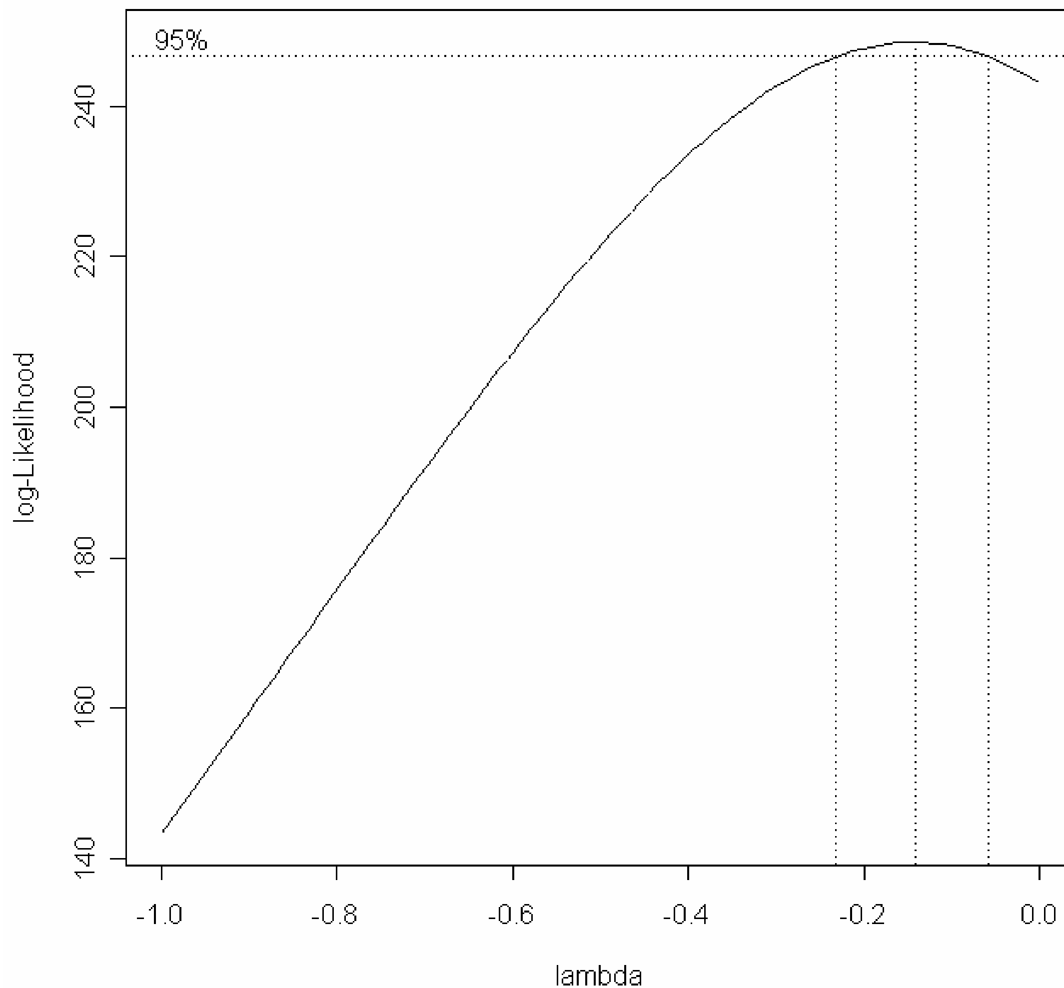

Figure 4.2: The Box-Cox likelihood plot. x axis is value of λ, and y axis is likelihood function. Likelihood achieves maximum when $\lambda = -0.148$. The three vertical dot line indicate 95% confidence interval. Plot by S-PLUS.

Chapter 5

Results and Discussion

In the chapter, the simulation results are shown and the statistical results are also discussed. First of all, the calibration of Ferry's effective potential is introduced. We use least square error to determine value of standard deviation of wave packet. Second, range of variables we simulation and some constraint of variables will be stated. There is collinearity phenomenon because of these constraint. At last, results will be shown and we will discuss according to the results, including double-gate and SOI MOSFET. And models will be presented. We will also compare the statistical results with simulation results.

5.1 Calibration of Ferry's Effective Potential

Figure 5.1 shows the classical carrier density and carrier density corrected by SP equations. Fig. 5.2 shows carrier density from Ferry's effective potential with various standard deviation of wave packet. However, different values of a cause quite different results. We calibrate the value by comparing with result from Schrödinger equation. We determine the value of standard deviation of wave packet by achieving the criterion

$$\min_{a} \sum_{i=1}^{n} (n_{SP,i} - n_{EP,a,i})^2 \tag{5.1}$$

where $n_{SP,i}$ is carrier density of mesh i from SP equations, $n_{EP,a,i}$ is carrier density of mesh i from Ferry's effective potential.

For every condition of device, we determine a value of a by above criterion. In simulation procedure, we scan a from 0 to 20 with step 0.001, unit is Å. Range of a we get is about in the range from four to twelve. The value generally used is 5 Å, and it is during the interval.

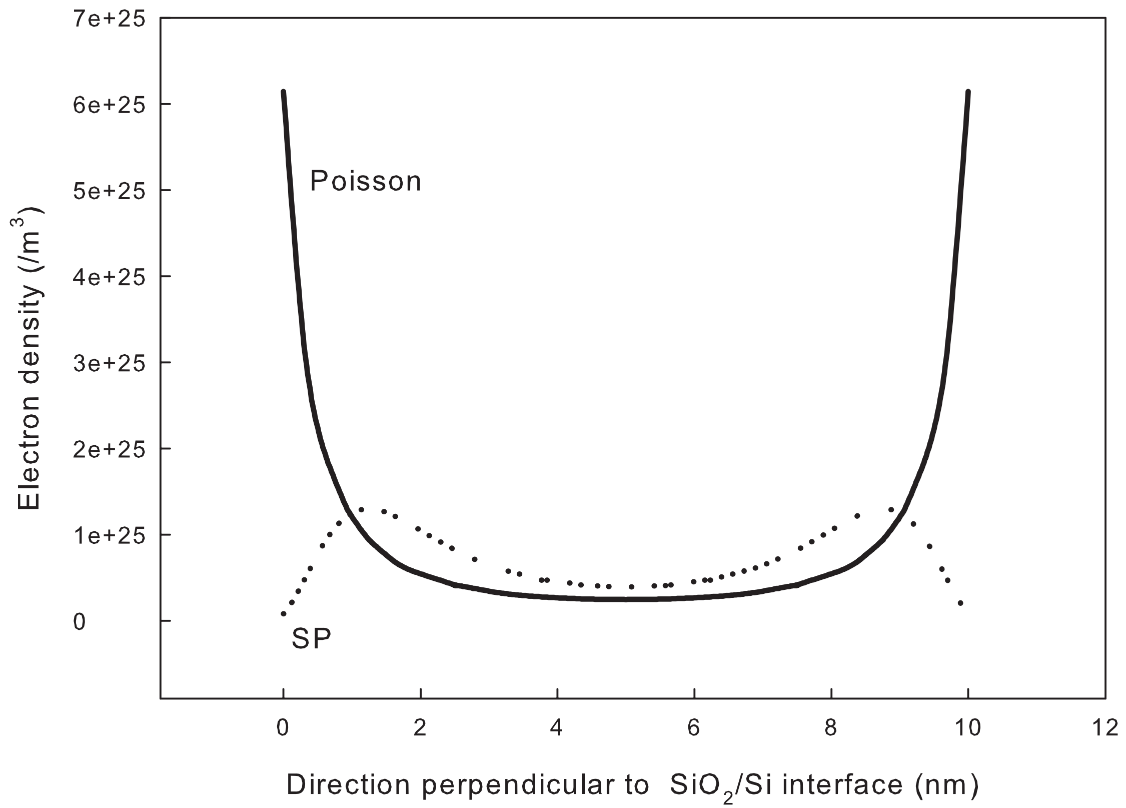

Figure 5.1: Classical electron density and electron density corrected by SP equations of double-gate MOSFET. And we treat result from SP equations as reference includes quantum effect.

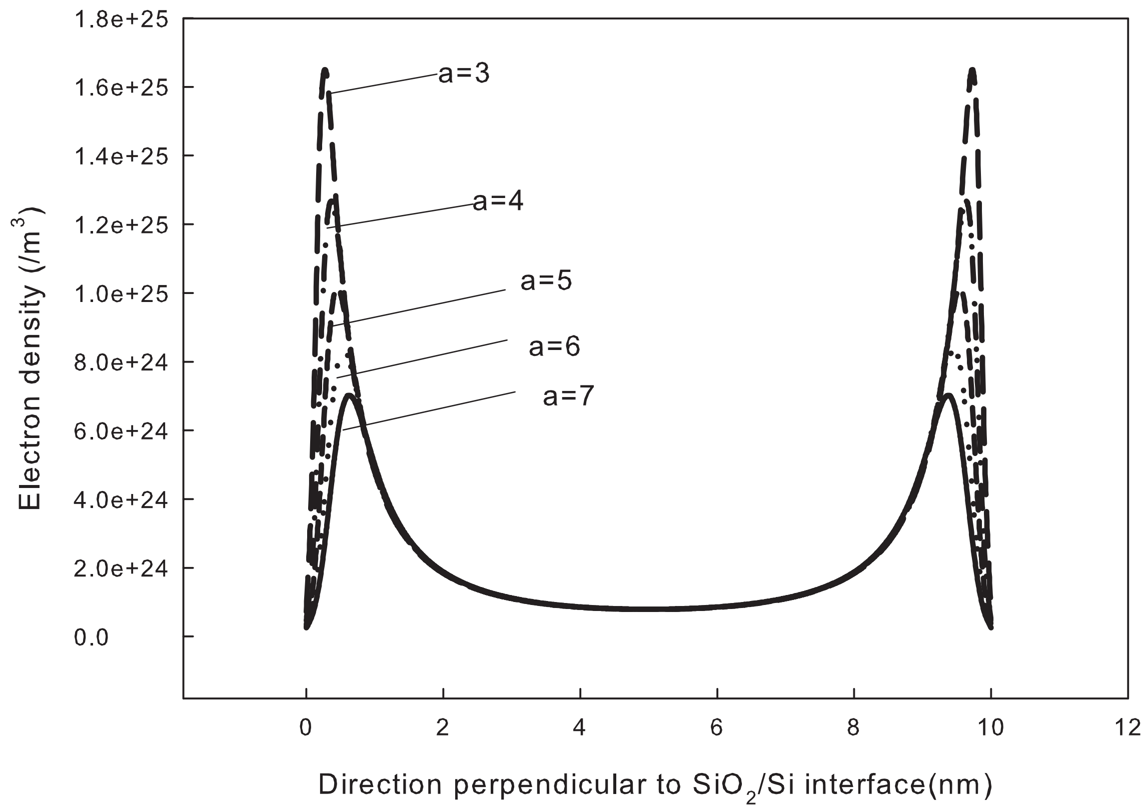

Figure 5.2: Electron density corrected by Ferry's effective potential with various standard deviation of wave packet of double-gate MOSFET. We will choose value of a such that result is close to the result from SP equations.

5.2 Data Collection by Using Device Simulation Tool

Here, we set several different conditions to find the suit values of standard deviation of wave packet. Values of standard deviation of wave packet is the dependent variable. And we consider following independent variables: 1. channel length (Lg), 2. gate voltage (Vg), 3. drain voltage (Vd) , 4. thickness of bulk (tsi), 5. thickness of oxide (tox) , 6. doping concentration (N). Beside, every variable has limiting of range.

1. Channel length : 20, 30, 40, 50 (nm) [43]

2. Gate voltage : 0.6, 0.7, 0.8, 0.9, 1.0, 1.1 (V)

3. Drain voltage : 0.6, 0.7, 0.8, 0.9 (V), if Vg=0.6

0.7, 0.8, 0.9, 1.0 (V), if Vg = 0.7 V

$\vdots$

1.1, 1.2, 1.3, 1.4 (V), if Vg = 1.1 V

(ensure device is in the saturation region)

4. Thickness of bulk : 8, 10, 12 (nm), if Lg = 20 nm

12, 15, 18 (nm), if Lg = 30 nm

$\vdots$

20, 25, 30 (nm), if Lg = 50 nm

(only discuss devices whose ratio of Thickness of bulk over Channel length $\approx$ 1/2

[44][45][46][47] proposes that device whose ratio of Thickness of bulk over Channel length

$\approx$ 1/2 has better characters.)

5. Thickness of oxide : 1, 1.5, 2 (nm)

6. Doping concentration : 1e16, 5e16, 1e17, 5e17 $(/cm^3)$

Here, we only discuss symmetric double-gate MOSFET. Besides, we will set thickness of one oxide is equal to 200 nm with gate voltage 0 V. And we will treat the latter be SOI structure.

5.3 Modelling and Simulation Results

5.3.1 Modelling Double-Gate MOSFET

In this part, we only consider double-gate MOSFET. First, Table 5.1 shows the correlation between every independent variables. Because of our design of experiments, we can find that there is collinearity phenomenon among some variables. Figs. 5.3, 5.4, 5.5, 5.6, 5.7, 5.8 show the scattering plots : each independent variable against standard deviation of wave packet. Obviously, we can find that there are not only linear correlations but also quadratic correlations between dependent variable and some independent variables. So, we will add square terms into the model. Because there is collinearity phenomenon, effect of some variables may be weakened so that variables are not significant. Besides, we also add interaction terms to check whether there are interaction effects or not.

All models we establish will be analyzed by stepwise method:

Independent variables : 1. Variables 1$\sim$ 6

2. Square terms of Variables 1$\sim$ 6

3. Second order interaction terms of Variables 1$\sim$ 6

Model I Dependent variable : Standard deviation of wave packet

Residual analyses of model I are shown as Fig. 5.9 and Fig. 5.10. Clearly, we can know model I is bad from Fig. 5.10.

We try to transform the dependent variable by power transformation. Fig. 5.11 is Likelihood plot of power transformation. Likelihood achieves maximum when $\lambda = -0.148$. By the reason stated before, we prefer to set $\lambda = 0$. So, we try to take log of standard deviation of wave packet.

Model II Dependent variable : $\ln$(Standard deviation of wave packet)

Figure 5.12 and Fig. 5.13 show the residual analyses of model II. Obviously, model II is not good, either.

1D quantum correction may be not enough for devices with ultra-short channel [48][49][50].Now, we reduce data and retain data whose channel length longer than 20nm only. Then we get model III and model IV.

Model III Dependent variable : Standard deviation of wave packet

Model IV Dependent variable : $\ln$(Standard deviation of wave packet)

Residual analyses are shown from Fig. 5.14 to Fig. 5.17.

We find that results of model IV is good from plots of residual analysis.

	Lg	Vg	Vd	tsi	tox	N
Lg	1	0.808	0.67	0.881	0	0
Vg		1	0.827	0.712	0	0
Vd			1	0.607	0.016	0.022
tsi				1	0	0
tox					1	0
N						1

Table 5.1: Correlation Table: pairwise correlation between every variables. There may be collinearity phenomenon if there is high correlation between two variables.

Following are ANOVA table, residual statistics, coefficient table, and formula.

Source	SS	DF	MS	F_0	R^2
Regression	9.729	9	1.081	21929.330	0.999
Residual	0.015	314	$4.93e-5$		
Total	9.744	324			

Table 5.2: ANOVA table for significance of regression in multiple regression in double-gate MOSFET. R^2 is almost equal to 1, so the model is good in terms of explanatory ability.

	Minimum	Maximum	Mean	Std. deviation
Predicted value	1.4146	2.1109	1.6934	0.17332
Residual	-0.009687	0.009424	0	0.00436

Table 5.3: Residual statistics in double-gate MOSFET: It shows points have maximum and minimum. Absolute value of residual are all less than 0.001.

Model	Coefficients	Std. Error	t
constant	4.297	0.016	261.890
Vg	-3.372	0.033	-100.897
tox^2	0.196	0.002	93.732
Vg^2	1.372	0.018	78.249
tox	-0.339	0.008	-42.779
Lg	-0.02	0.0008	-41.989
Lg^2	0.00018	0.001	32.470
N	-0.003	0.0006	-20.360
Vg*tox	-0.143	0.007	-19.367
Lg*tox	0.0001	0.0002	4.727
Vd	-0.005	0.003	-1.942
tsi	0.000018	0.0002	-2.41

Table 5.4: Coefficients table in double-gate MOSFET: the first frame is name of variable; second is the coefficient of variable; third is standard deviation of coefficient; the last frame is value of t distribution.

$$\begin{aligned}\ln(a) &= 4.297 + (1.372Vg^2 - 3.372Vg) + (0.196tox^2 - 0.339tox) \\ &+ (0.00018Lg^2 - 0.02Lg) - 0.005Vd - 0.003N - 0.000018tsi \\ &+ 0.0001Lg \times tox - 0.143Vg \times tox,\end{aligned} \tag{5.2}$$

where unit of N is $1e17/cm^3$.

After generating formula, we have to check whether the model is reasonable. From scattering plots, we can find that response variable appears monotone decreasing or increasing. On the other hand, our model is a second order formula. If maximum or minimum occur during the interval we simulate, then the results are suspect. In our model, there are three second order terms, Vg, tox, and Lg. Maximum or minimum occur about at Vg=1.23, tox=0.86, Lg=55.55. All of them are out of range of simulation. So, the formula is reasonable.

Because we used stepwise method to select variables. Variable selected into the model earlier has larger effect. In table 5.4, effect of variable is decreasing according to the order of variables. We know that gate voltage, thickness of oxide, and channel length dominate the variation of standard deviation of wave packet. In fact, effects of drain voltage and thickness of bulk are insignificant. It may resulted from collinearity of variables. It doesn't mean that drain voltage and thickness of bulk will not influence the results.

Form table 5.3, maximum of residual occurs when $\ln(a) = 2.1112$. In the other word, maximum of residual is 0.08146 when $a = 8.258$. If we want to simplify the model, we may delete some variables whose effects are too small and estimate model again.

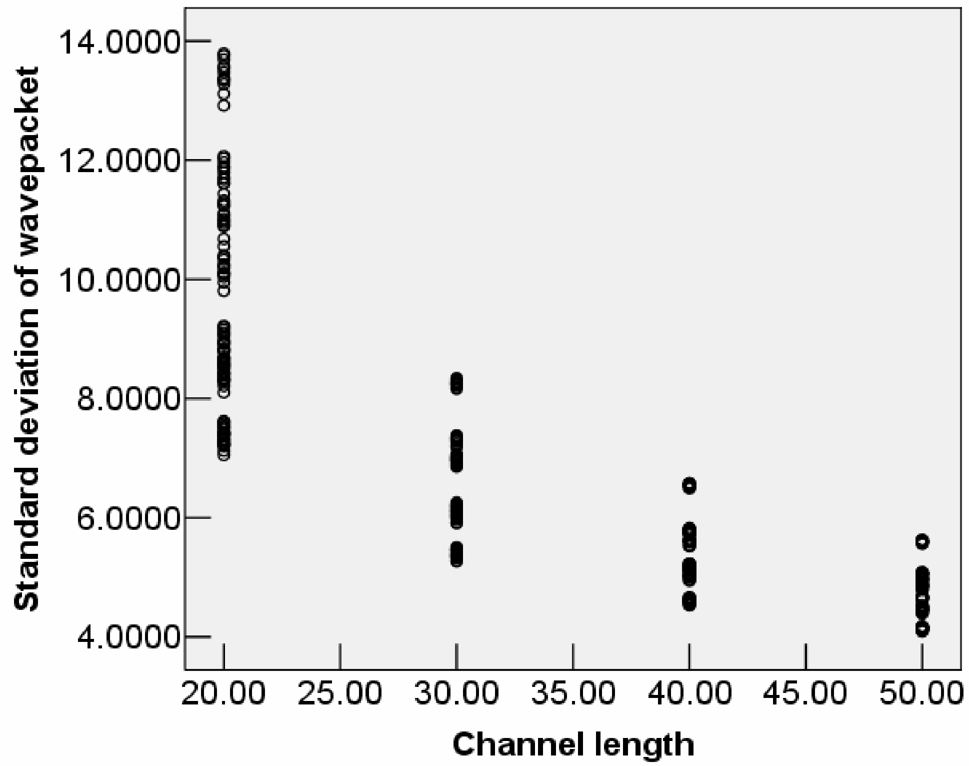

Figure 5.3: Scattering Plot : Channel length vs. Standard deviation of wave packet. It appears quadratic trend. Therefore, we will add the quadratic terms into the model.

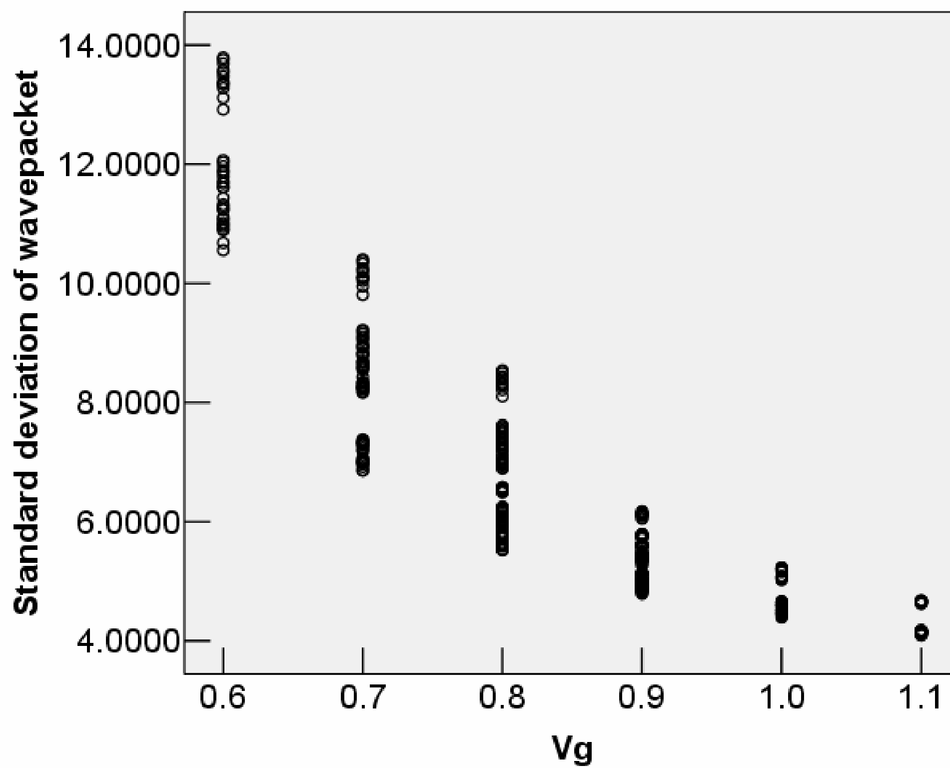

Figure 5.4: Scattering plot : Gate voltage vs. Standard deviation of wave packet. It appears quadratic trend. Therefore, we will add the quadratic terms into the model.

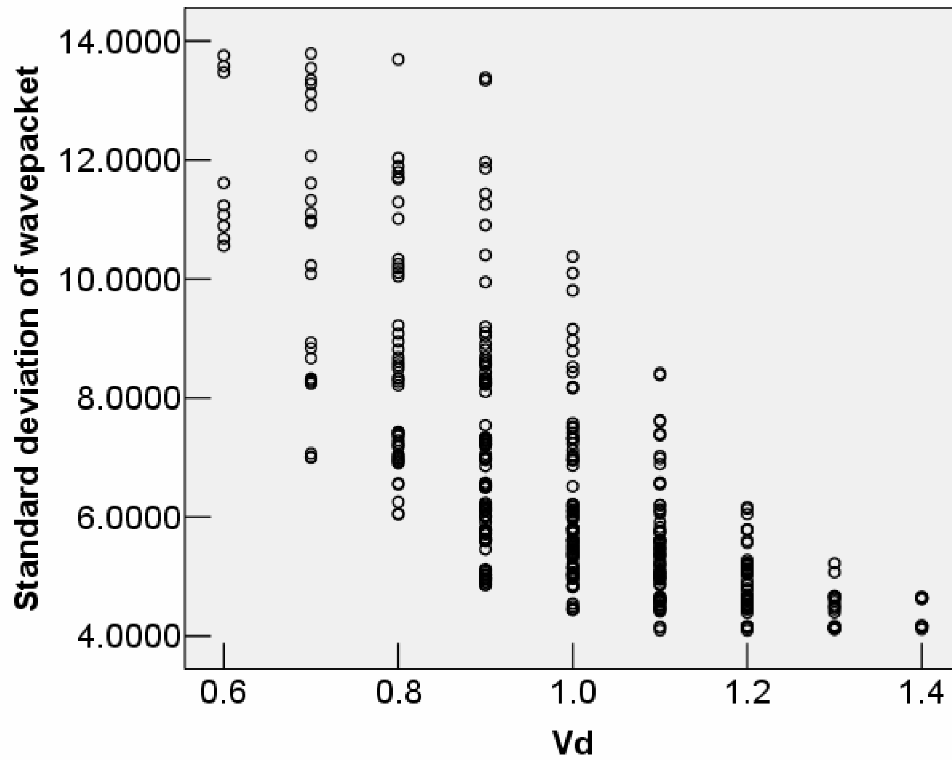

Figure 5.5: Scattering plot : Drain voltage vs. Standard deviation of wave packet. It appears quadratic trend. Therefore, we will add the quadratic terms into the model.

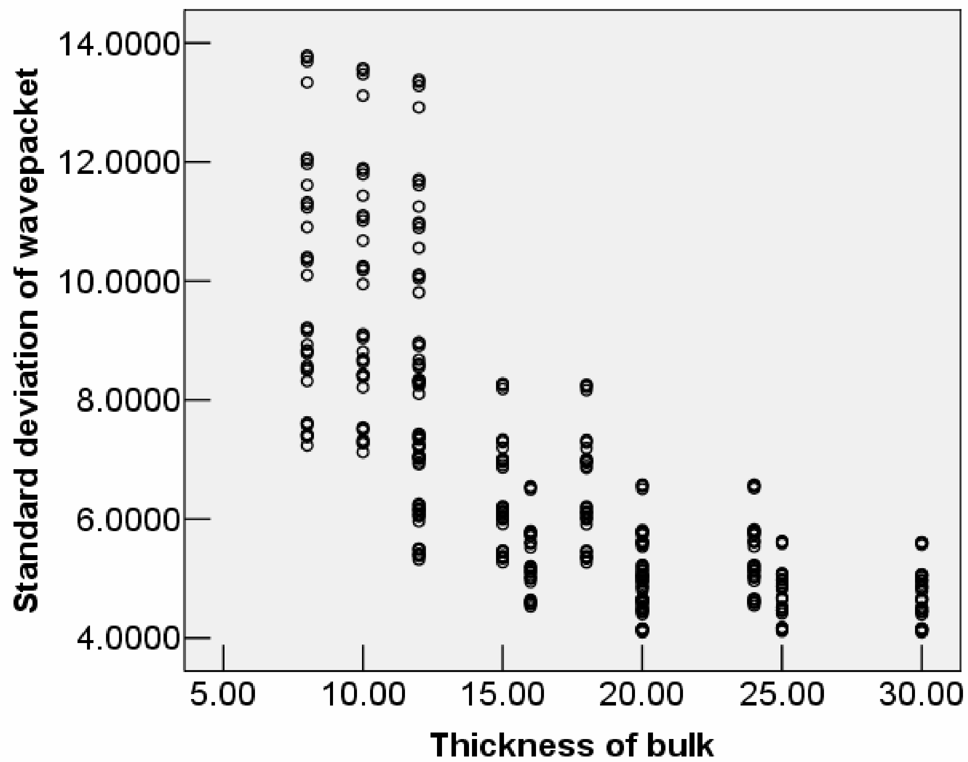

Figure 5.6: Scattering plot : Thickness of bulk vs. Standard deviation of wave packet. It appears quadratic trend. Therefore, we will add the quadratic terms into the model.

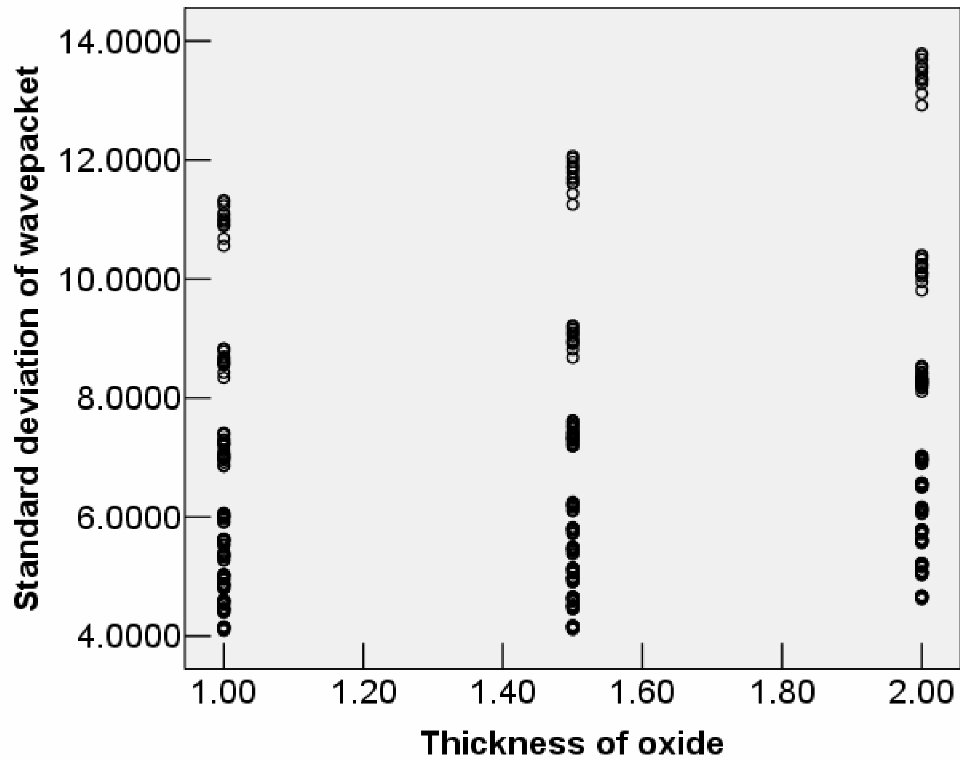

Figure 5.7: Scattering plot : Thickness of oxide vs. Standard deviation of wave packet. It appears quadratic trend. Therefore, we will add the quadratic terms into the model.

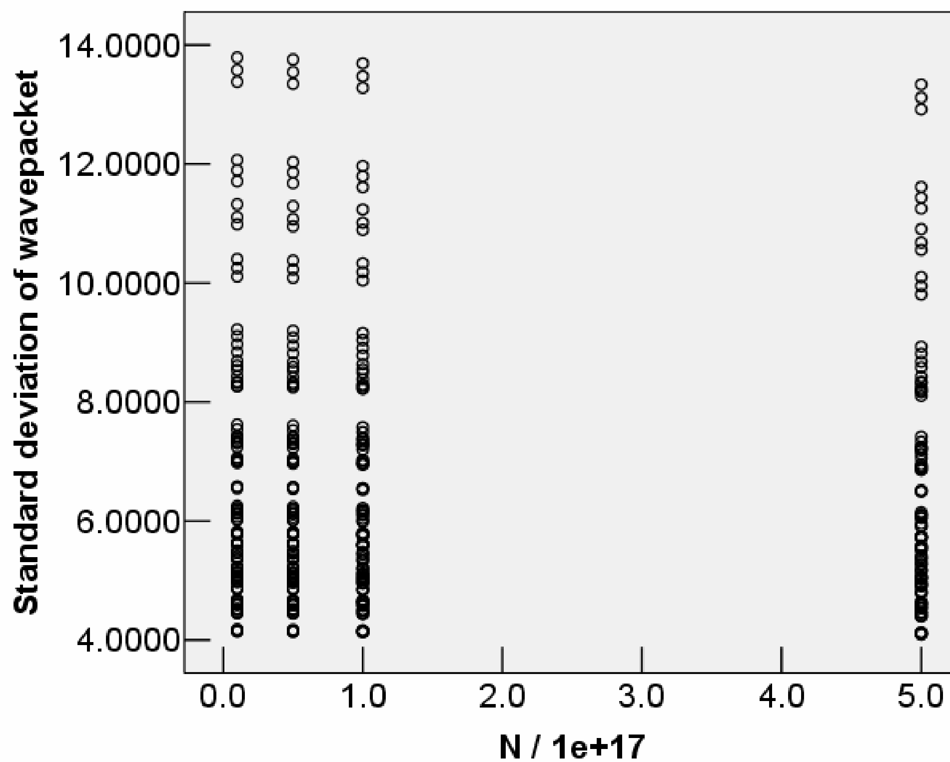

Figure 5.8: Scattering plot : Doping concentration vs. Standard deviation of wave packet. From this figure, the effect of doping concentration may be not so evident.

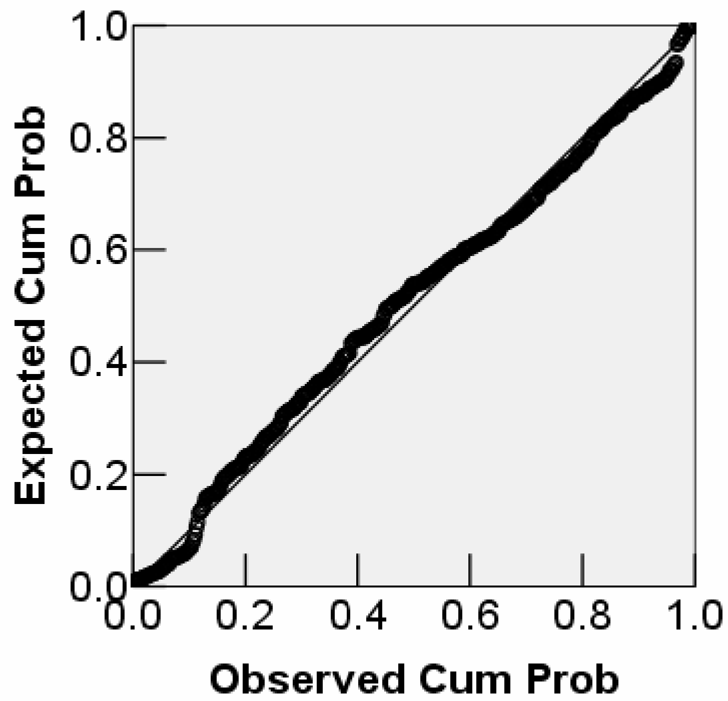

Figure 5.9: Normal plot of Model I. Y axis is cumulate probability of normal distribution, and X axis is cumulate probability of observed residual. The result is satisfied.

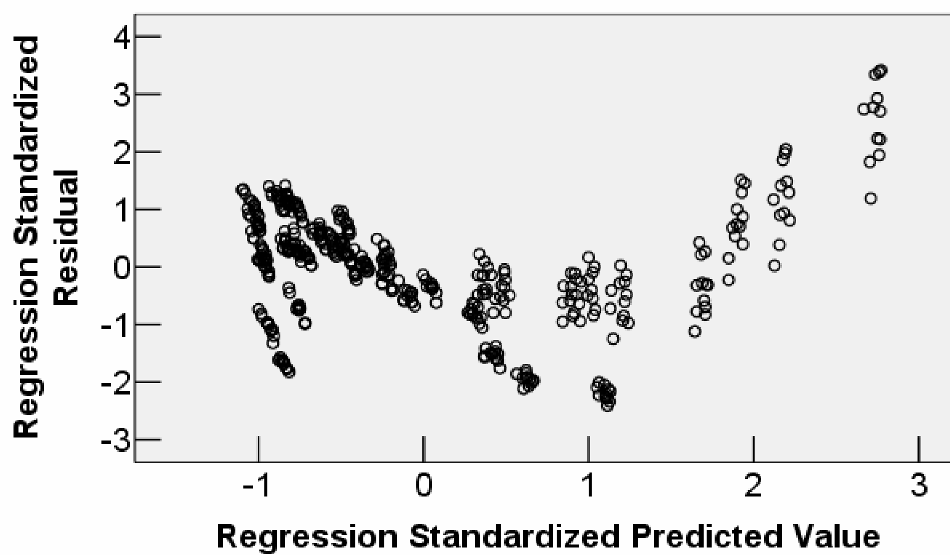

Figure 5.10: Scattering plot : Fitted value against residual of model I. It appears nonlinear pattern. Therefore, we may conclude that the model I is not good.

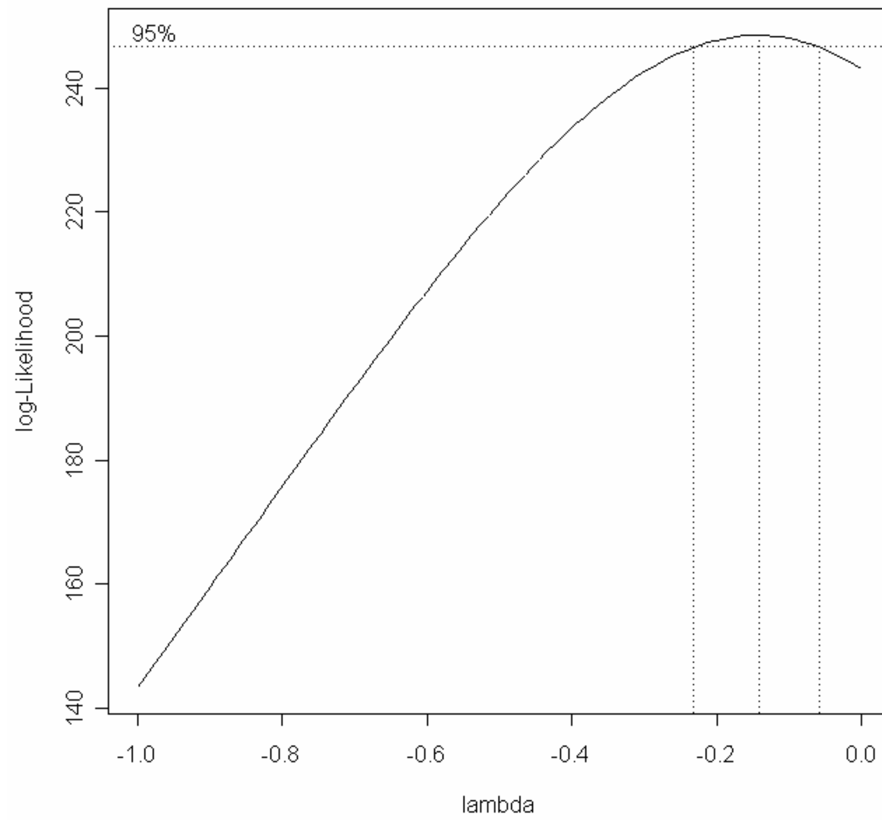

Figure 5.11: Likelihood plot of power transformation. Likelihood achieve maximum when $\lambda = -0.148$. We prefer to set $\lambda = 0$.

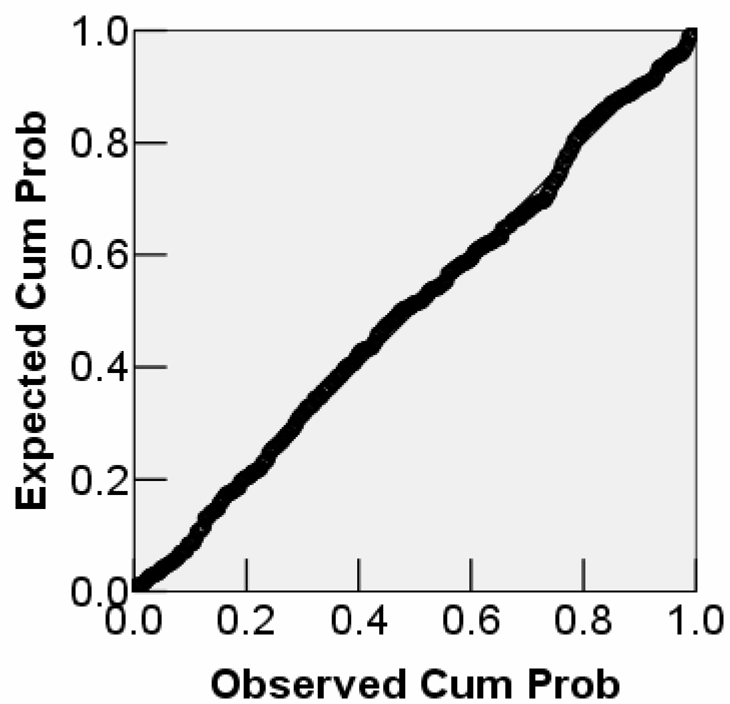

Figure 5.12: Normal plot of Model II. Y axis is cumulate probability of normal distribution, and X axis is cumulate probability of observed residual. The result is satisfied.

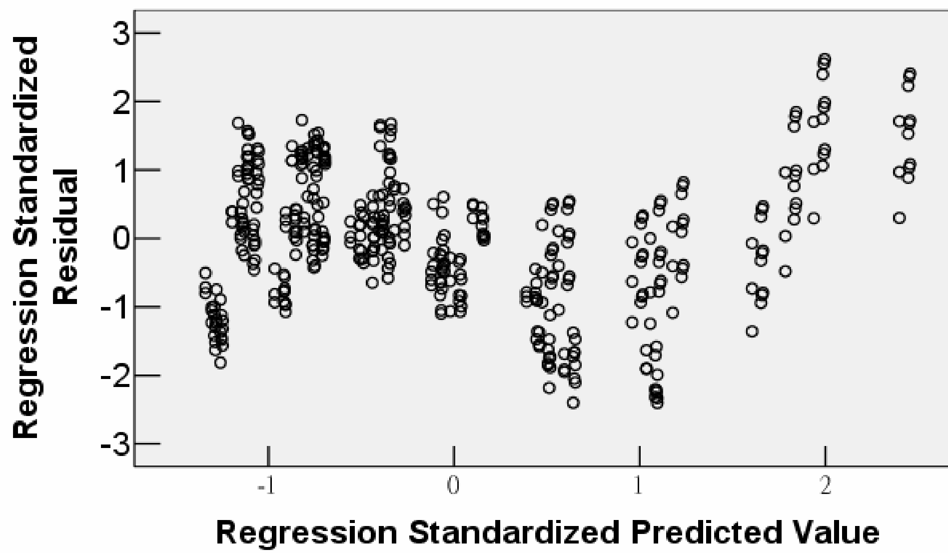

Figure 5.13: Scattering plot : Fitted value against residual of model II. It appears nonlinear pattern. Therefore, we may conclude that the model II is not good.

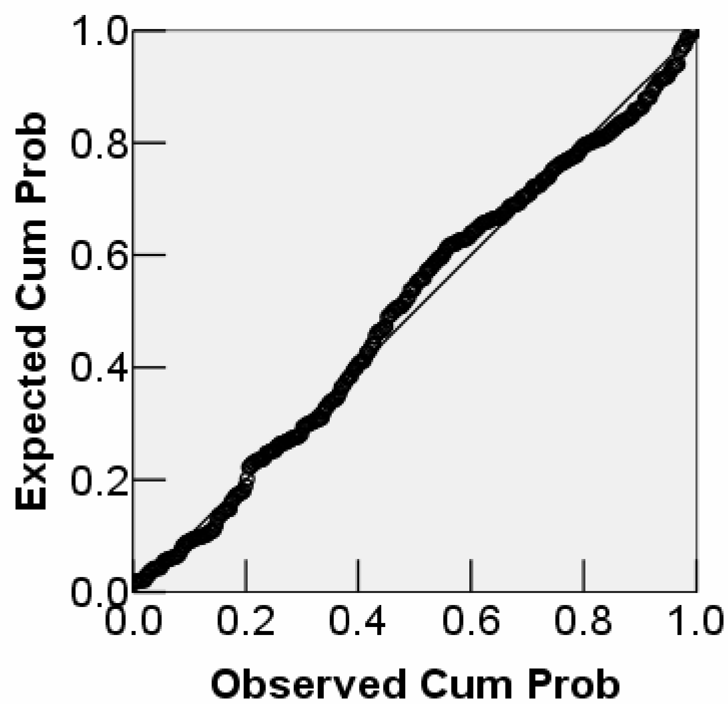

Figure 5.14: Normal plot of Model III. Y axis is cumulate probability of normal distribution, and X axis is cumulate probability of observed residual. The result is satisfied.

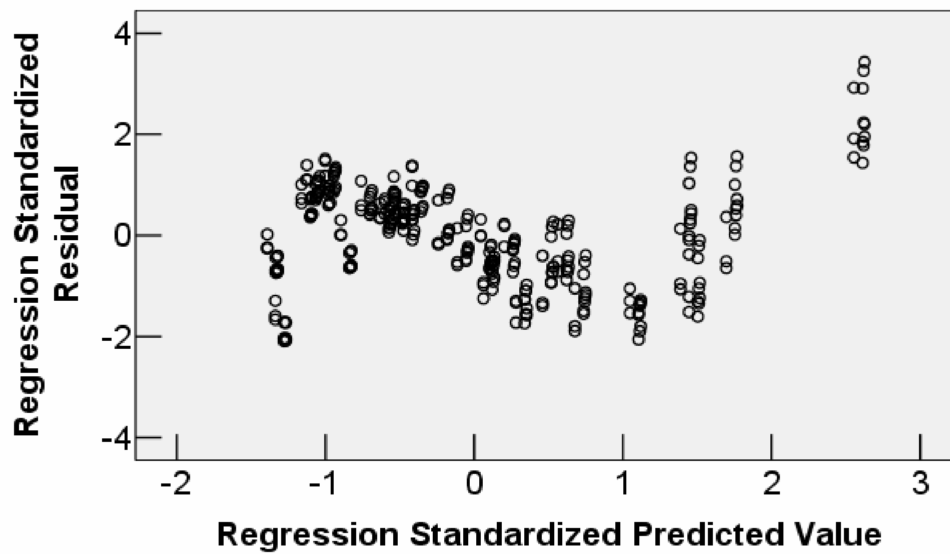

Figure 5.15: Scattering plot : Fitted value against residual of model III. It appears nonlinear pattern. So the model III is not good.

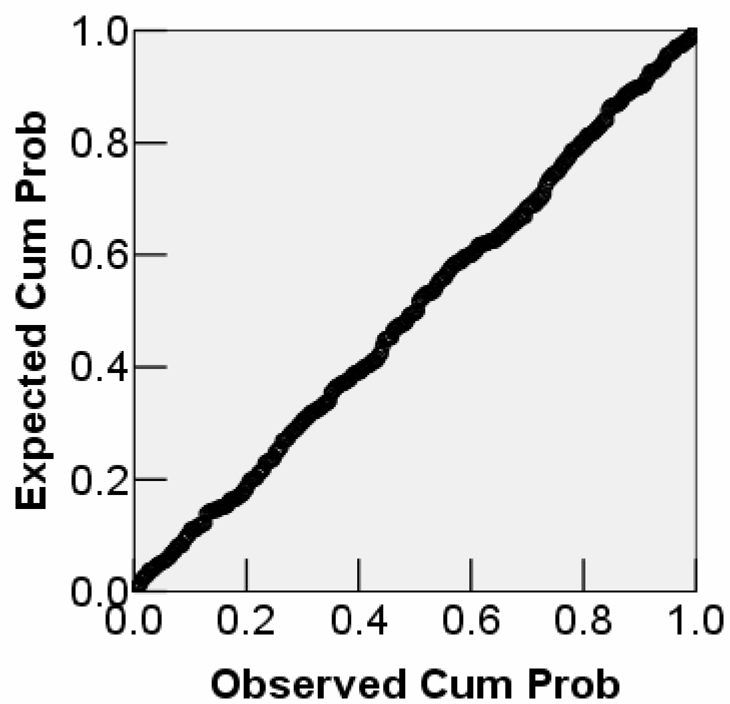

Figure 5.16: Normal plot of Model IV. Y axis is cumulate probability of normal distribution, and X axis is cumulate probability of observed residual. The result is satisfied.

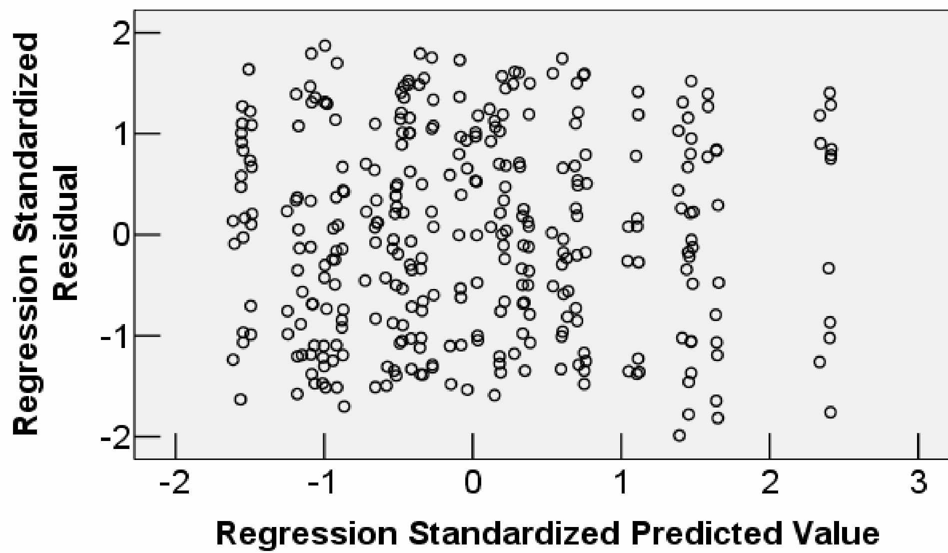

Figure 5.17: Scattering plot : Fitted value against residual of model IV. It appears flat band pattern, so the model IV is good. Combining result of normal plot. The model IV is good.

5.3.2 Accuracy of Model of Double-Gate MOSFET

In this part, some comparison of characters will be presented. And the conditions of devices are: tox = 1 nm, Lg = 40 nm, tsi = 24 nm, Vg = 0.9 V, Vd = 1V, and N = 5e23 / m^3.

First, we show the comparison of electron density among SP model, optimized effective potential, and effective potential from regression model, Fig. 5.18. From magnified figure, we can find results from effective potential both shift to right side. How the degree of displacement will be produced? Now, we define

$$\bar{X} = \frac{\int xndx}{\int ndx}$$

as the expectation value of electron density. In case shown in Fig. 5.18, $\bar{X}_{sp} = 1.817, \bar{X}_{optimize} = 2.031, \bar{X}_{model} = 2.046$. Displacement of $\bar{X}$ is about $2\AA$.

Following, we show the comparison of $Id - Vg$ curves, Fig. 5.31. Drain current solved form effective potential is always lower than solved from SP equations. Besides, curves solved from effective potential with optimized a and a from model are almost equal. Maximum of different between SP equations and effective potential about 0.3 mA.

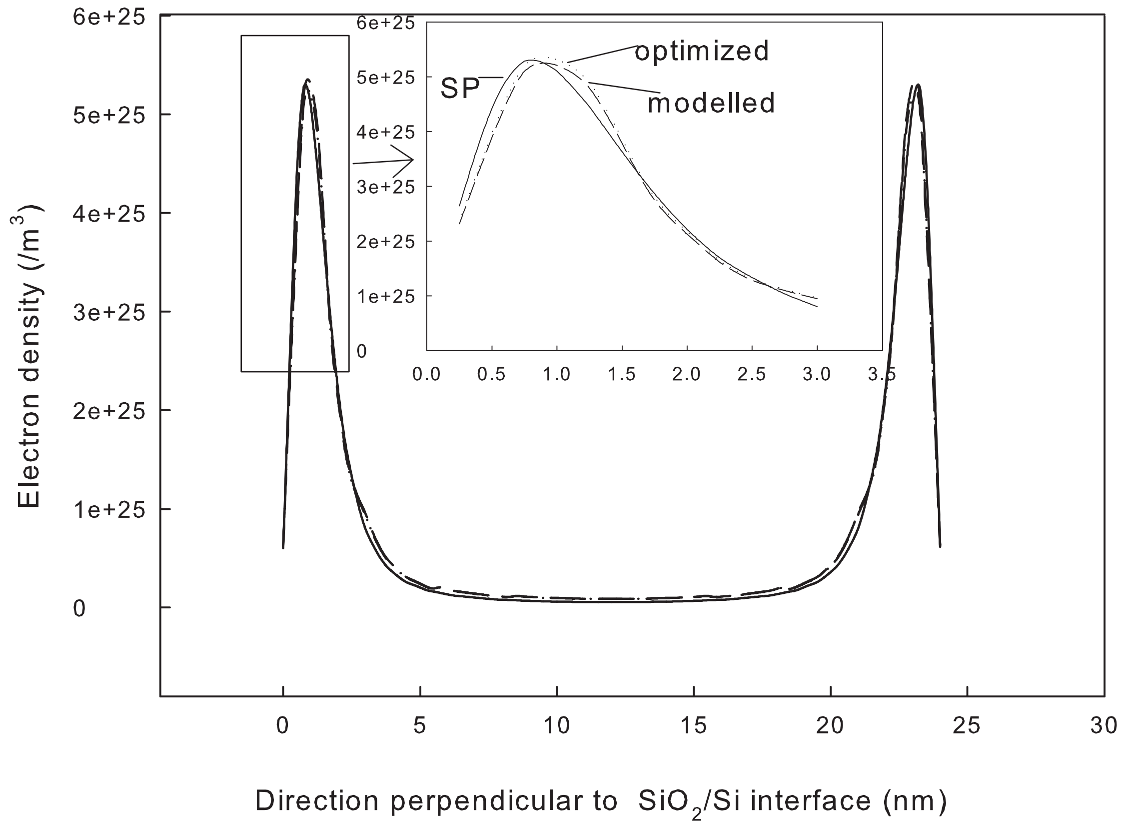

Figure 5.18: Comparison of electron density: peaks of electron density solved from Ferry's effective potential both shift to right side.

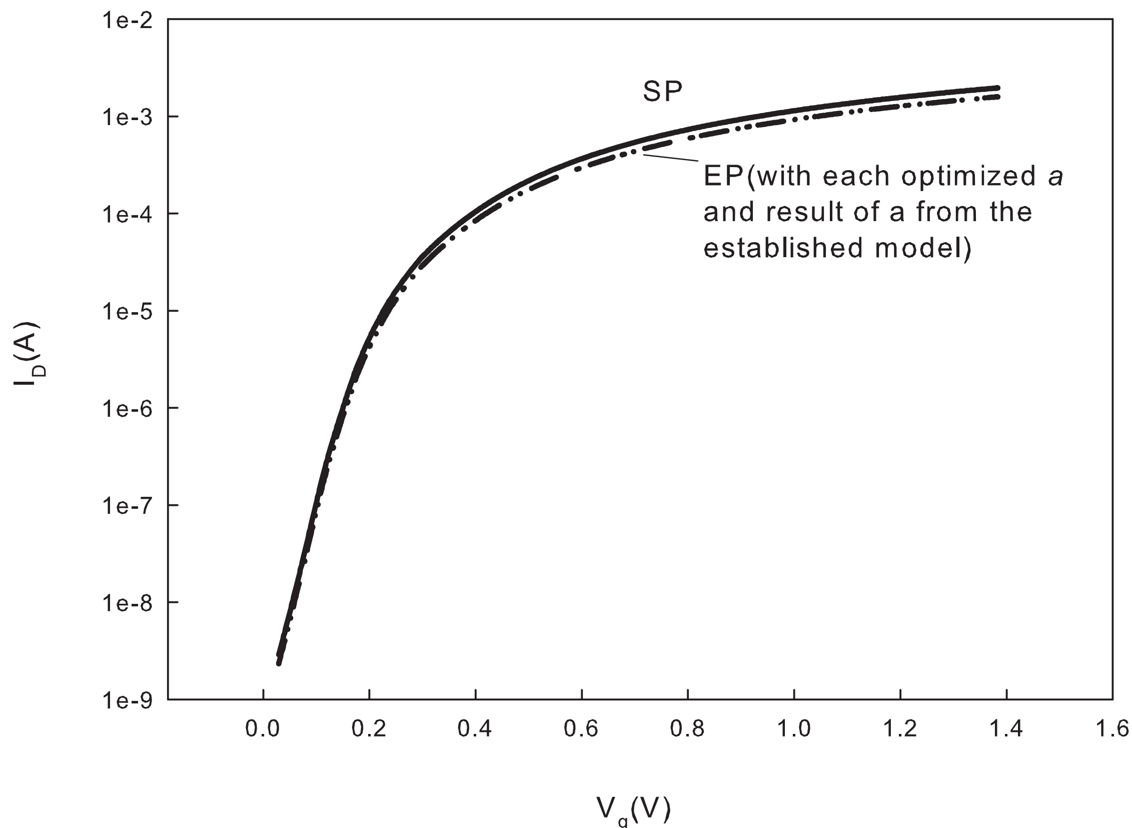

Figure 5.19: Id-Vg curve:solid line is solved from SP equations while dash line is solved from effective potential. curves solved from effective potential with optimized a and a from model are almost equal. Curve of effective potential is some lower than SP equations. Maximum of different between SP equations and effective potential is about 0.3 mA.

5.3.3 Modelling Double-Gate and SOI MOSFETs

In this part, we will analyze data of double-gate and SOI structure together. In other words, we want to construct a model more general, suitable for double-gate and SOI MOSFET simultaneous.

By previous experience, we proceed power transformation (Fig. 5.20). Similarly, we take log of standard deviation of wave packet and establish model by stepwise method. Scattering plots of response variable against independent variables are shown form Fig. 5.21 to Fig. 5.27. Following are ANOVA table, residual statistics, coefficients table and model after analyzing.

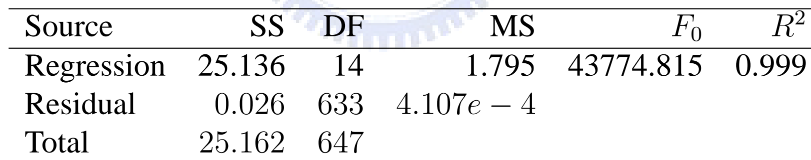

Source	SS	DF	MS	F_0	R^2
Regression	25.136	14	1.795	43774.815	0.999
Residual	0.026	633	$4.107e-4$		
Total	25.162	647			

Table 5.5: ANOVA table for significance of regression in multiple regression. R^2 is equal to 0.99. Explanatory ability of the model is good.

	Minimum	Maximum	Mean	Std. deviation
Predicted value	1.2254	2.1107	1.5999	0.19711
Residual	-0.011223	0.01284	0	0.00633

Table 5.6: Residual statistics : It shows points have maximum and minimum. We can find that residual of new model is some larger than previous.

Model	Coefficients	Std. Error	t
constant	4.281	0.02	214.278
Vg1	-3.295	0.04	-81.523
tox1^2	0.196	0.003	77.711
Vg1^2	1.341	0.021	63.424
Lg	-0.0205	0.006	-36.042
S	-0.185	0.005	-35.941
tox1	-0.338	0.01	-35.2
Lg^2	0.00018	0.001	27.161
Vg1*tox1	-0.159	0.009	-17.862
N	-0.003	0.0007	-17.416
Lg*tox	0.0008	0.001	6.65
Vd	-0.008	0.003	-2.364
tsi	-0.0000874	0.0003	0.974

Table 5.7: Coefficients table: the first frame is name of variable; second is the coefficient of variable; third is standard deviation of coefficient; the last frame is value of t distribution.

$$\begin{aligned} \ln(a) &= 4.277 + (1.341Vg1^2 - 3.295Vg1) + (0.196tox1^2 - 0.338tox1) \\ &+ (0.00018Lg^2 - 0.0205Lg) - 0.008Vd - 0.003N - 0.0000874tsi \\ &+ 0.0008Lg \times tox1 - 0.159Vg1 \times tox1 - 0.185S \end{aligned} \tag{5.3}$$

In Eq. 5.3, there is a new variable, S. This variable has only two values, 0 and 1. When $S = 0$, it indicates double-gate MOSFET. While $S = 1$, it indicates SOI structure. Other variables are the same as before. This formula is extended to suit for two structure. From Eq. 5.2 and Eq. 5.3, we can find that change of coefficient of variables in both equations is not evident. It indicates that trends in these two structures are similarly. However, residual of Eq. 5.3 is some larger than formula only for double-gate MOSFET.

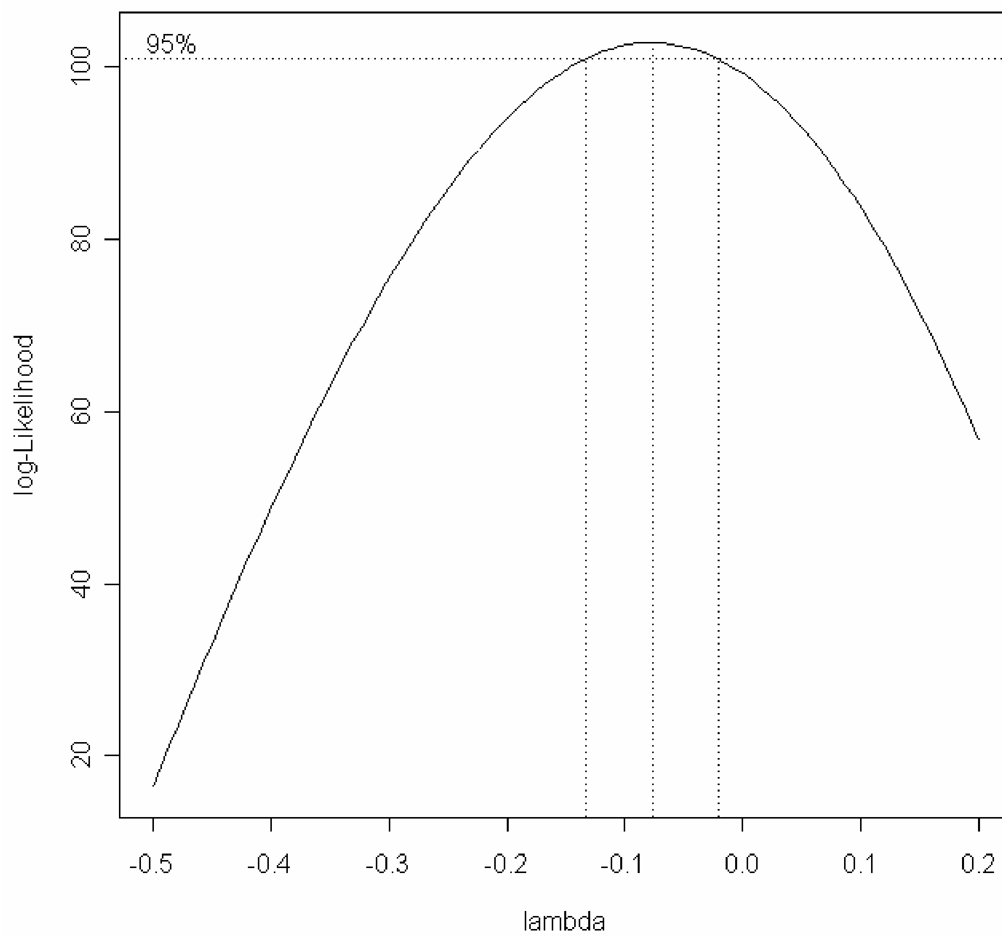

Figure 5.20: Likelihood plot of power transformation. Likelihood achieve maximum when $\lambda = -0.082$. It is more close to 0. So we still prefer to set $\lambda = 0$.

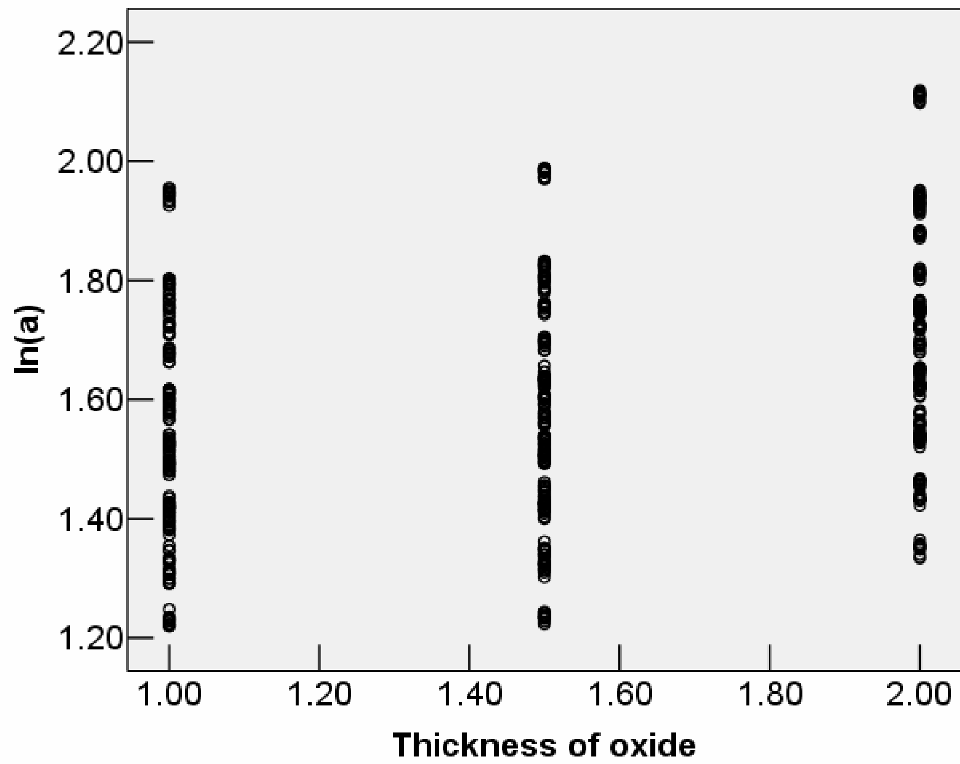

Figure 5.21: Scattering plot : Thickness of oxide vs. Standard deviation of wave packet. It appears quadratic trend. So we will add the quadratic terms into the model.

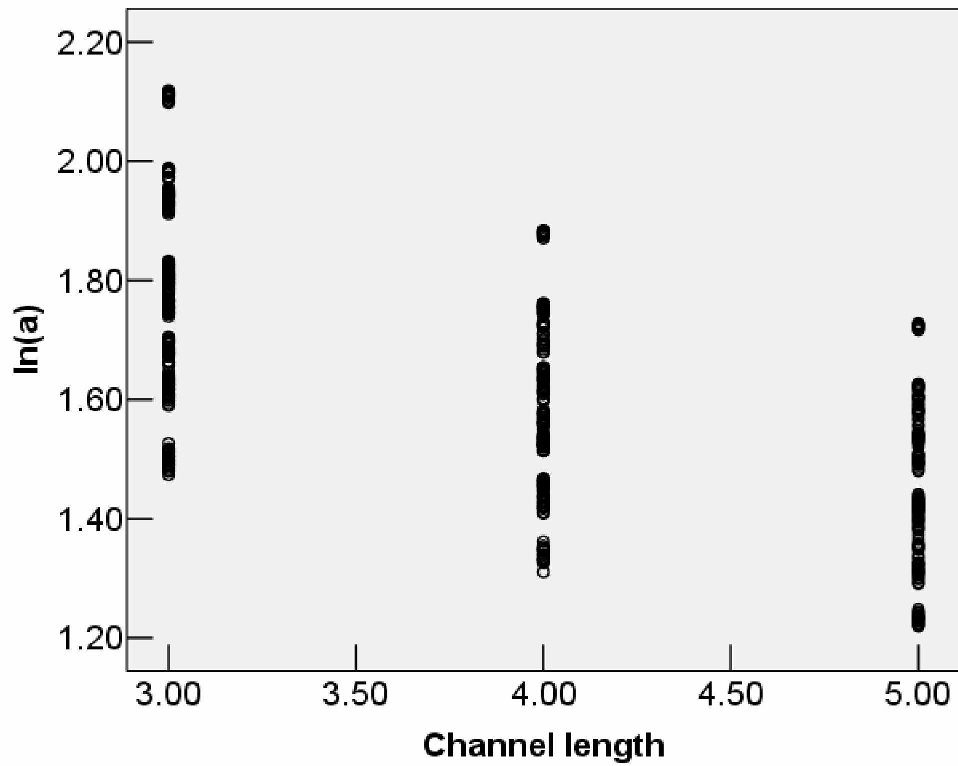

Figure 5.22: Scattering Plot : Channel length vs. Standard deviation of wave packet. It appears quadratic trend. So we will add the quadratic terms into the model.

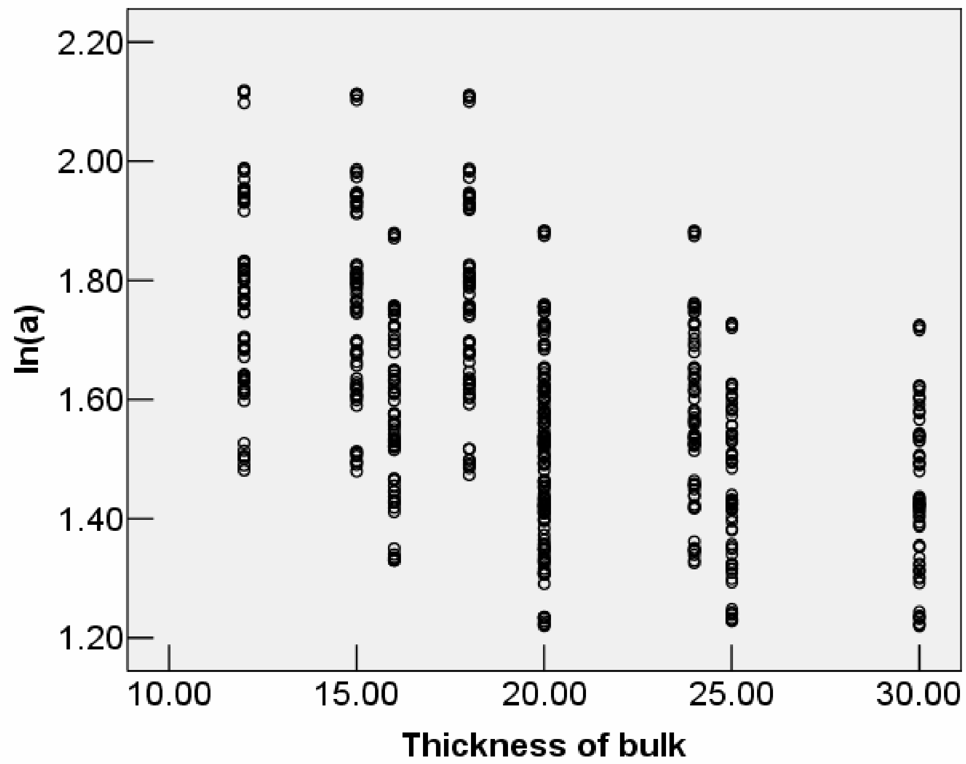

Figure 5.23: Scattering plot : Thickness of bulk vs. Standard deviation of wave packet. It appears quadratic trend. So we will add the quadratic terms into the model.

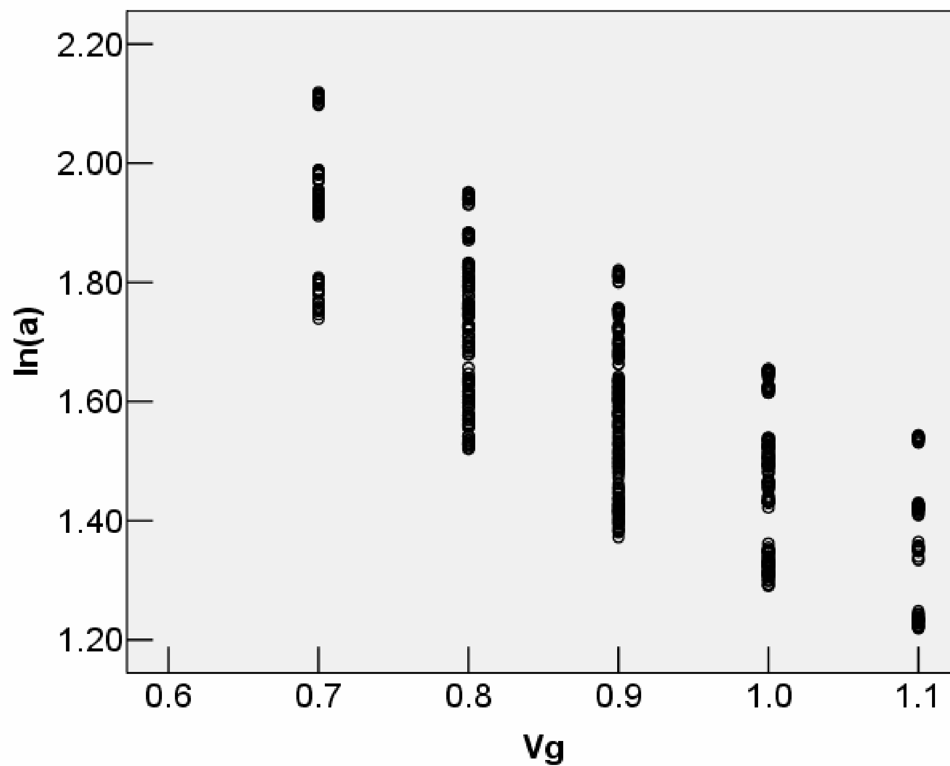

Figure 5.24: Scattering plot : Gate voltage vs. Standard deviation of wave packet. It appears quadratic trend. So we will add the quadratic terms into the model.

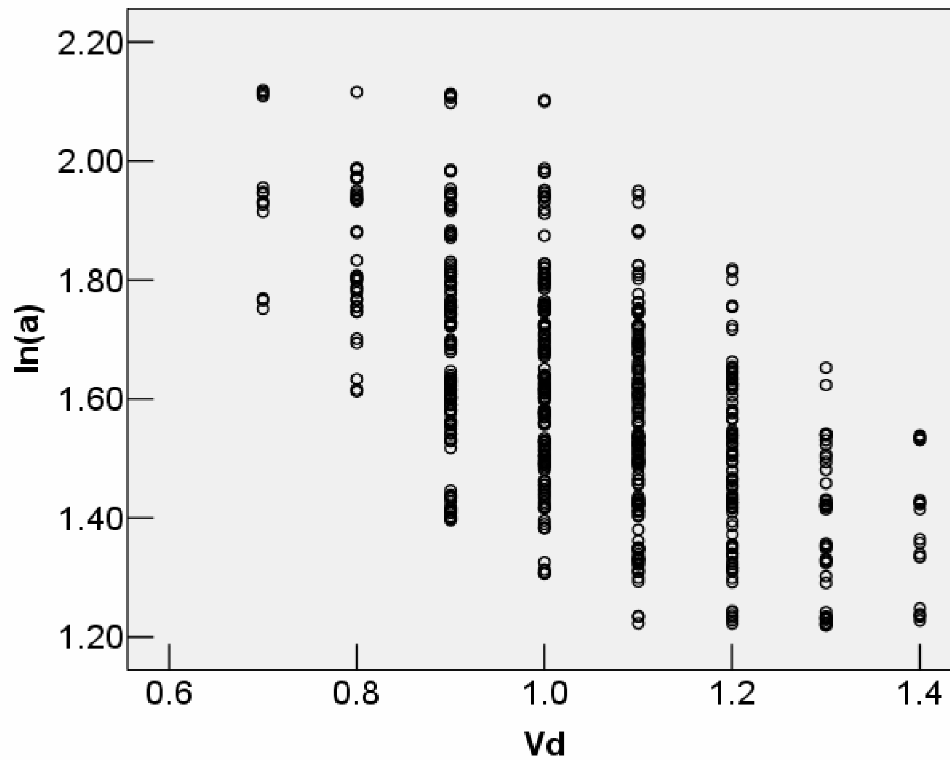

Figure 5.25: Scattering plot : Drain voltage vs. Standard deviation of wave packet. It appears quadratic trend. So we will add the quadratic terms into the model.

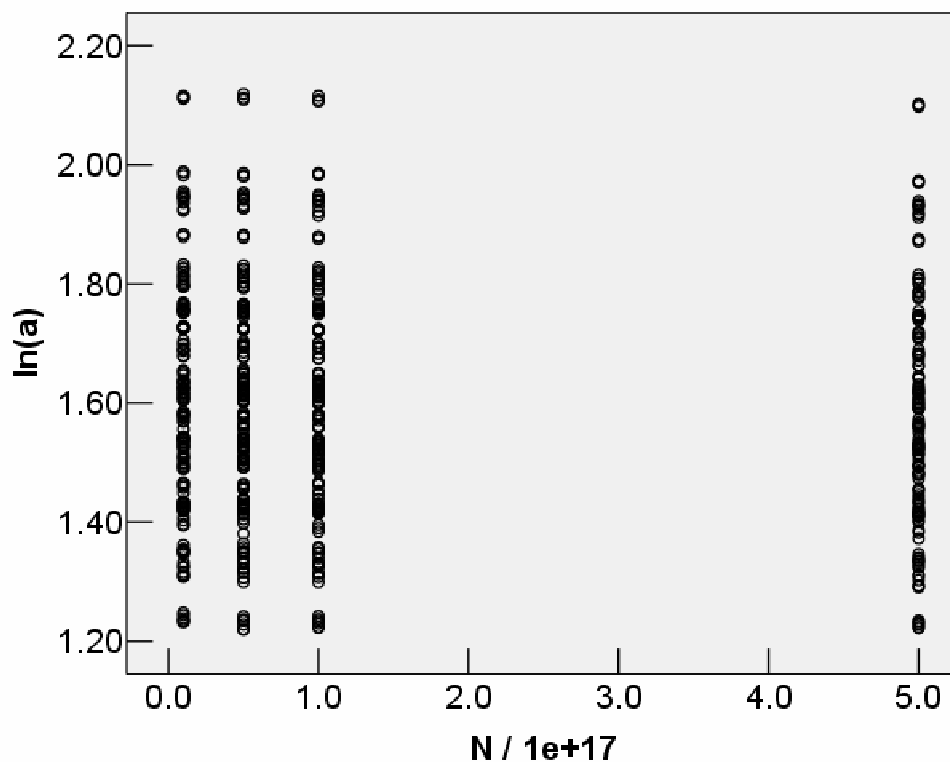

Figure 5.26: Scattering plot : Doping concentration vs. Standard deviation of wave packet. From this figure, the effect of doping concentration may be not so evident.

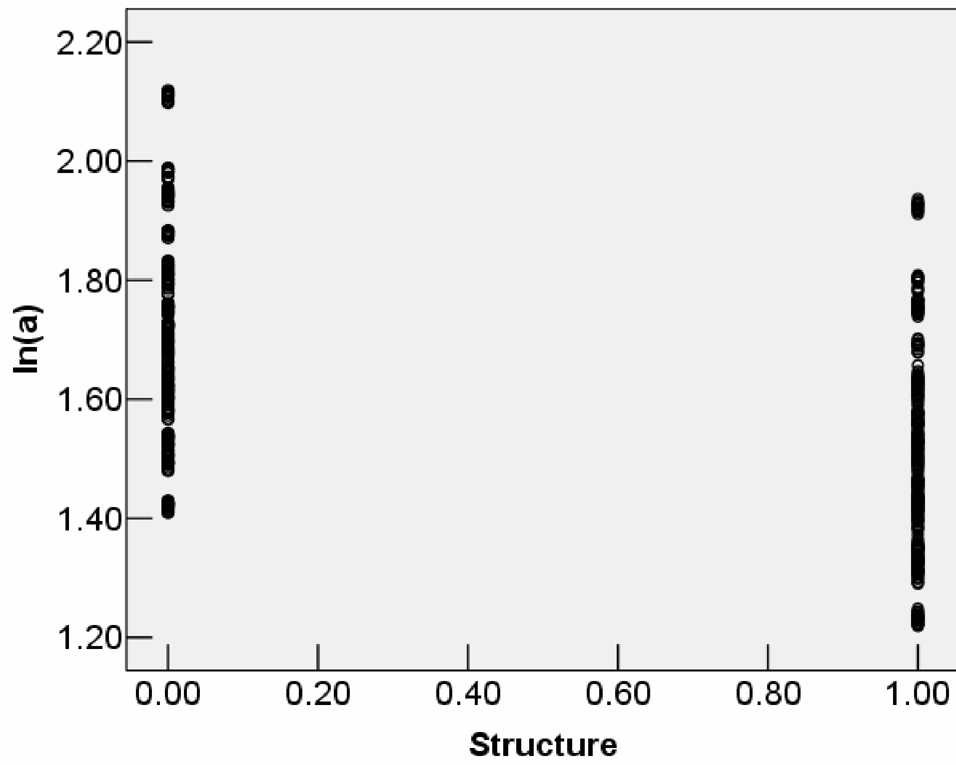

Figure 5.27: Scattering plot : Structure vs. Standard deviation of wave packet. 0 indicates double-gate, 1 indicates SOI structure.

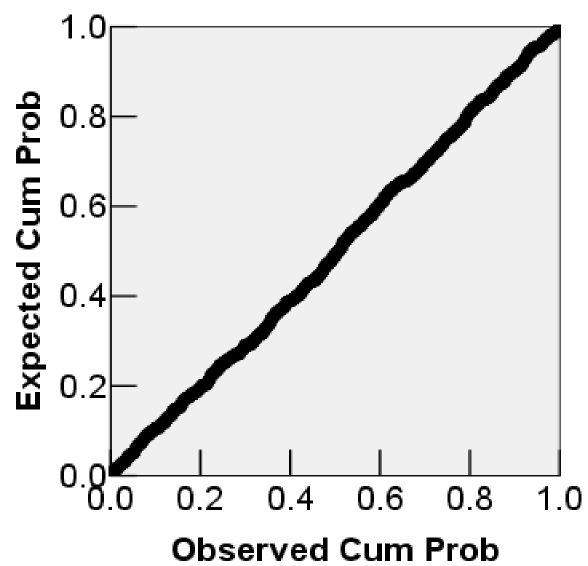

Figure 5.28: Normal plot. Y axis is cumulate probability of normal distribution, and X axis is cumulate probability of observed residual. The result is satisfied.

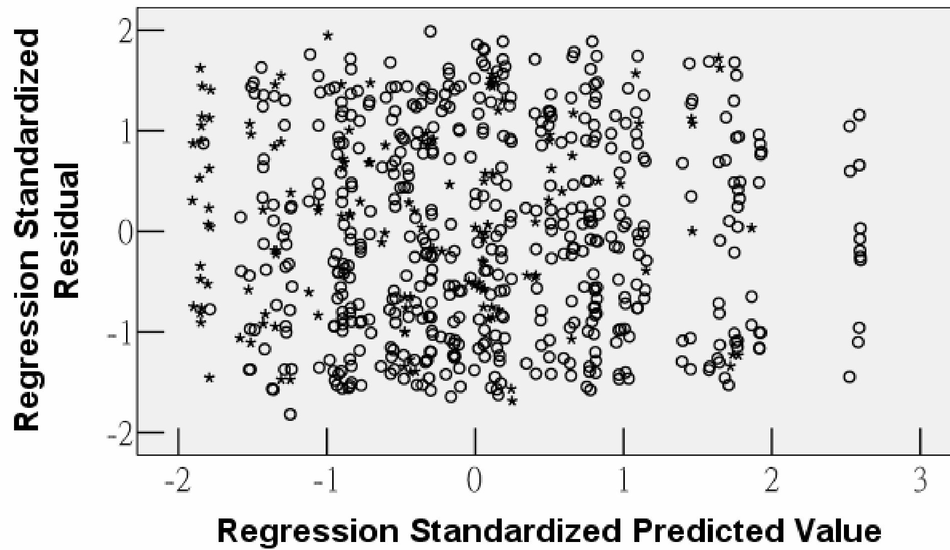

Figure 5.29: Scattering plot : Fitted value against residual of formula 5.3. It appears flat band pattern, so the model is good. Combining result of normal plot. The model is good. Circles indicate cases of double-gate, and stars indicate cases of SOI.

5.3.4 Accuracy of Model of Double-Gate and SOI MOSFET

We establish another model which is suit for double-gate and SOI MOSFETs at the same time. We will discuss how accurate the model is. Similarly, we calculate $\bar{X}$ for the new model of device with the same conditions used before, Fig. 5.30 . Then we get $\bar{X}_{model} = 2.067$. The change seems not so evident. Result of the new model is some worse than model in section 5.3.1 in this case. Maybe result of new model is better in other case. What we can say is that variation of residual of new model is larger. Besides, Id-Vg curves are almost the same, Fig. 5.31.

Of course, we will check accuracy in SOI. $\bar{X}_{sp} = 2.07, \bar{X}_{optimize} = 2.157, \bar{X}_{model} = 2.136$. Though $\bar{X}_{model}$ is closer to $\bar{X}_{sp}$, but the error of curve of electron density is larger, Fig. 5.32.

From results of double-gate and SOI structure, we can find that residual of the latter is larger than the former. Model suit for two kinds of devices is more general, but the accuracy will be worse. Nevertheless, the accuracy seems acceptable.

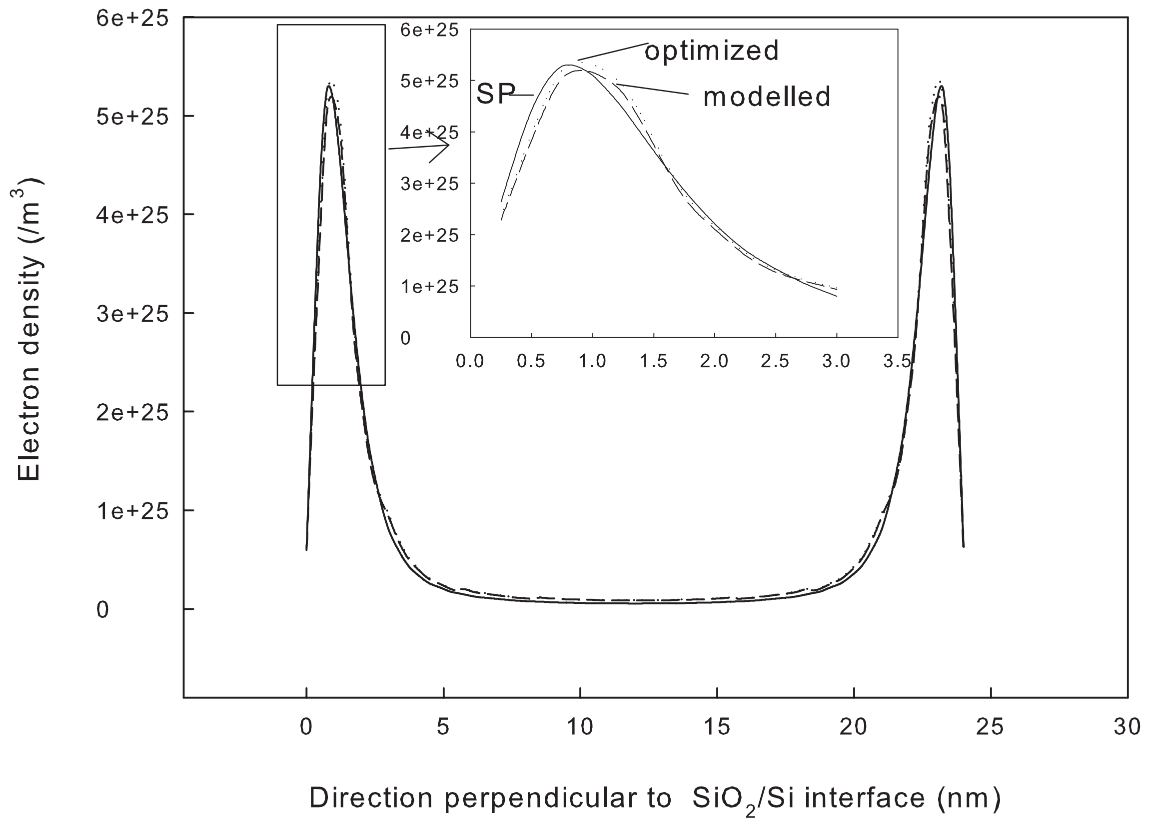

Figure 5.30: Comparison of electron density: peaks of electron density solved from Ferry's effective potential both shift to right side.

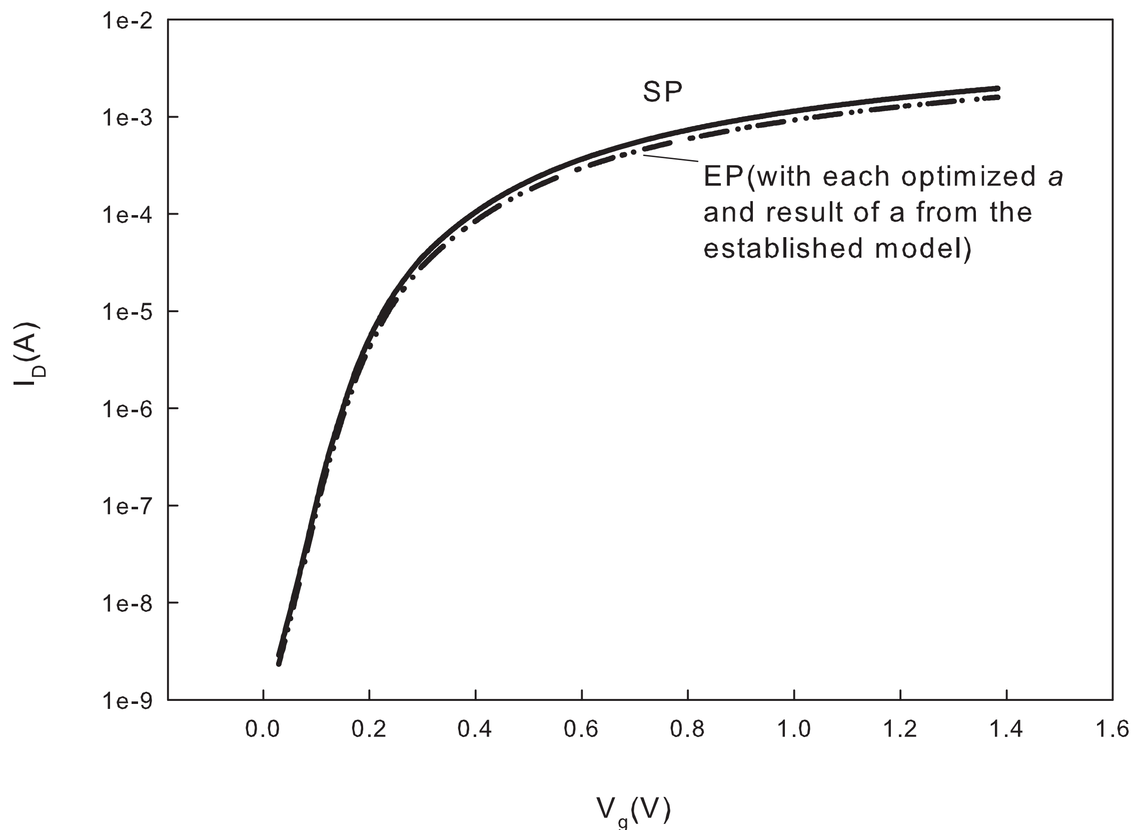

Figure 5.31: Id-Vg curve:solid line is solved from SP equations while dash line is solved from effective potential. curves solved from effective potential with optimized a and a from model are almost equal. Curve of effective potential is some lower than SP equations. Maximum of different between SP equations and effective potential is about 0.3 mA.

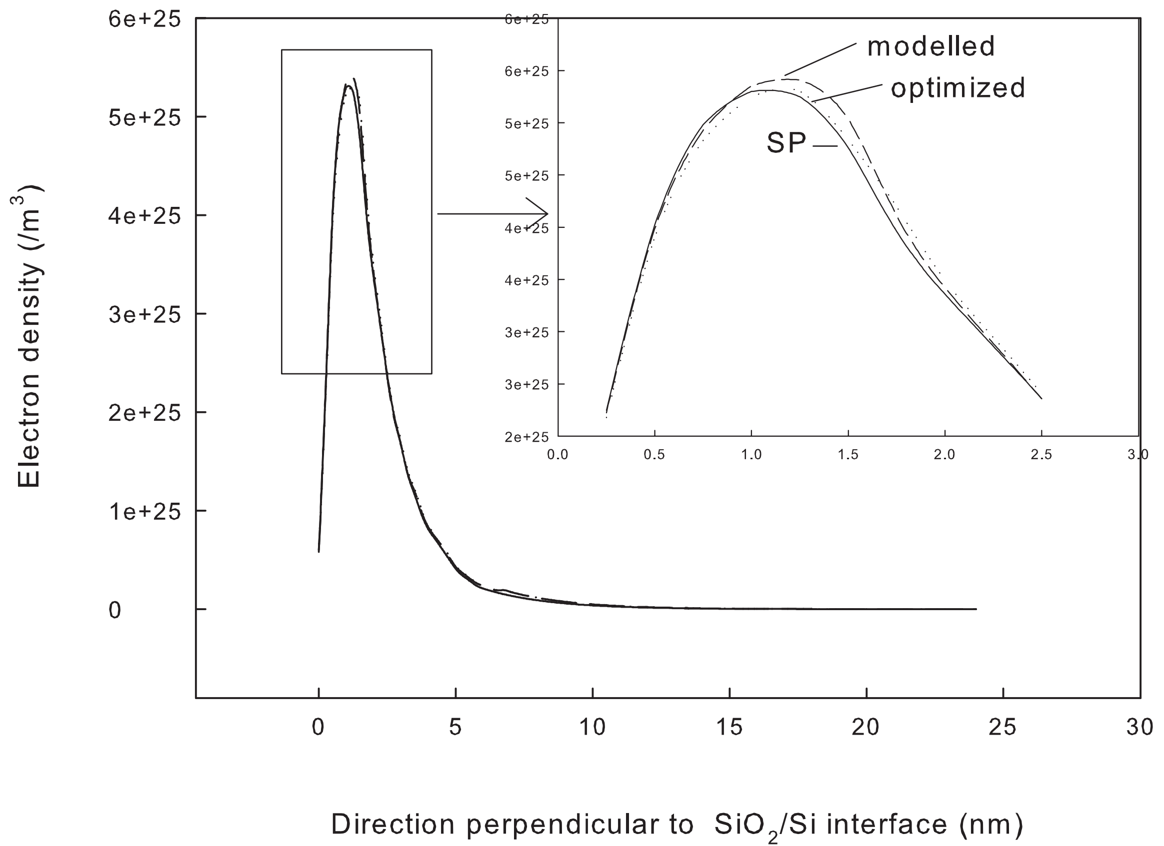

Figure 5.32: Comparison of electron density: From this case, we can find that residual of this model is larger.

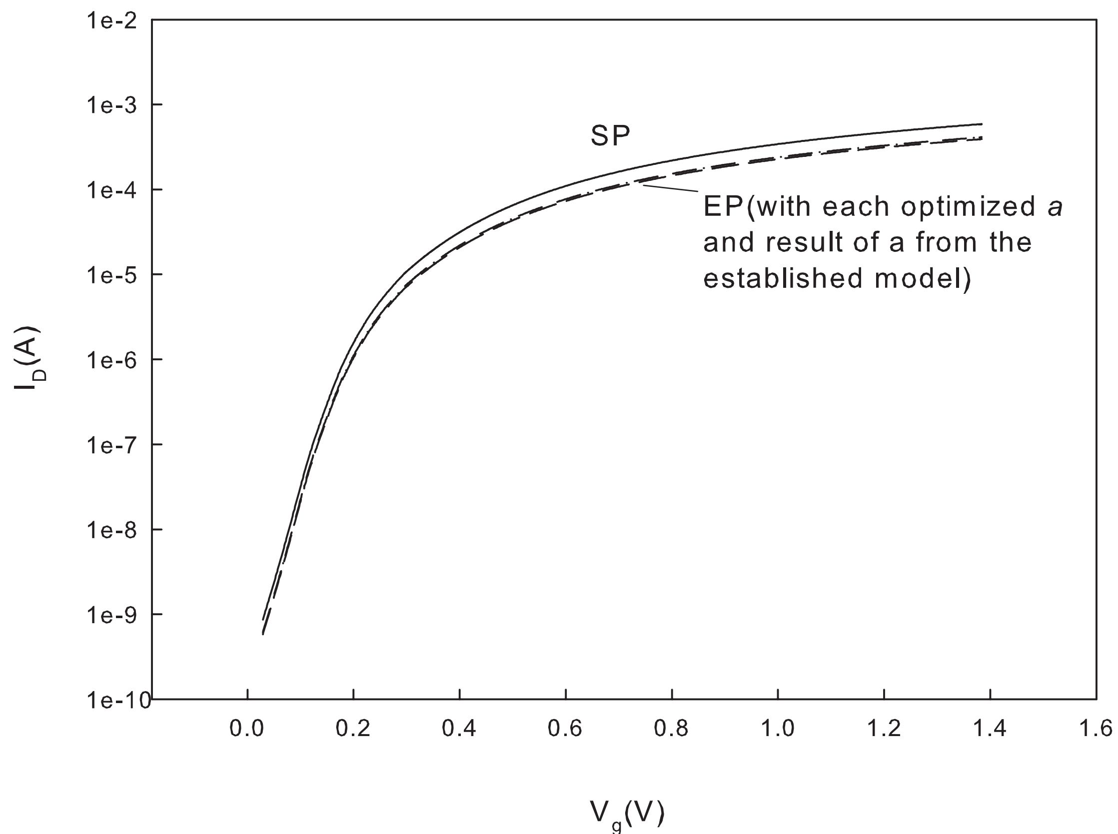

Figure 5.33: Id-Vg curve:solid line is solved from SP equations while dash line is solved from effective potential. curves solved from effective potential with optimized a and a from model are still almost equal. But different is more clear. Curve of effective potential is some lower than SP equations. Maximum of different between SP equations and effective potential is about 0.35 mA.

5.4 Discussion

We simulate devices with channel length which is equal to 20 nm, 30 nm, 40 nm and 50 nm, respectively in double-gate MOSFET. We can't get a better model if we analyze all data. However, if we delete data whose channel length equal to 20 nm, then we establish a model not bad. On the other hand, people have proposed that quantum effective will appear in channel direction when channel length is shorter than 20 nm. So, 1D Ferry's effective is not suit for those devices.

From our simulation, we get formula for double-gate MOSFET and SOI structure. And from formula, we know how the outer factors effect value of standard deviation of wave packet. Effects of drain voltage and thickness of bulk are not significant in our results. Collinearity of data may be one of the reason. Their influence may be increasing while collinearity is decreasing.

In terms of structure, double-gate and SOI MOSFET are similarly. However, characters of these structure may be some different. So, formula for both structures is not as good as formula only for one structure.

From scattering plots, we can know there are simple correlations between regressors variables and response variable. So we using the simplest model to fit it first. And results are satisfied. Therefore, we don't establish model which is more complicated.

Chapter 6

Conclusions

In this thesis, models of standard deviation of wave packet have been established successfully. Accuracy was also presented with comparing to the results solved from SP equations, including electron density and I-V curve. From previous models, we can know what outer conditions effect the standard deviation of wave packet evidently. Both models have their own merit and shortcoming. Models seems acceptable in terms of error. In this chapter, the contributions of the thesis will be addressed firstly, and followed by the future works.

6.1 Summary

In this thesis, we focus on the Ferry's effective potential and try to find the behavior of standard deviation of wave packet with various outer conditions. We use statistical methods to build multiple linear regression model. We don't use advanced model because we have gotten good results.

Models of standard deviation of wave packet are established under some constraint of conditions. Under these constraint, we know that channel length, gate voltage,and thickness of oxide dominate the variation of standard deviation of wave packet form models. From these results, we can't say drain voltage and thickness of bulk are marginal with certainty because of collinearity of our data. In addition to model for double-gate MOSFETs, we also establish a model suit for double-gate and SOI MOSFETs simultaneously. Perhaps residual of the latter is larger than the former. But the different seems not so evident. The model may be not suitable for devices whose conditions exceed these constraint or with other structures. However, statistical methods presented in this thesis can be extend to analysis similar problem.

6.2 Future Work

Besides double-gate MOSFET and SOI, there are still many structures of devices. In thesis, we discuss these two structures because of similarity in structure. Recently, ultra thin barrier device is proposed. Its structure is between double-gate and SOI MOSFET. On the other hand, double-gate structure will become single gate if we set thickness of bulk thicker and only one gate in our condition. In terms of structure, we can discuss several kinds of structures or characteristics of devices at the same time to make formula more general. By experience in this thesis, model more general may lose accuracy. Here, we only consider those direct outer conditions as regressor variables. Transformation of regressor variables may be important and efficient factors. Besides, we only use the most popular model - linear regression model. Advanced model may arise better results for more complicated data.

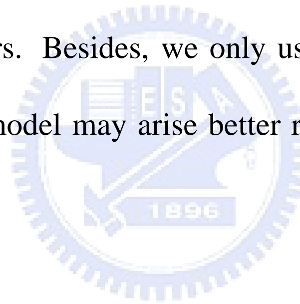

Bibliography

[1] M. Choi, L. Milor, and L. Capodieci, ”Simulation of the circuit performance impact of lithography in nanoscale semiconductor manufacturing”, *Proceedings of International Conference on Simulation of Semiconductor Processes and Devices*, 3-5 Sep. 2003, pp. 219-222.

[2] Y. Li, T. W. Tang, and S. M. Yu, ”A Quantum Correction Model for Nanoscale Double-Gate MOS Devices Under Inversion Conditions”, *Journal of Computational Electronics*, Vol. 2, No. 2-4, Dec. 2003, pp. 491-495.

[3] J. W. Lee and Y. Li, ”Silicidation Enhanced Poly-Depletion and Flat Band Voltage Shift in Nanoscale Metal-Oxide-Silicon Structures”, *Book of Abstracts of The 1st International Meeting on Applied Physics*, Badajoz, Spain, Oct. 14-18, 2003, p. 798.

[4] S. C. Lo, J. H. Tsai, J. M. Hsu, and Y. Li, ”Quantum Mechanical Gate Current Simulation in MOSFETs with Ultrathin Oxides”, *Proceedings of The 2003 International*

Conference on VLSI, CSREA Press, Las Vegas, Nevada, USA June, 23-26, 2003, pp. 244-250.

[5] S. C. Lo, Y. Li, and J. H. Tsai, ”Quantum Mechanical Simulation of High-k Gate Dielectrics Metal-Oxide-Semiconductor Structures”, *WSEAS Transactions on Electronics*, Vol. 1, No. 1, Jan. 2004, pp. 170-175.

[6] Y. Li, ”A Quantum Correction Poisson Equation for Metal-Oxide-Semiconductor Structure Simulation”, *Semiconductor Science and Technology*, Vol. 19, No. 7, July 2004, pp. 917-922.

[7] S. M. Ramey and D. K. Ferry, ”Implementation of Surface Roughness Scattering in Monte Carlo Modeling of Thin SOI MOSFETs Using the Effective Potential”, *IEEE Transactions on Nanotechnology*, Vol. 2, No. 2, June 2003, pp. 110-114.

[8] J. R. Watling, A. R. Brown, A. Asenov and D. K. Ferry, ”Quantum Corrections in 3-D Drift Diffusion Simulations of Decanano MOSFETs Using an Effective Potential”, *Simulation of Semiconductor Processes and Devices*, 2001.

[9] Y. Li and S. M. Yu, ”A unified quantum correction model for nanoscale single- and double-gate MOSFETs under inversion conditions”, *Nanotechnology*, 2004, pp. 1009-1016.

[10] R. Akis, S. N. Miličić, D. K. Ferry and D. Vasileska, ”An Effective Potential Method for Includeing Quantum Effects Into the Simulation of Ultra-Short and Ultra-Narrow Channel MOSFETs”, Proceedings of the 4th International Conference on Modeling, 2001.

[11] J. R. Schrieffer, Semiconductor Surface Physics, *University of Pennsylvania press*, 1957, Philadelphia.

[12] Sze, S. M., Physics of semiconductor devices, 1981, John Wiley & Sons,Inc

[13] Sze, S. M., Semiconductor devices, physics and technology-2nd ed, 1985, John Wiley & Sons,Inc

[14] Y. Li, H.-M. Lu, T.-W. Tang, and S. M. Sze, ”A Novel Parallel Adaptive Monte Carlo Method for Nonlinear Poisson Equation in Semiconductor Devices”, *Mathematics and Computers in Simulation*, Vol. 62, No, 3-6, March 2003, pp. 413-420.

[15] Y. Li and S.-M. Yu, ”A Parallel Adaptive Finite Volume Method for Nanoscale Double-Gate MOSFETs Simulation”, *Journal of Computational and Applied Mathematics*, Vol. 17., No. 1, March 2005, pp. 87-99

[16] D. J. Roulston, An Introduction to the physics of Semiconductor Devices, Oxford University Press, New York, 1999.

[17] Y. Li, S.S. Chung, and J.-L. Liu, ”A Novel Approach for the Two-dimensional Simulation of Submicron MoSFETs Using Monotone Iterative Method”, *Proceedings of International Symposium onVLSI Technology, Systems, and Applications*, pp. 27-30, 8-10 June 1999.

[18] Y. Li, J.-W. Lee, T.-W. Tang, T.-S. Chao, T.-F, Lei, and S. M. Sze,” Numerical Simulation of Quantum Effects in High-k Gate Dielectrics MOS Structures using Quantum Mechanical Models”, *Computer Physics Communications*, Vol. 147, No. 1-2, August 2002, pp. 214-217.

[19] M. G. Ancona, ”Quantum Correction to the Equation of State of an Electron Gas in a Semiconductor”, *Physical Review B*, Vol. 39, NO. 13, 1989, pp. 9536-9540.

[20] T. Ando, A. B. Fowler, and F. Stern, ”Electronic properties of two-dimensional systems”, *Review Modern Physics*, Vol. 54, 1982, pp. 437.

[21] A. S. Spinelli, A. Benvenuti, ”Self-consistent Model for Quantum Effect in n-MOS Transistors”, *IEEE Transactions on Electron Devices*, Vol. 45, NO.6, 1998, pp. 1342-1349.

[22] T. Janik and B. Majkusiak, ”Influence of carrier energy quantization on the threshold voltage of metal-oxide-semiconductor transistor”, *J. Appl. Phys.*, 1994, Vol. 75, pp. 5186-5190

[23] T. Ando, A. B. Fowler, and F. Stern, ”Electronic properties of twe-dimensional systems”, *Rev. Mod. Phys.*, 1982, Vol. 54, pp. 437-672.

[24] R. Rios and N. D. Arora, ”Determination of ultra-thin gate oxide thickness for CNOS structures using quantum effects”, in *IEDM Tech. Dig.*, 1994, pp. 613-616.

[25] C. Ringhofer, C. Gardner and D. Vasileska, ”Effective potentials and quantum fluid models: A thermodynamic approach,” *Inter. J. on High Speed Electronics and Systems* 13, 771, 2003.

[26] C. Dewdney and B, J, Hiley, ”A quantum potential description of one-dimensional time-dependent scattering from square barriers and square wells,” *Round. Phys*., vol. 12, pp. 27-48, 1982.

[27] D. K. Ferry and J.-R. Zhou, ”Form of the quantum potential for use in hydrodynamic equations for semiconductor device modelling,” *Physical Review B*, vol. 48, pp. 7944-7950, 1993.

[28] P. Feynman amd H. Kleinert, ”Effective classical partition functions,” *Physical Review A*, vol. 34, pp. 5080-5084, 1986.

[29] Y. Li, ”A Comparative Study of Numerical Algorithms in Calculating Eigenpairs of the Master Equation for Portein Folding Kinetics”, *Abstracts of the 10th International Workshop on Computational Electronics* (IWEC-10), 24-27 Oct. 2004, pp. 201-202.

[30] G. J. Iafrate, H. L. Grubin, and D. K. Ferry, ”Utilization of quantum distribution functions for ultra-submicron device transport”, *Journal de Physique*, Vol. 42(Colloq. 7), 1981, pp. 307-312.

[31] E. Wigner, ”On the quantum correction for thermodynamic equilibrium”, *Phys. Rev.*, Vol. 40, 1932, pp. 749-759.

[32] D. K. Ferry, J. R. Barker, ”Open problems in quantum simulation in ultra-submicron devices”, *VLSI Design*, Vol.8, 1998, pp. 165-172.

[33] D. K. Ferry, ”Effective potential and the onset of quantization in ultrasmall MOSFETs”, *Superlattices and Microstructures*, Vol. 28, 2000, pp.419-423.

[34] D. Vasileska and D. K. Ferry, ”Scaled Silicon MOSFETs: Universal Mobility Behaviou”, *IEEE Trans. Electron Dev.*, Aprial 1997, Vol. 44, pp. 577-583

[35] D. K. Ferry, ”Simulation at the start of the new millennium: Crossing the quantum mechanical threshold”, *VLSI Design*, inpress.

[36] D. K. Ferry adn W. Howard, ”Negative Field-Effect Mobility on (100) Si Surfaces”, *Rhys. Rev. Lett.*, Vol. 16, May 1966, pp. 797-799.

[37] Peter T. Brockwell, Richard A. Davis, Introduction to Time Series And Forecasting, 2nd ed, 2002, Springer-Verlag New ork, Inc.

[38] Douglas C. Montgomery, Elizabeth A.Peck, G. Geoffrey Vining, Introduction to Linear Regression Analysis, 3rd ed, 2001, John Wiley & Sons, Inc.

[39] Wu, C.-F. Jeff, Experiments: planning, analysis. and parameter design optimization, 2000, John Wiley & Sons, Inc.

[40] Raymond H. Myers, Douglas C. Montgomery, Response Surface Methodology : process and product optimization using designed experiments, 2nd ed, 2002, John Wiley & Sons, Inc.

[41] G. E. P. Box and Norman R. Draper, Empirical Model-Building and Response Surfaces, New York, Wiley, 1987.

[42] D. K. Ferry,R. Akis, D. Vasileska, ”Quantum effects in MOSFETs: Use of and effective potential in 3D Monte Carlo simulation of ultra-short channel devices”, *IEDM Technical Digest, Electron Devices Meeting*, 2000, pp. 287-290

[43] D. K. Ferry, ”The onset of quantization in ultra-submicron semiconductor devices,” *Superlattices and Microstructures*, Vol. 27, No. 2/3, 2000.

[44] Y. Li, H.-M. Chou, ”A comparative study of electrical characteristic on sub-10-nm double gate mosfets”, *IEEE Transactions, Nanotechnology*, Vol. 4, 2005, pp. 645-647.

[45] M. leong, H.-S. Wong, E. Nowak, J. Kedzierski, and E. C. Hones. ”High performande double-gate device technology challenges and opportunities”, in *Proc. Int. Quality electronic Design Symp.*, Mar. 18-21, 2002, pp. 492-495.

[46] L. Wei, Z. Chen, and K. Roy, ”Design and optimization of double gate SOI MOS-FET’s for low voltage low power circuits”, in *Proc. IEEE Int. Silicon-on-Insulator Conf.*, Oct. 5-8, 1998, pp. 69-70.

[47] Y. Li and S. M. Yu, ”A two-dimensional quantum transport simulation of nanoscale double-gate MOSFET’s using parallel adaptive technique”, *IEICE Trans. Inform. Syst.*, Jul. 2004, Vol. E87-D, No. 7, pp. 1751-1758.

[48] J. Bude, ”MOSFET modeling into the ballistic regime,” *in Proc. Int. Conf, Simulation Semiconductor Processes and Devices*, 2000, pp. 23-26

[49] A. Abramo, A Cardin, L. Selmi, and E. Sangiorgi, ”Two-dimensional quantum mechanical simulation of charge distribution in silicon MOSFETs”, *IEEE Trans. Electron Devices*, Oct. 2000, Vol. 47, pp. 1858-1863.

[50] H. Tsuchiya and T. Miyoshi, ”Quantum transport modeling of ultrasmall semiconductor device”, *IEICE Trans. Electron.*, 1999, Vol. E82-C, 880-888.

Appendix A

Effective Potential Source Code of Matlab

We simulate classical transport model and SP model by software-ISE. There is no command of effective potential. So we simulate classical transport model to get potential without quantum mechanism first. And then use following code to get Ferry's effective potential.

EP

According to the equation,

$$V_{eff}(x) = \int V(x+y)G(y,a_0)dy.$$

We evaluate 1D effective potential by using potential solved from classical transport model.

Following is code of previous equation:

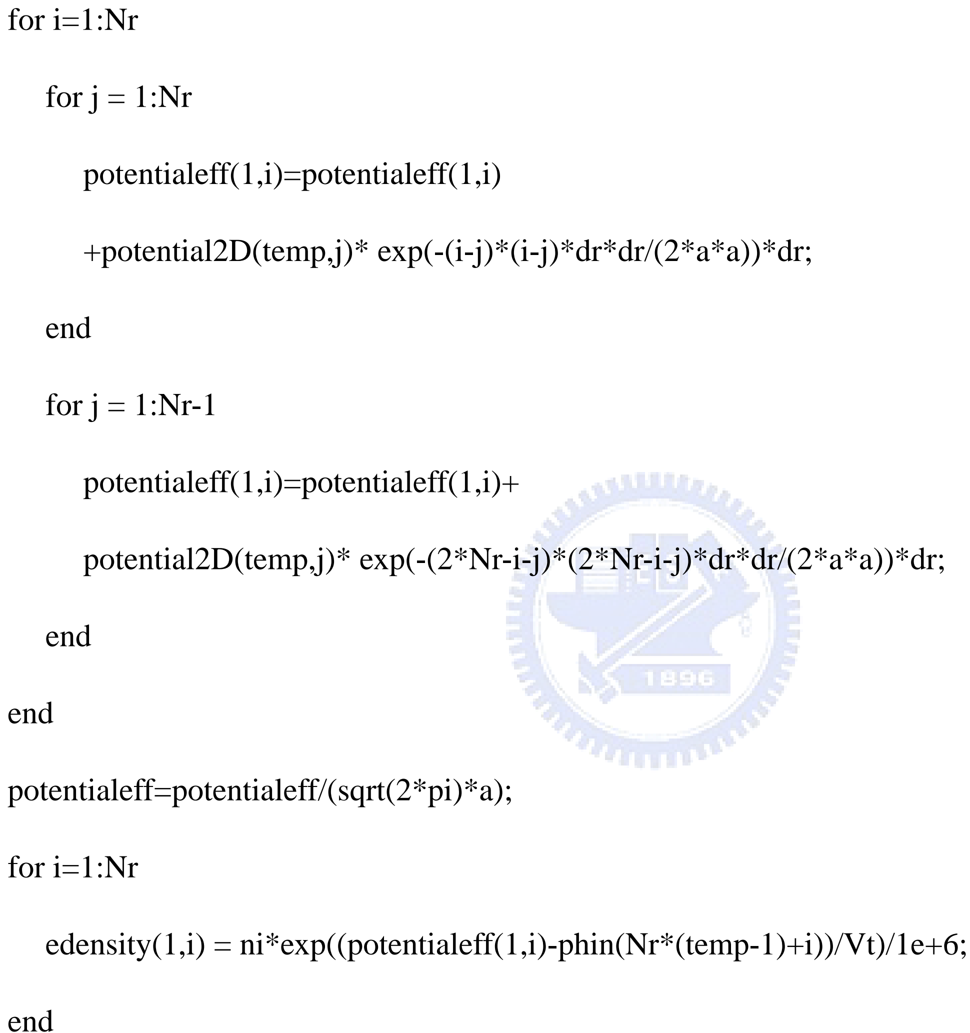

```
for i=1:Nr
    for j = 1:Nr
        potentialeff(1,i)=potentialeff(1,i)
        +potential2D(temp,j)* exp(-(i-j)*(i-j)*dr*dr/(2*a*a))*dr;
    end
    for j = 1:Nr-1
        potentialeff(1,i)=potentialeff(1,i)+
        potential2D(temp,j)* exp(-(2*Nr-i-j)*(2*Nr-i-j)*dr*dr/(2*a*a))*dr;
    end
end
potentialeff=potentialeff/(sqrt(2*pi)*a);
for i=1:Nr
    edensity(1,i) = ni*exp((potentialeff(1,i)-phin(Nr*(temp-1)+i))/Vt)/1e+6;
end
```

Appendix B

ISE Commands for Classical Transport and Schrödinger Equation

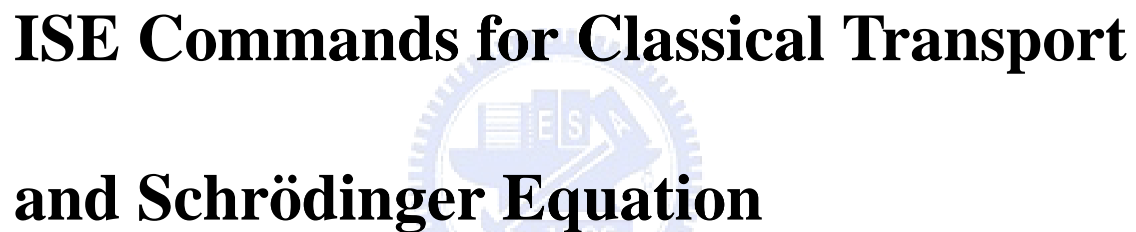

We use ISE in most of our simulation. Here, we will present commands in ISE. First part, we define mesh and doping concentration. Second part, we present the model we used and some outer conditions. Last, we show keywords of Drift-Diffusion model and Schrödinger equation. If we want to coupled these models, we have to add these commands into second part.

B.1 MDraw Commands

Title ”Untitled”

% Definition of mesh. We can set several commands to build irregular mesh.

Definitions{

#Refinement regions

Refinement”name”

{

MaxElementSize=(0.0005 0.0005)

MinElementSize=(0.0001 0.0001) }

#Profiles

% Definition of Doping. Here, we can set not only doping concentration, but also meterial.

Constant”S” {

Species=”ArsenicActiveConcentration”

Value=1e+20

}

Constant"D" {

Species="ArsenicActiveConcentration"

Value=1e+20

}

Constant"B" {

Species="BoronActiveConcentration"

Value=1e+17

}

}

B.2 Dessis Commands

% Here, we can set outer conditions and models.

% Initial setting.

Electrode{

```
{Name="source" Voltage=0.0}
{Name="drain" Voltage=0.0}
{Name="gate" Voltage=0.0 Barrier=-0.4}
}
% File need to include.
File{
Grid = "@grid@"
Doping ="@doping@"
Plot = "@dat@"
current ="@plot@"
Output = "@log@"
Param = "@parameter@"
}
%model will be included
Physics{
Mobility(
PhuMob
HighFieldsaturation(GradQuasiFermi)
Enormal
```

```
)
}
%numerical setting
Math{
Extraploate
Derivatives
RelErrControl
Figits=5
ErRef(electron)=1e10
ErRef(hole)=1e10
Notdamped=50
Iterations=30
Newdiscretization
ConstRefPot
DirectCurrent
}
%model will be included
Solve{
#initial solution
```

```
NewCurrentFile=”INIT”
CoupledPoisson Electron Hole Quasistationary(
InitialStep=1e-2 Increment=1.2
Minstep=1e-5 MaxStep=0.5
Goal{Name=”drain” Voltage=0.8}
)
NewCurrentFile=””
Quasistationary(
InitialStep=1e-2 Increment=1.2
Minstep=1e-5 MaxStep=0.5
Goal{Name=”gate” Voltage=0.8}
)
}
```

B.2.1 key words

If we want to include Drift-Diffusion model or Schrödinger equation, we can adding follow code into dessis commands.

(a) Drift-Diffusion

```
Solve{ Coupled{Poisson Electron Hole}}
```

(b) Schrödinger

```
Physics(RegionInterface=”name of interface”)
    {Schroedinger (
    Electron
    MaxSolutions=8)}
```

Appendix C

Energy Band of Double-Gate MOSFET

Here, we only consider double gate devices and set device with thickness of oxide1= thickness of oxide2 = 1.5 nm, channel length = 30 nm, gate1 voltage = gate2 voltage = 0.9 V, drain voltage = 1.0 V, doping concentration = $1e16 / cm^3$, thickness of bulk = 15 nm be the reference. And we change thickness of bulk, doping concentration, gate voltage, thickness of oxide, drain voltage and channel length in turn. We draw plots of energy band corresponding to each condition as follows. When we focus on the neighborhood of SiO_2/Si interface (potential well), we can find that gate voltage, thickness of oxide, channel length and doping concentration influence the shape of well significantly. Thickness of bulk and drain voltage just shift the position of well and variation is not significant. Degree of effects from these figures and results from statistical analysis are unanimous.

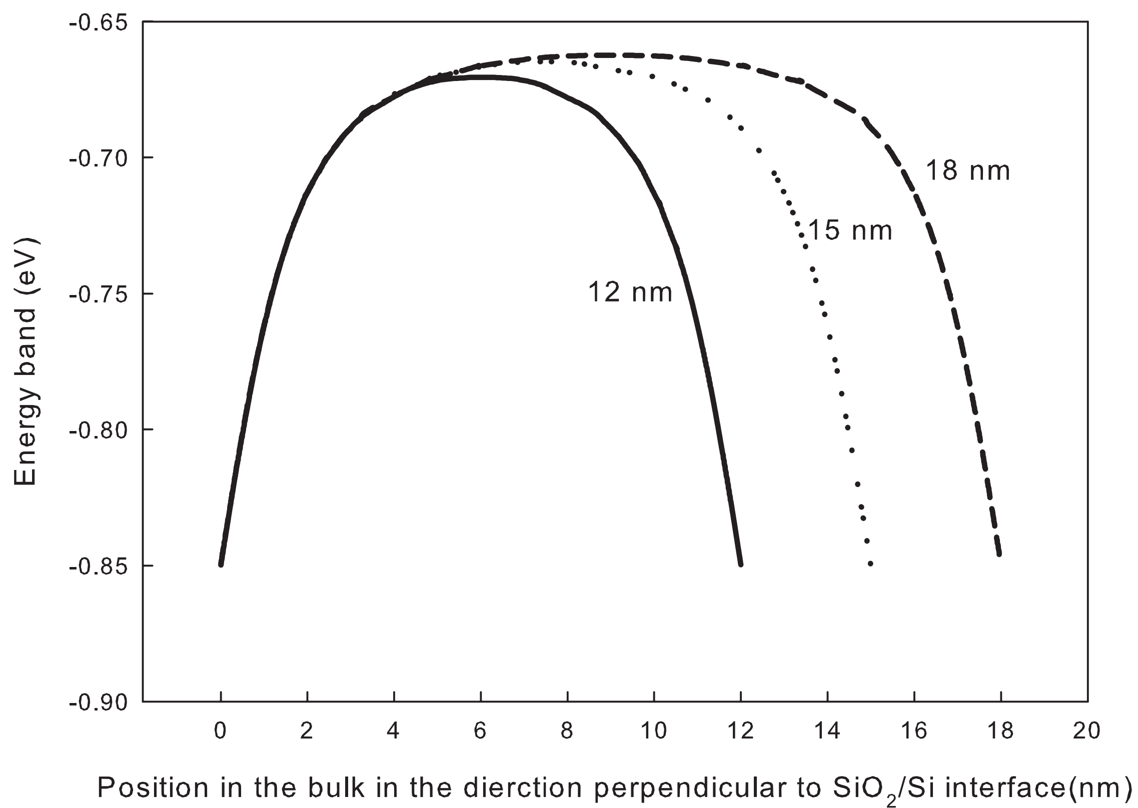

Figure C.1: Energy band plot of various thickness of bulk. The main effect of change of thickness of bulk is the range of flat band. Change of band nearby the SiO_2/Si interface is not evident.

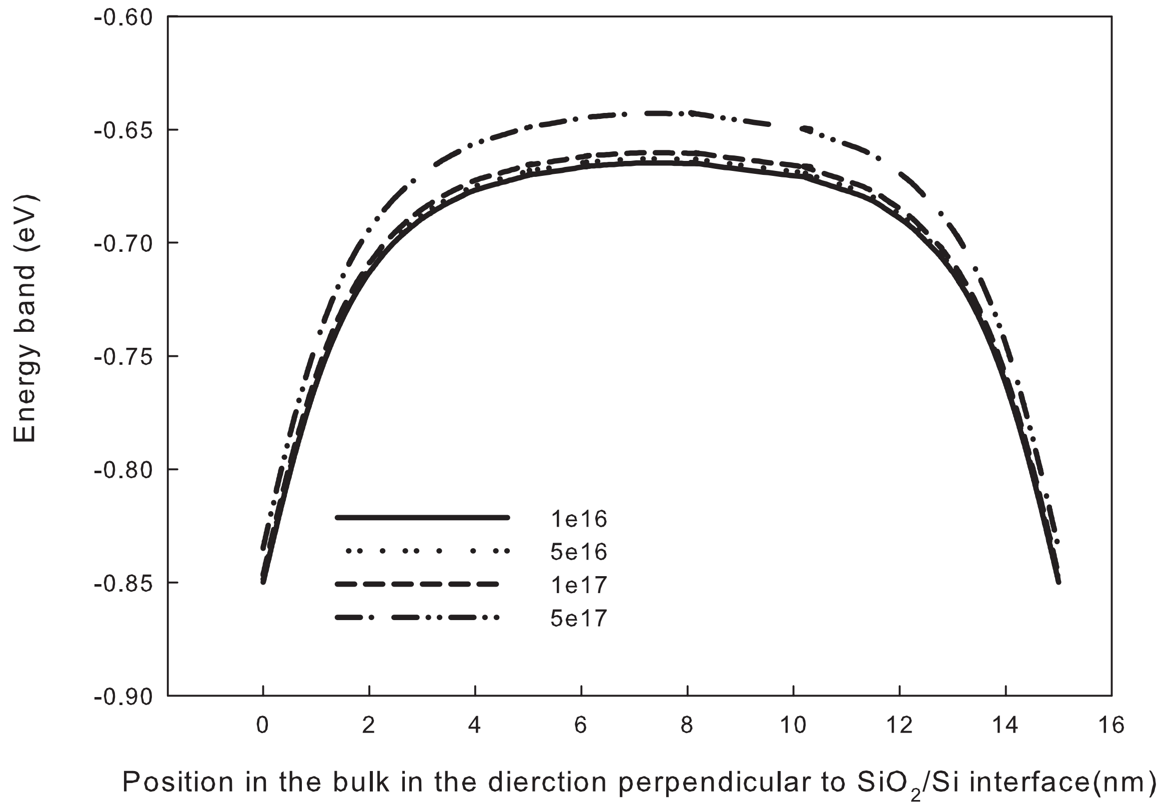

Figure C.2: Energy band plot of various doping concentration. As increasing of doping concentration, energy band shift up. There is some change of shape of band nearby the SiO_2/Si interface.

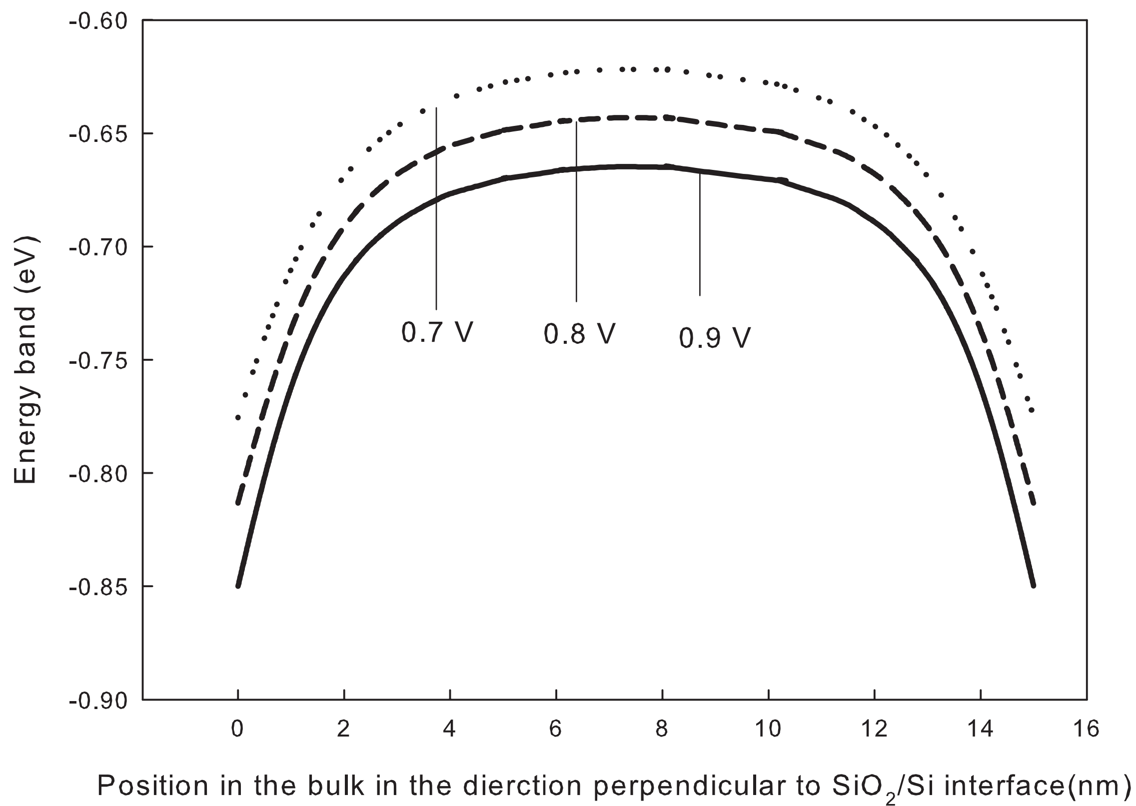

Figure C.3: Energy band plot of various gate voltage. Increase of gate voltage not only shifts down the energy band, but also deepens the depth of energy band nearby the interface.

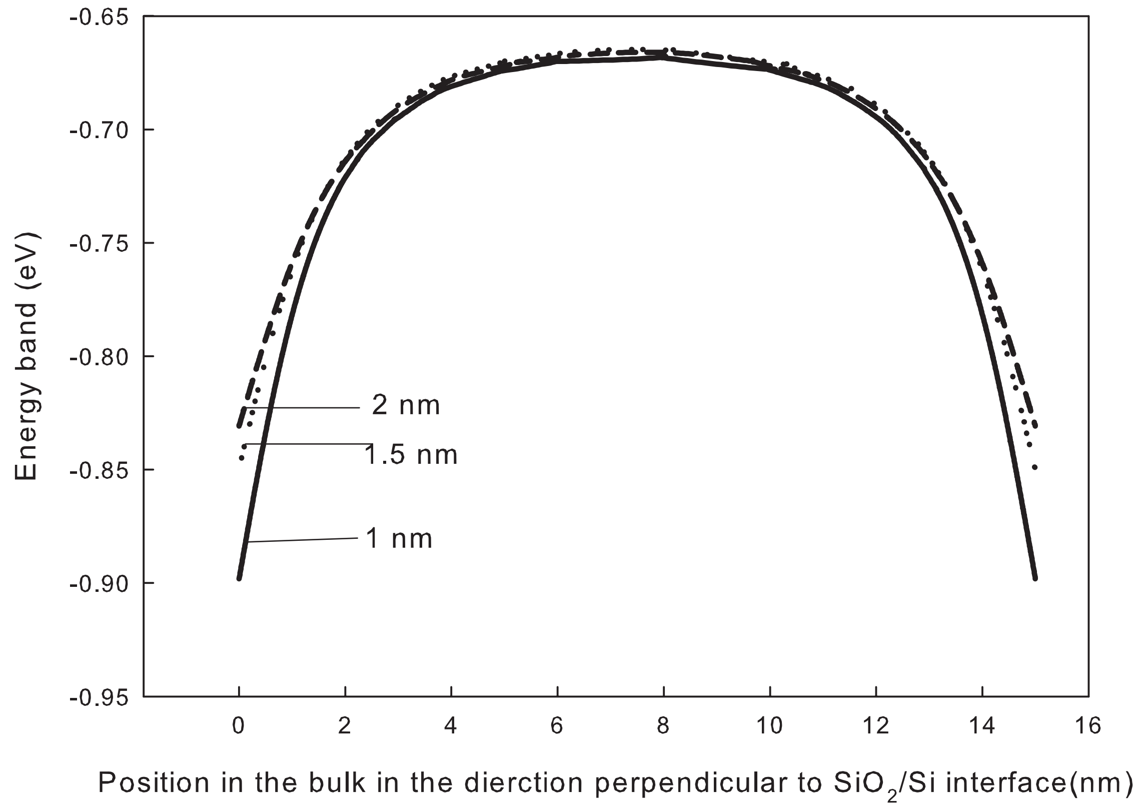

Figure C.4: Energy band plot of various thickness of oxide. Decrease of thickness of oxide influences the shape of energy band nearby the interface.

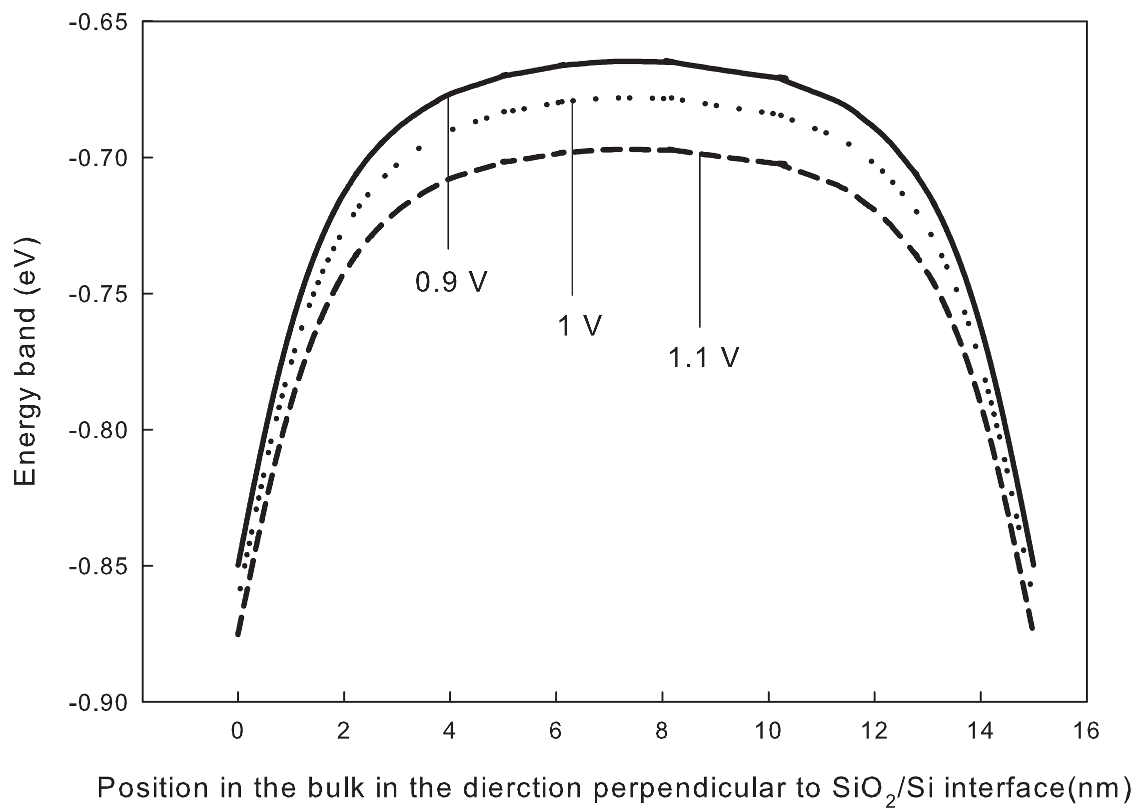

Figure C.5: Energy band plot of various drain voltage. Change of drain voltage shift the energy band. Change of shape energy band is not evident.

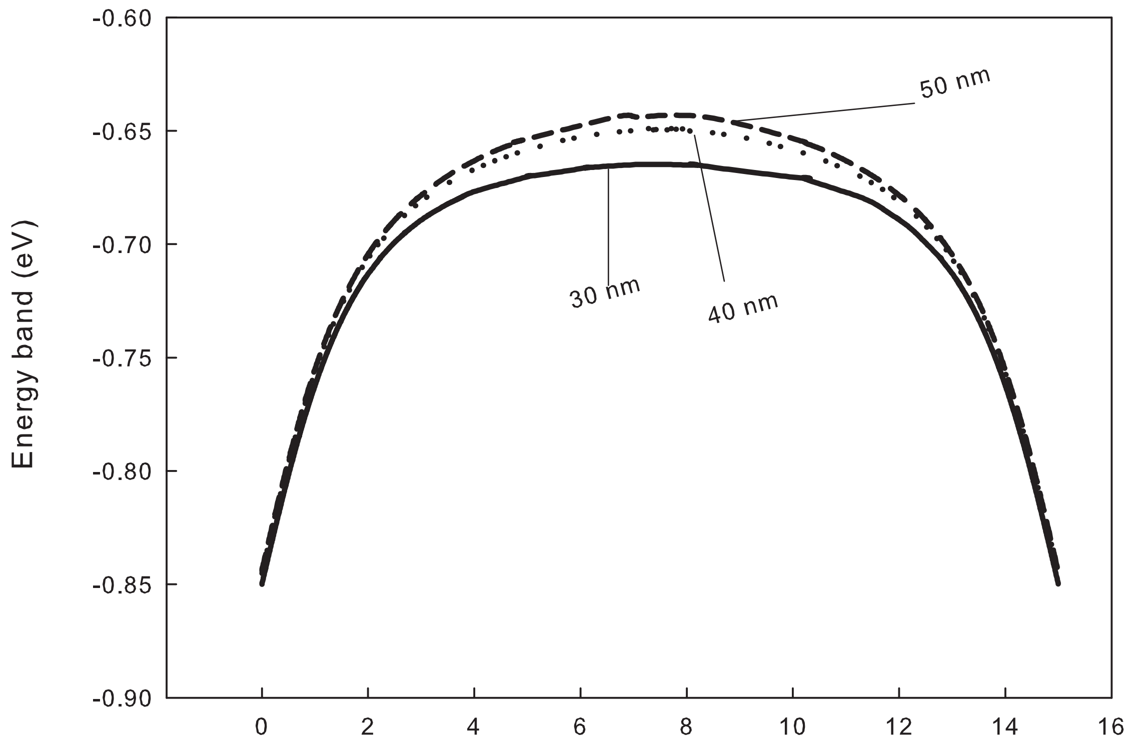

Figure C.6: Energy band plot of various channel length. Increase of channel length will deepen the depth of energy band obviously.

Appendix D

A Brief Instruction to SPSS

SPSS is a Data Analysis with Comprehensive Statistics Software. It is a modular, tightly integrated for the analytical process: planning, data collecting, data access, data management and preparation, data analysis, reporting, and deployment. In this research, scattering plot, multiple linear regression and residual analysis. In this Appendix, the adopted features are introduced.

final_data.sav - SPSS Data Editor

File Edit View Data Transform Analyze Graphs Utilities Window Help

1 : t_ox 1

	a	ln_a	t_ox	Lg	t_si	Vg1	Vd	N
1	11.3240	2.43	1.00	2.00	8.00	.6	.7	1]
2	8.8380	2.18	1.00	2.00	8.00	.7	.7	1]
3	7.4160	2.00	1.00	2.00	8.00	.8	.8	1]
4	11.2920	2.42	1.00	2.00	8.00	.6	.8	5]
5	8.8170	2.18	1.00	2.00	8.00	.7	.9	5]
6	7.4020	2.00	1.00	2.00	8.00	.8	1.1	5]
7	11.2340	2.42	1.00	2.00	8.00	.6	.6	1]
8	8.7820	2.17	1.00	2.00	8.00	.7	1.0	1]
9	7.3770	2.00	1.00	2.00	8.00	.8	1.1	1]
10	10.9070	2.39	1.00	2.00	8.00	.6	.9	5]
11	8.5780	2.15	1.00	2.00	8.00	.7	.9	5]
12	7.2360	1.98	1.00	2.00	8.00	.8	1.0	5]
13	11.1060	2.41	1.00	2.00	10.00	.6	.7	1]
14	8.6900	2.16	1.00	2.00	10.00	.7	.9	1]
15	7.3070	1.99	1.00	2.00	10.00	.8	.9	1]
16	11.0730	2.40	1.00	2.00	10.00	.6	.6	5]

Data View / Variable View

SPSS Processor is ready

Figure D.1: Table of data: every column indicates a variable; and every row indicates a case.

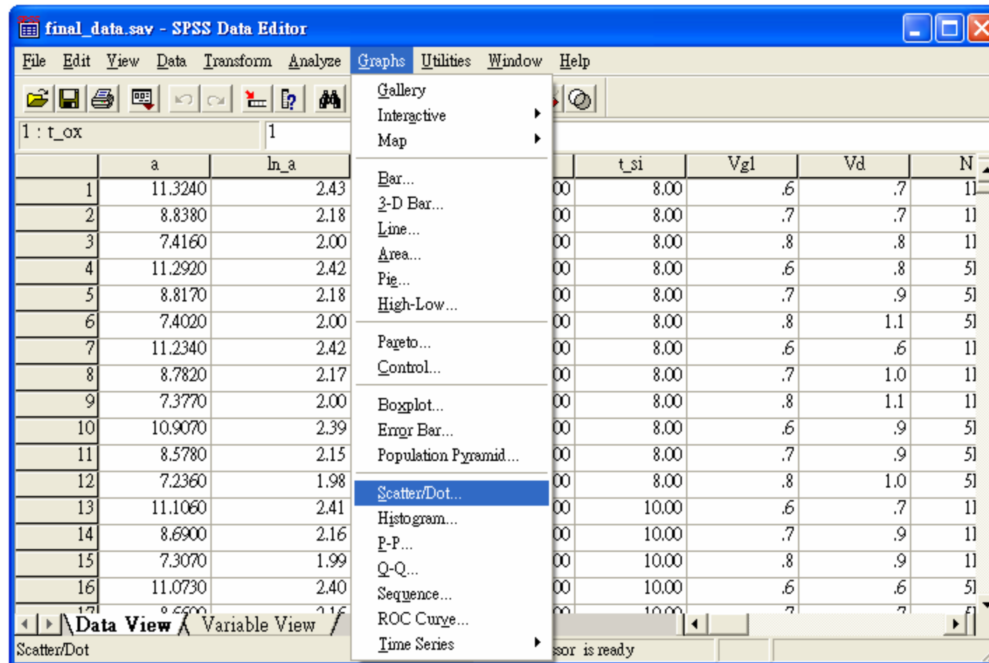

Figure D.2: Before processing model analysis, usually we will observe scattering plots to assist our variables setting.

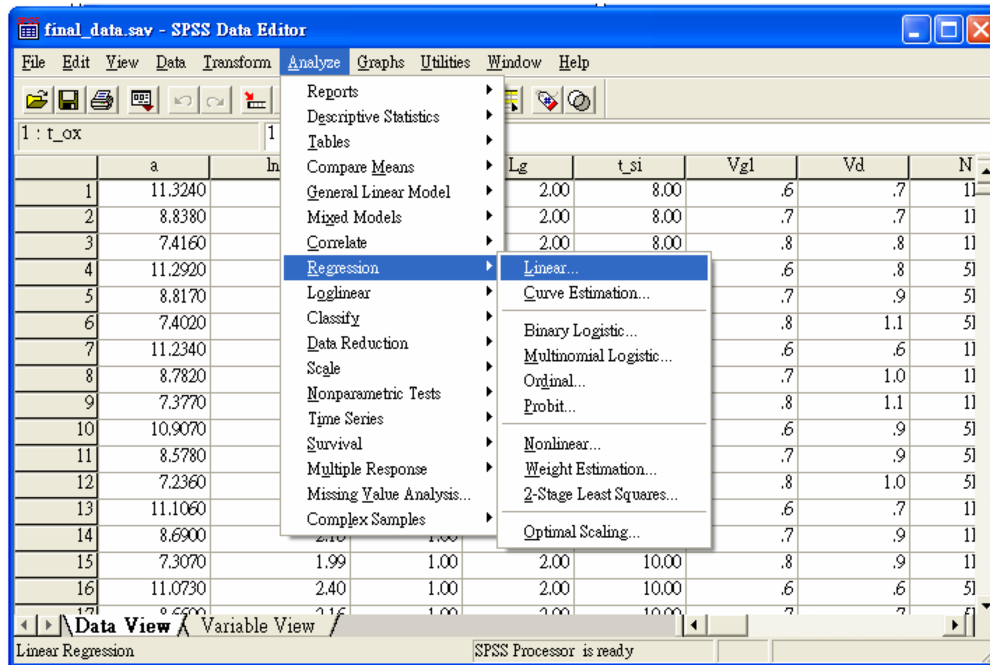

Figure D.3: In our analysis, we use linear regression. So, we have to choose bottom : Analyze / Regression / Linear.

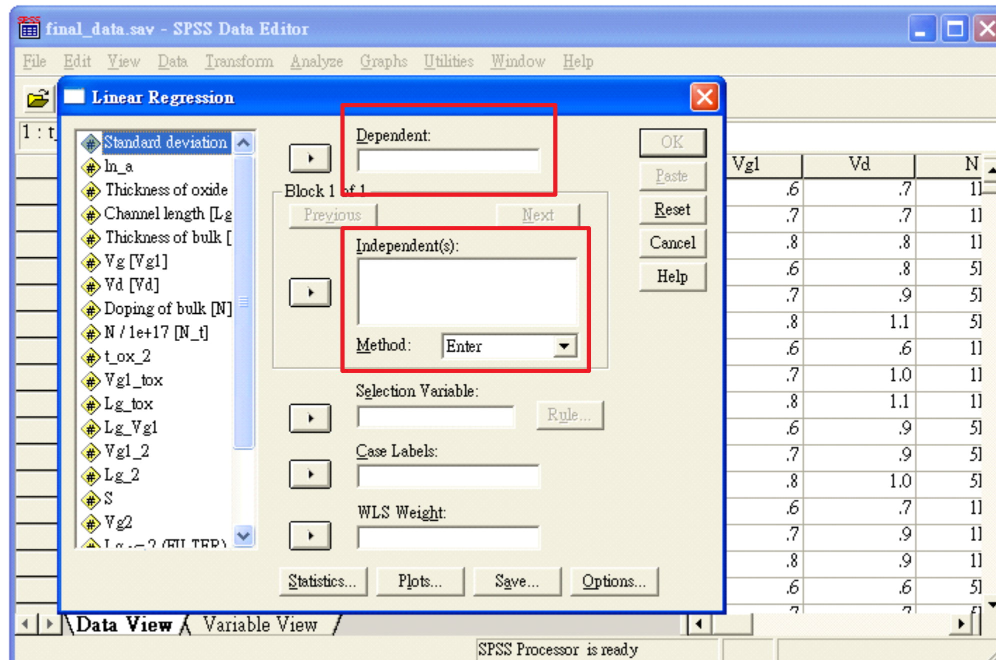

Figure D.4: We have to set response variable into the "Dependent" frame, and choose regressor variables into the "Independent" frame. Besides, we can choose methods to select regressor variables.

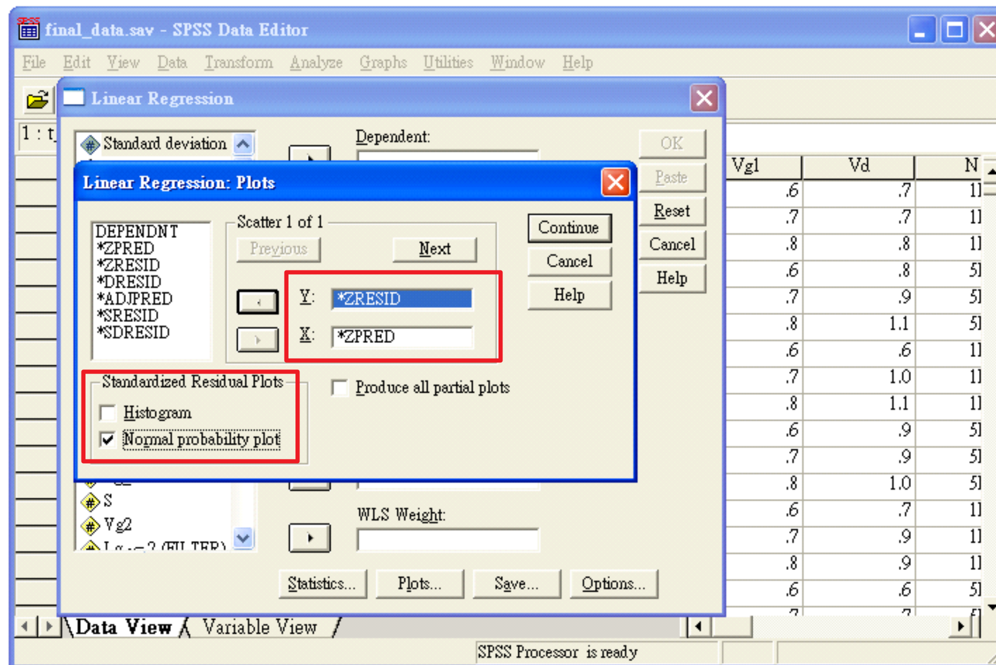

Figure D.5: After setting model, we can mark Normal probability plot and choose residual terms to check residual analysis.